

https://dspace.org/

Review of stokes flow past a sphere

Banda, Sipho

2019

https://hdl.handle.net/10539/27075

Banda, Sipho, (2019) Review of stokes flow past a sphere, University of the Witwatersrand, Johannesburg, https://hdl.handle.net/10539/27075.

Downloaded from a DSpace repository. https://dspace.org/

Review of Stokes Flow Past a Sphere

Student Number : 0506068D
Author : Sipho Banda
Supervisor : Dr. Sheldon Herbst

January 2019



A Dissertation submitted to the Faculty of Science, University of the Witwatersrand, Johannesburg, in fulfilment of the requirements for the degree of Master of Science.

Declaration

I, Sipho Banda, declare that this Dissertation is my own, unaided work. It is being submitted for the Degree of Master of Science at the University of the Witwatersrand, Johannesburg. It has not been submitted before for any degree or examination at any other University.

Signed: Sipho Banda



Date: 25 January 2019

Abstract

The slow viscous incompressible flow past a stationary sphere is studied. We review Stokes and Oseen approximations. The stream function approach is used to derive the solutions of incompressible fluid flow that were obtained by Stokes and Oseen. We solve the Stokes expansion using Mathematica and the code is given in the algorithms. The explicit finite difference method (FDM) is used to solve the fourth order differential equation that was derived from the full Navier-Stokes equations. We also investigate numerical solutions to the Stokes expansion using standard (FDM) in Mathematica. Using FDM iteratively we can find approximate solutions to higher moments in the stream function and compare these solutions with those found from the numerical solutions to the full Navier-Stokes equations.

Acknowledgements

I would like to thank my supervisor, Dr. Sheldon Herbst for guidance and support throughout the research. Dr. Sheldon Herbst also provided his advice and ideas which have helped me a lot.

I am also thankful to my family and friends for the support and encouragement.

Contents

Declaration ii

Abstract iii

Acknowledgements iv

Contents v

List of Figures vii

List of Tables ix

Glossary x

List of Symbols xi

1 Introduction 1

2 Governing Equations 11
2.1 Stokes Approximation 11
2.1.1 Navier-Stokes and continuity equations 11
2.1.2 Boundary Conditions 18
2.1.3 Perturbation Expansion 20
2.2 Oseen Approximation 21

3 Analytical Method 24
3.1 Stokes Approximation 24
3.1.1 Stoke's solution for zero order problem 24
3.1.2 Solution of the first order problem 28
3.1.3 Whitehead Paradox 34
3.1.4 Solution of second order problem 34
3.2 Oseen Approximation 40
3.2.1 Leading term of Oseen expansion 40
3.2.2 Second term of Oseen expansion 40
3.3 Improved Approximation 43
3.3.1 Improved solution of the first order problem 43
3.3.2 Improved solution of the second order problem 46
3.4 Conclusion 47

4 Numerical Method **48**
4.1 Finite Difference Method 48
4.1.1 Navier-Stokes Equations 48
4.1.2 Method 51
4.2 Numerical Methodology for Direct Simulation of the Navier-Stokes equations 54
4.2.1 Navier-Stokes Equations 54
4.2.2 Method 55

5 Numerical Results **57**
5.1 Results 57
5.2 Comparison of the Analytical and Numerical Results of the stream function 62
5.3 Comparison of the numerical results of the direct numerical simulation (DNS) and finite difference method (FDM) 69
5.4 Conclusion 80

6 Stability Analysis **81**
6.1 Von Neumann Stability Analysis 81
6.2 Results 85
6.3 Conclusion 88

7 Conclusion **89**

A Algorithms **93**
A.1 Analytical Code for ψ_0 93
A.2 Analytical Code for ψ_1 94
A.3 Numerical Code for Ψ 95

References **107**

List of Figures

1 The streamlines illustrating the zeroth order flow of fluid around the sphere. 27
2 The streamlines illustrating the flow of fluid around the sphere for ψ up to ψ_1 at Re = 0.50 32
3 The streamlines illustrating the flow of fluid around the sphere for ψ up to ψ_1 at Re = 3.00 33
4 Streamlines for flow around the sphere for Oseen solution at Re = 0.30 42
5 Streamlines illustrating the flow past a sphere for the improved solution of ψ up to ψ_1 at Re = 0.50. 44
6 Streamlines illustrating the flow past a sphere for the improved solution of ψ up to ψ_1 at Re = 3.00. 45
7 Streamlines illustrating the flow past a sphere for the improved solution of ψ up to ψ_2 at Re = 0.50 46
8 The graph shows that ξ gets to 1 quickly. ξ gets closer to 1 before r gets to 10. 49
9 Streamlines for Ψ up to Ψ_1 for various values of Reynolds numbers using 40×40 grid points for r interval [1, 3.30259] (ξ interval [0, 0.9]). 57
10 Streamlines for Ψ up to Ψ_1 using 80×80 grid points for r interval [1, 3.30259] (ξ interval [0, 0.9]). 58
11 Streamlines for Ψ up to Ψ_5 for various values of Reynolds numbers using 80×80 grid points for r interval [1, 3.30259] (ξ interval [0, 0.9]). 59
12 Streamlines for Ψ up to Ψ_{10} for various values of Reynolds numbers using 80×80 grid points for r interval [1, 3.30259] (ξ interval [0, 0.9]). 60
13 Streamlines for Ψ up to Ψ_{10} for various values of Reynolds numbers using 80×80 grid points for$r$ interval [1, 10.2103] (ξ interval [0, 0.9999]) 61
14 Streamlines of the analytical results for various values of Reynolds numbers using 40×40 grid points. 67
15 Streamlines of the numerical results for various values of Reynolds numbers using 40×40 grid points. 68
16 Streamlines of the direct numerical simulation (DNS) results for various values of Reynolds numbers using 40×40 grid points for $r = 3.30259$. 78

17 Streamlines of the finite difference method (FDM)results for various values of Reynolds numbers using 80×80 grid points for $r = 3.30259$ 79
18 Region plot for $\delta\xi = 0.1$ and $\delta\mu = 0.22$ at various Reynolds numbers. The stable region is blue and unstable is white. . . . 85
19 Region plots for $\delta\xi = 0.0230769$ and $\delta\mu = 0.0507692$ at various Reynolds numbers. The stable region is blue and unstable is white. 86
20 Region plot for $\delta\xi = 0.0113924$ and $\delta\mu = 0.0250633$ at various Reynolds numbers. The stable region is blue and unstable is white. 87

List of Tables

1 Comparison of the analytical ($\psi_0 + Re\psi_1$) and numerical ($\Psi_0 + Re\Psi_1$) results of the stream function for $Re = 0.01$. The analytical values are in bold font and numerical values in normal font. The vertical and horizontal values represents θ and r respectively. 63

2 Comparison of the analytical ($\psi_0 + Re\psi_1$) and numerical ($\Psi_0 + Re\Psi_1$) results of the stream function for $Re = 1.00$. The analytical values are in bold font and numerical values in normal font. The vertical and horizontal values represents θ and r respectively. 64

3 Comparison of the analytical ($\psi_0 + Re\psi_1$) and numerical ($\Psi_0 + Re\Psi_1$) results of the stream function for $Re = 10.00$. The analytical values are in bold font and numerical values in normal font. The vertical and horizontal values represents θ and r respectively. 65

4 Comparison of the analytical ($\psi_0 + Re\psi_1$) and numerical ($\Psi_0 + Re\Psi_1$) results of the stream function for $Re = 50.00$. The analytical values are in bold font and numerical values in normal font. The vertical and horizontal values represents θ and r respectively. 66

5 Comparison of the direct numerical simulation (DNS) and finite difference method (FDM) results of the radial velocity (V_r) for $Re = 0.01$. The DNS values are in bold font and FDM values in normal font. The vertical and horizontal values represents θ and r respectively. 70

6 Comparison of the direct numerical simulation (DNS) and finite difference method (FDM) results of the tangential velocity (V_θ) for $Re = 0.01$. The DNS values are in bold font and FDM values in normal font. The vertical and horizontal values represents θ and r respectively. 71

7 Comparison of the direct numerical simulation (DNS) and finite difference method (FDM) results of the radial velocity (V_r) for $Re = 1.00$. The DNS values are in bold font and FDM values in normal font. The vertical and horizontal values represents θ and r respectively. 72

8 Comparison of the direct numerical simulation (DNS) and finite difference method (FDM) results of the tangential velocity (V_θ) for $Re = 1.00$. The DNS values are in bold font and FDM values in normal font. The vertical and horizontal values represents θ and r respectively. 73
9 Comparison of the direct numerical simulation (DNS) and finite difference method (FDM) results of the radial velocity (V_r) for $Re = 10.00$. The DNS values are in bold font and FDM values in normal font. The vertical and horizontal values represents θ and r respectively. 74
10 Comparison of the direct numerical simulation (DNS) and finite difference method (FDM) results of the tangential velocity (V_θ) for $Re = 10.00$. The DNS values are in bold font and FDM values in normal font. The vertical and horizontal values represents θ and r respectively. 75
11 Comparison of the direct numerical simulation (DNS) and finite difference method (FDM) results of the radial velocity (V_r) for $Re = 50.00$. The DNS values are in bold font and FDM values in normal font. The vertical and horizontal values represents θ and r respectively. 76
12 Comparison of the direct numerical simulation (DNS) and finite difference method (FDM) results of the tangential velocity (V_θ) for $Re = 50.00$. The DNS values are in bold font and FDM values in normal font. The vertical and horizontal values represents θ and r respectively. 77

Glossary

Stream Function Approach (SFA) - Navier-Stokes equations via the stream function formulation.

Finite Difference Method (FDM) - Finite difference method that approximates the solution of the stream function.

Direct Numerical Simulation (DNS) - Direct numerical simulation that solves the full Navier-Stokes equations.

Homotopy Analysis Method (HAM) - A method that solves nonlinear partial differential equations in fluid mechanics.

Large Eddy Simulation (LES) - A mathematical model used in fluid mechanics.

Charles David Pierce (CDP) - Finite volume solver created by Charles David Pierce at the Stanford University

List of Symbols

$\underline{V}$	-	Velocity vector
U	-	Characteristic speed
P	-	Pressure
a	-	Characteristic length
∇	-	Nabla
ρ	-	Uniform density
ν	-	Kinematic viscosity
V_r	-	Radial Velocity
V_θ	-	Tangential Velocity
V_ϕ	-	Velocity in the ϕ direction.
Re	-	Reynolds Number
ω	-	Vorticity of the flow
ψ	-	Stokes Stream Function
n	-	Unit vector in the direction of the Mainstream Flow
Φ	-	Oseen Stream Function
p	-	Oseen variable
Ψ	-	Approximation to the Stokes Stream Function
$N\xi$	-	Step size change in the i direction
$N\mu$	-	Step size change in the j direction
Ψ_t	-	Sum of the terms of Ψ
$\underline{r}$	-	Radial coordinate of the position vector.
θ	-	Azimuthal angle in spherical coordinates.
ϕ	-	Zenith angle in spherical coordinates.

1 Introduction

The slow viscous incompressible flow has been investigated in numerous parts of science and engineering. It is governed by the conservation of momentum and mass. The mass and conservation of momentum equations for an incompressible fluid of constant density and viscosity leads to the continuity and Navier-Stokes equations of motion. The Navier-Stokes equations contains the velocity of the flow, pressure, density, kinematic viscosity, characteristic length and the Reynolds number. When the Reynolds Number is small, the flow is called the slow viscous incompressible flow. The Reynolds number is given by $Re = Ua/\nu$ where U is the characteristic speed, a is the characteristic length and ν is the viscosity. The Reynolds number is small when the viscosity is large or the length a is small.

The Navier-Stokes equations are used to model the flow through porous medium, pump design, chemical reactor behavior, aircraft flight component design, atmospheric events and weather patterns [1]. The Navier-Stokes equations are also considered to be a good model for the flow of blood in heart, arteries and veins. The flow of blood is also governed by the continuity equation [2]. The equations are also used in rivers, circulatory systems, respiratory systems and air conditioning systems.

The problem of slow viscous incompressible flow past a sphere was first investigated by Stokes [3]. He obtained the solution of flow past a sphere by neglecting the inertia of fluid. He obtained the solution for small Reynolds number where the viscous forces are greater than inertial forces. Whitehead [4] attempted to solve the problem by obtaining higher approximations when the Reynolds number is not negligibly small. He developed an iterative procedure that calculates the inertial terms in the equation of motion for lower order approximations. The iterative procedure involved the expansion of the flow in powers of the Reynolds number since the boundary conditions at each stage of the iteration are independent of the Reynolds number. He established that the second approximation of the velocity remains finite at infinity and does not satisfy the boundary condition at infinity. Higher approximations to the velocity distribution diverge at infinity [5]. The breakdown of the expansion of the flow in powers of the Reynolds number is called the Whitehead Paradox.

The Whitehead Paradox was resolved by Oseen [6]. He investigated the source of non-uniformity by linearising the inertia term far from the sphere. He showed that the approximation of velocity and its derivatives is a linear problem and it can be solved analytically. The problem was later investigated by Kaplun and Lagerstrom [7] who introduced the method of singular pertubation method/matched asymptotic expansions. The method was then used by Proudman and Pearson [5] to obtain higher approximations to the flow past the sphere and a circular cylinder. Proudman and Pearson [5] noted that the Oseen expansion is uniformly valid along the whole flow and each successive term does not give a higher uniform approximation but it is always possible to find a finite number of terms which give to any required accuracy, a uniform approximation to the solution.

Van Dyke [8] presented the solution of viscous flow at low Reynolds numbers. He matched the Stokes expansion with the Oseen expansion to present a resolution of the Whitehead paradox using the method of matched asymtotic expansions. Many authors used the method of matched asymptotic expansions and pertubation to solve fluid mechanics problems. Gajjar [9] also discussed the incompressible fluid flows at low Reynolds numbers. He considered Stokes flow past a cylinder and sphere by expressing the Navier-Stokes and continuity equations in terms of the stream function and vorticity of the flow. He then used the asymptotic expansions and pertubation methods to find the solution of the first and second order problems. He also provided the resolution of the Whitehead paradox by matching the Stokes expansion to the Oseen expansion as given by Van Dyke [8]. The method was also used by Kohr [10] to solve the governing equations of the low Reynolds number flow of an incompressible fluid past a cylinder. Datta and Singhal [11] extended the problem by presenting a solution of the steady flow past a sphere with a source at its centre. The Reynolds number was assumed to be small so that the inertia of the fluid can be neglected. He also used the matched asymptotic method to solve the Navier-Stokes equations in terms of the stream function and vorticity. He defined the Stokes expansion as the inner expansion and Oseen expansion as the outer expansion. He then used the inner and outer expansions to find the undetermined constants in both expansions. He was able to find higher order approximations and also evaluated the $\mathrm{O}(R^2 \log R)$ terms in the inner expansion. Other authors used the matched asymptotic expansions method to solved the Navier-Stokes equations for fluid flows past a cylinder. Umemura [12] studied the low Reynolds number flow past two cylinders using the method of matched asymptotic expansions.

Srivastava et al. [13] presented an analytical approach for Oseen's flow past a deformed sphere. The Brenner's formula was used to calculate Oseen's correction to the Stokes drag on a deformed sphere. The results were found to be in agreement with the results from existing literature. An analytical solution for viscous incompressible Stokes flow in spherical shell was also presented by Thieulot [14]. He obtained a solution that is depended on the assumption that the pressure, velocity, viscosity and density satisfies the equations of the flow at every point.
Stokes flow problems were also solved using the Brinkman's model in the past. Higdon and Kojima [15] used Brinkman's [16] equations to study Stokes flow past porous particles. They obtained the asymptotic results using Green's functions for small and large permeabilities. Brinkman's model was also used by Padmavathi et al. [17] to model the Stokes flow past a porous particle. They considered the Stokes flow to be non-axisymmetric and the governing equations were described by the Brinkman's model. The boundary conditions were defined by the continuity of stress and velocity components at the surface of the sphere. They then used Faxen's law to calculate the torque and drag on the sphere. The results are comparable to existing literature and are similar to the results that were obtained by Higdon and Kojima.

Housiadas et al. [18] investigated the creeping flow past a sphere with pressure-dependent viscosity. The governing equations were described by the continuity equation and momentum balance. A regular perturbation scheme was used to solve the governing equations where the dimensionless viscosity-pressure coefficient is the small parameter of perturbation. They found that the solution exist only for the three-dimensional simple shear case and it does not exist for the axisymmetric sedimentation case. The analytical solution of a highly viscous flow past a compound particle was investigated by Zhao [19]. He considered a uniform flow past a sphere with a rigid kernel and a fluid coating. He also derived the stream function and analysed the contours of the stream function. The results indicated that a spherical object covered with a fluid coating experiences less drag than a pure rigid sphere.
The homotopy analysis method has been used to solve nonlinear partial differential equations in fluid mechanics. Ragab et al. [20] used the homotopy analysis method to find the solution of the time-fractional Navier-Stokes equations. The results indicated that the homotopy analysis method is powerful and efficient in solving nonlinear fractional partial differential equations. Murthy and Kumar [21] also obtained the solution for the stream function and vorticity using the Homotopy Analysis Method (HAM) and the expansion of Gegenbauer polynomials. The nonlinear momentum equation for stream function was solved using the Homotopy Analysis Method and the

stream function was taken in terms of the Gegenbauer polynomials to match the uniform flow far away from the sphere.

Some of the authors used the operator splitting methods to provide the solution of the Navier-Stokes equations. Bristeau et al. [22] discussed the numerical solution of the Navier-Stokes equations. They considered both incompressible and compressible viscous fluid flows past any geometry. The solution of the incompressible fluid was found using the time discretization by operator splitting methods. The method allowed them to bypass the difficulties of the problem. The problem was difficult to solve because the fluid is incompressible and the governing equations are nonlinear. They also used the time discretization by operator splitting method to solve the compressible Navier-Stokes equations. The results showed that the time discretization by operator methods is efficient and accurate for the incompressible flow and it may still be efficient for compressible flows. Li and Li [23] also presented the solution of the Navier-Stokes equations using operator splitting methods. The Navier-Stokes equations were solved with a nonlinear slip boundary conditions. The numerical results indicated that the Navier-Stokes equations with the nonlinear slip conditions must be solved using large time steps. Recently, Djoko and Koko [24] also studied the Navier-Stokes equations with the threshold slip boundary conditions. They solved the Navier-Stokes system using the combination of time discretization by operator splitting, augmented Lagrangian and finite element approximation method.

The finite difference method is a numerical method that is used to solve partial differential equations by approximating the derivatives in the equations. The method is easy to implement for rectangular domains and circles or annulus but it can be difficult to implement for complicated geometries. Many authors used the finite difference method to solve the Navier-Stokes equations for incompressible or compressible fluid flows past a sphere. Chorin [25] developed the finite difference method to solve the Navier-Stokes equations for an incompressible fluid. The Navier-Stokes equations were expressed in terms of velocity and pressure. The results showed that the finite difference method is able to solve problems in two and three dimensional space. Christov and Volkov [26] presented the numerical solution of the steady viscous flow past a stationary deformable bubble. They introduced a coordinate transformation so that the unknown region is mapped to a known region. Infinity was moved to a large value that satisfies the boundary conditions. The Navier-Stokes equations were solved using the second-order difference scheme for a range of Reynolds and Webber numbers. The results are comparable to experimental and theoretical results. Fornberg [27] also presented the nu-

merical solution of the steady incompressible flow past a sphere. The equations of motion were described by the steady-state Navier-Stokes equations. He expressed the Navier-Stokes equations in terms of the stream function and the vorticity of the flow in cylindrical coordinates and used the centred second-order finite differences to approximate the solution. He applied the boundary conditions at the surface of the body and axis of symmetry. The results suggested that the wake takes the form of a Hill's spherical vortex. The second-order finite difference scheme was also used by Zhang [28] to solve the steady Navier-Stokes equations in primitive variables in a driven cavity. He applied the combination of the second-order backward and forward difference to discretize the nonlinear terms and the usual second-order centred differences to discretize the linear terms. The system of equations was then solved using a multi grid method. The results were found to be in agreement with the vorticity-stream function results. Later on, Juncu [29] obtained the numerical solution of the steady viscous flow past a fluid sphere using the finite difference method for external Reynolds numbers up to 500. He also expressed the Navier-Stokes equations in terms of the dimensionless stream-function and vorticity in spherical coordinates. He considered the fluid to be newtonian and the flow to be laminar, axisymmetric and steady. He then used the second-order finite difference scheme to approximate the solution because second-order schemes predicts the flow accurately. The results that were presented showed that the finite difference scheme converged for all Reynolds numbers and the convergence rate of the finite difference scheme decreases as the Reynolds number decreases. The results are also comparable to the solution that was provided by published predictive equations. The finite difference method was also used by Johnston and Liu [30] to approximate the solution of the unsteady incompressible Navier-Stokes equations based on local pressure boundary conditions. The second-order numerical scheme was based on the velocity-pressure formulation because it is suitable for Reynolds numbers from moderate to large. The results showed that method is feasible and effective. Lai [31] developed a fourth-order finite difference scheme to solve the incompressible Navier-Stokes equations in a disk. He expressed the Navier-Stokes equations in terms of the vorticity and stream function. The results were found to be in good agreement with previous authors results. Li and Wang [32] also solved the incompressible Navier-Stokes equations using the fast finite difference method on a irregular domains. They expressed the Navier-Stokes equations in terms of vorticity and stream function and solved the Navier-Stokes equations numerically using a Cartesian grid. The Cartesian grid is good for solving problems with complex geometry. The Poisson equation was then solved on the irregular domain using the Poisoon solver which is based on the fast immersed inter-

face method. Numerical results showed that the finite difference scheme is second-order accurate. De Angeli et al. [33] presented a numerical solution for incompressible fluid flows using the finite difference method which was designed for parallel computing platforms. The results indicated that the parallel code improves the efficiency for large-scale simulations. A numerical method was presented by Quadrio and Luchini [34] for the direct numerical simulation of the incompressible Navier-Stokes equations on a parallel computer. The numerical method uses the commodity hardware that is designed for efficient shared-memory and distributed-memory parallel computing. It also uses the finite difference schemes and Fourier expansions. They used the finite difference scheme in the wall-normal direction and the Fourier expansions in the homogeneous direction. Svärd et al. [35] constructed a stable high-order finite difference scheme to solve the compressible Navier-Stokes equations. They found that the finite difference schemes have second, third, fourth and fifth-order accuracy. Usov [36] proposed a semi-implicit finite difference scheme to solve the Navier-Stokes equations for nonlinear viscous compressible flow. The scheme reduces computational costs. Mcgee and Seshaiyer [37] presented a numerical solution for coupled flow interaction transport models. They used the Navier-Stokes equations to model the blood flow in the vessel and Darcy's flow to model the plasma flow through the vessel wall. They used the finite difference method to discretize the coupled equations and the Schwarz method to solve the resulting system of equations. Kumar and Rajathy [38] investigated the flow of steady incompressible viscous electrically conducting fluid past a sphere using the finite difference method. The fluid was in the presence of a uniform magnetic field parallel to the undisturbed flow. Reis et al. [39] presented a numerical solution of the incompressible Navier-Stokes equations using an exact projection method. They used the fourth-order compact finite difference scheme to discretize the boundary conditions and the Poisson equation that followed from the projection method. The results indicated that the method converges and were verified through analytical solutions and manufactured techniques.

The Runge-Kutta method is also efficient for solving the Navier-Stokes equations. Sterner [40] used the Runge-Kutta method to solve the Navier-Stokes equations. He used a semi-implicit Runge-Kutta scheme by combining the explicit time-integration in the direction of the stream with the implicit integration in the body normal direction. The flow of an incompressible viscous fluid past a sphere was also investigated by Johnson and Patel [41]. They solved the Navier-Stokes equations using a four-stage Runge-Kutta method and investigated the problem experimentally over flow regimes. The results were found to be in agreement with previous studies.

The immersed boundary method is also used to solve the Navier-Stokes equations. The method was developed by Peskin [42] and it has been used by several authors to simulate flow problems including flow patterns in the heart. Campregher et al. [43] used an immersed boundary method to present the computations of the flow past a still sphere for moderate Reynolds numbers. They used the momentum equation to calculate the Lagrangian forces field by applying the no-slip condition indirectly. They also used the virtual physical model which was proposed by Silva et al. [44] in 2003 to evaluate the force field using the flow of momentum equation. They remodelled the version of the virtual physical model by extending it to 3D domains. The codes is able to solve the Navier-Stokes equations which requires large memories and it is also able to do parallel processing. The results are found to be in good agreement with data from existing literature. Muhammad and Shah [45] calculated the slow flow past the sphere using the direct boundary element method. They discretized the surface of the sphere into quadrilateral elements and applied the direct boundary element method to calculate the creeping flow solution around the sphere. The results were found to be comparable with the analytical approximations. Poon et al. [46] investigated the flow past a stationary and rotating sphere at high Reynolds numbers using the finite volume solver CDP. The finite volume solver CDP was created by Charles David Pierce at the Stanford University. The governing equations of the fluid are described by the incompressible Navier-Stokes equations. They performed a direct numerical simulation (DNS) for Re = 250 and 1000 because it is computationally expensive to directly compute the Navier-Stokes equations as Reynolds number increases. They used a large eddy simulation (LES) modelling approach for Re = 10000 to minimize the computation cost. The LES method was developed in 1963 by Smagorinsky [47] but was only used in engineering in the early 90's. Large eddies were captured by the LES method while the mathematical model was used to approximate the small-scale homogeneous motions. The results are in agreement with the available data from literature for both the stationary and rotating sphere.

The finite element method is one of the prominent numerical techniques that have been developed to solve partial differential equations. The method has been used by many authors to solve the Naveir-Stokes equations. Mikulencak and Morris [48] presented the numerical solutions of stationary shear flows past free and fixed bodies for a range of Reynolds numbers. The flow is described by the steady Navier-Stokes equations as governing equations. They used a finite element method to approximate the solutions of the Navier-Stokes equations. They used the Newton's method to solve the two-

dimensional problems and an iterative solver to solve the three-dimensional problems. The iterative solver was used to resolve the non-linearity of the three-dimensional problem by employing a conjugate gradient linear solver with a non-linear least-squares conjugate gradient method. The results are comparable to the asymptotic low Reynolds number theory and experimental results from previous studies. A multiscale finite difference method was used by Masud and Khurram [49] to solve the incompressible Navier-Stokes equations. They decomposed the velocity field into fine-scales and coarse. They also introduced the model for the fine-scale velocity to correct the lack of stability of the Galerkin formulation of the Navier-Stokes equations. The stability analysis showed that the method exhibits good stability and accuracy. Li et al. [50] also used the finite element method to solve the transient Navier-Stokes equations. The method was based on two local Gauss integrations and the lowest equal-order pair of finite elements. The results indicated that the numerical tests are in good agreement with theoretical results and the method is accurate and stable. Aigo [51] also presented the numerical solution of the Navier-Stokes equations. He used the projection and finite element method to solve the Navier- Stokes equations. He solved the Navier-Stokes equations using the projection method which is based on projection technique and finite element method. He also used the control volume approach method to find the solution of the Navier-Stokes equations. The results showed that methods will improve the computational results. Camano et al. [52] presented a new fixed finite element method to solve the Navier-Stokes equations. They considered an incompressible fluid with variable viscosity and constant density. They produced numerical results that indicated good perfomance of the augmented mixed finite element method. Danilov et al. [53] used the finite element method to solve the Navier-Stokes equations in a time-dependent domain. The finite element method was also used by Abdelwahed et al. [54] to solve the Navier-Stokes equations. They express the Navier-Stokes equations in terms of the stream function and vorticity. They used a parallel numerical algorithm to optimize the computing time.

The finite volume method is one of the methods that are used to solve partial differential equations. It has been used in many problems of fluid mechanics. Boivin et al. [55] studied the incompressible flows on unstructured meshes. They solved the Navier-Stokes equations using the finite volume method and fractional time step scheme. Chandrashekar [56] also used the finite method to discretize the heat equation and compressible Navier-Stokes equations. He applied a weak Dirichlet boundary conditions on the temperature and velocity. The results indicated that the iterative converged better when weak

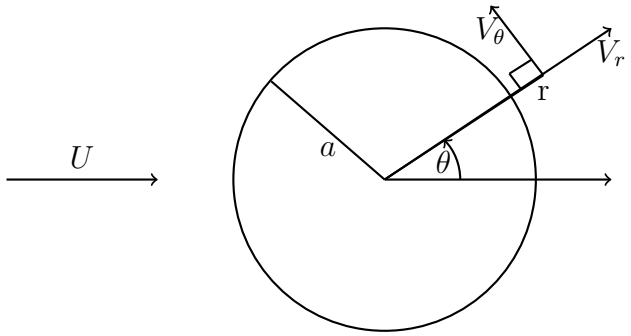
boundary conditions are applied on temperature and velocity. Sadikin et al. [57] presented the unsteady three dimensional flow simulation around a sphere using a numerical simulation computational fluid dynamic. The flow regimes and separation around the sphere were analyzed for Reynolds numbers between 20 and 500. They found that the behaviour of the flow changes and the flow separates as the Reynolds number increases. Verman [58] analyzed the incompressible Navier-Stokes equations using an explicit staggered projection method. He replaced the continuity equation with the Poisson equation and used the projection method to resolve issues that were related to the pressure boundary condition. Krasnov et al. [59] presented the numerical solution of the Navier-Stokes equations by using the discontinuous Galerkin method. The results are in good agreement with existing numerical data and experimental results. Langtangen et al. [60] also presented the numerical methods for incompressible Navier-Stokes equations. The methods includes finite differences, finite volumes , spectral and finite element methods. They mentioned that the lattice gas or lattice Boltzman methods can also be used to compute incompressible viscous flow.

The simulation of a sphere with a small radius through an incompressible viscous fluids was presented in 2003 by Valladares et al. [61]. The forces acting on the sphere were due to gravity, buoyancy and viscocity. Stokes calculation for the drag force was used and the stochastic force was proposed which depended on the temperature. The governing equations of the sphere through the viscous fluid were given by a Langevin type equation. The Langevin type equations were solved numerically by using the Verlet algorithm. Wilson [62] presented the numerical solution of the Stokes flow past three spheres. The numerical method was based on the method of reflections and Lamb's solution to the Stokes flow. The governing equations were described by the incompressible Navier-Stokes equations and the boundary conditions were applied on the spheres velocity and angular velocity for each sphere or on the external force and torque acting on each sphere. The general solution of the Navier-Stokes equations was presented using Lamb's solution in spherical polar coordinates. The results were comparable to existing literature based on the Stokesian Dynamics.

The aim of the research is to review the problem of flow past a sphere and solve the Navier-Stokes equations via the stream function approach. We attempt to derive the solution that was obtained by Stokes using the analytical methods, via symbolic computation as well as numerical methods in the form of explicit finite difference method. It is important to understand the solution that was derived by Stokes. We also analyse the problems encountered by Whitehead in his attempt to obtain higher approximations when the Reynolds number is not small. We do a full review of the work done by Oseen to solve the Whitehead paradox. We use the finite difference method in terms of the stream function, for various values of Re with the aim of investigating the validity of the solution as Re approaches unity. Lastly, we generate code to numerically solve and plot solutions for higher moments of stream function and we perform stability analysis of the finite difference method utilised here. We compare the finite difference method (FDM) solution of the stream function with the direct numerical simulation (DNS) solution of the full Navier-Stokes equations.

2 Governing Equations

We consider a slow viscous incompressible fluid flow past a sphere of radius a. We choose the spherical coordinates (r, θ, ϕ) with the origin at the centre of the sphere. The axis $\theta = 0$ is chosen to lie in the direction of the free stream velocity U. The body force due to gravity is neglected. The physical components of the velocity are V_r, V_θ and V_ϕ. The flow is symmetric about the axis $\theta = 0$, there is no change in the variable in the ϕ direction. $V_r = V_r(r, \theta)$, $V_\theta = V_\theta(r, \theta)$ and $V_\phi = 0$.



2.1 Stokes Approximation

2.1.1 Navier-Stokes and continuity equations

The Navier-Stokes and continuity equations for steady state are given by equations (2.1.1) and (2.1.2) where the velocity and pressure is $\underline{V}$ and P respectively. In equation (2.1.2), ρ is the uniform density and ν is kinematic viscosity of the incompressible fluid. The form of equation (2.1.1) is due to the incompressibility of the fluid. The Navier-Stokes and continuity equations are defined as:

$$\underline{\nabla} \cdot \underline{V} = 0, \tag{2.1.1}$$

$$(\underline{V} \cdot \underline{\nabla})\, \underline{V} = -\frac{1}{\rho} \underline{\nabla} P + \nu \nabla^2 \underline{V}, \tag{2.1.2}$$

subject to the boundary conditions below.

• The no slip boundary condition at the surface of the sphere ($r = 1$). It implies that there is no velocity in the θ direction and since the fluid catches to the surface due to viscosity, the boundary condition is defined by

$$V_\theta(1, \theta) = 0. \tag{2.1.3}$$

• The no cavities form boundary condition at the surface of the sphere ($r = 1$). It implies that the fluid cannot move radially away from the surface of the sphere as this would cause cavities (regions where there is no fluid i.e a vacuum). Thus the boundary condition on the radial velocity must be given by

$$V_r(1, \theta) = 0. \tag{2.1.4}$$

• Boundary condition far from the sphere as $r \to \infty$. The boundary condition as $r \to \infty$ must be given by the mainstream velocity. Then boundary condition far from the sphere is given by

$$\underline{V_r} = U \cos\theta \tag{2.1.5}$$

and

$$\underline{V_\theta} = -U \sin\theta. \tag{2.1.6}$$

We now write the equations in dimensionless form by defining the following

$$\overline{V} = \frac{V}{U}, \tag{2.1.7}$$

$$\overline{P} = \frac{P}{pU^2}, \tag{2.1.8}$$

$$\overline{r} = \frac{r}{a}. \tag{2.1.9}$$

where U is the mainstream velocity far from the sphere and $\underline{r}$ is the radial coordinate of the position vector.

The Reynolds number is given by

$$Re = \frac{Ua}{\nu}. \tag{2.1.10}$$

The Reynolds number is a non-dimensional parameter which gives a measure of the ratio of inertial to viscous forces [9]. The inertial forces are neglected for Stokes flow which is also known as creeping flow and the Reynolds number is very small.

By substituting (2.1.7), (2.1.8) and (2.1.9) into (2.1.1) and (2.1.2), we obtain

$$\overline{\nabla} \cdot \overline{V} = 0, \tag{2.1.11}$$

$$\left(\overline{V} \cdot \overline{\nabla}\right) \overline{V} = -\overline{\nabla}\, \overline{P} + \frac{1}{Re} \nabla^2 \overline{V}. \tag{2.1.12}$$

By suppressing the overhead bars then the Navier-Stokes and continuity equations in dimensionless form are

$$\nabla \cdot V = 0, \tag{2.1.13}$$

$$(V \cdot \nabla)\, V = -\nabla P + \frac{1}{Re} \nabla^2 V. \tag{2.1.14}$$

The vorticity of the flow is the curl of the velocity field and it is defined as

$$\omega = \nabla \times V. \tag{2.1.15}$$

It describes the local rotation of the flow and it is perpendicular to the plane of the fluid flow. A region of the flow is irrotational when $\omega = 0$ and flows that are initially irrotational remain irrotational if all forces that are acting on the flow are conservative [63].

We use vector identities to define

$$(V \cdot \nabla)\, V = \nabla(\frac{1}{2} V^2) - V \times (\nabla \times V), \tag{2.1.16}$$

$$\nabla^2 V = \nabla(\nabla \cdot V) - \nabla \times (\nabla \times V). \tag{2.1.17}$$

By using (2.1.16) and (2.1.17) then equation (2.1.14) becomes

$$\underline{\nabla}(\frac{1}{2}V^2) - \underline{V} \times (\underline{\nabla} \times \underline{V}) = -\underline{\nabla}P + \frac{1}{Re}\left(\underline{\nabla}(\underline{\nabla} \cdot \underline{V}) - \underline{\nabla} \times (\underline{\nabla} \times \underline{V})\right) \tag{2.1.18}$$

We substitute (2.1.15) into equation (2.1.18) and use the incompressible condition (2.1.13) to get

$$\underline{\nabla}(\frac{1}{2}V^2) - \underline{V} \times \underline{\omega} = -\underline{\nabla}P - \frac{1}{Re}(\underline{\nabla} \times \underline{\omega}) \tag{2.1.19}$$

Rearrange equation (2.1.19) to get

$$\underline{\nabla} \times \underline{\omega} = Re(\underline{V} \times \underline{\omega} - \underline{\nabla}(P + \frac{1}{2}V^2)) \tag{2.1.20}$$

We now apply $\underline{\nabla}\times$ on (2.1.20) to get

$$\underline{\nabla} \times \underline{\nabla} \times \underline{\omega} = Re(\underline{\nabla} \times \underline{V} \times \underline{\omega} - \underline{\nabla} \times \underline{\nabla}(P + \frac{1}{2}V^2)). \tag{2.1.21}$$

We use

$$\underline{\nabla} \times (\underline{\nabla}V) = 0, \tag{2.1.22}$$

then (2.1.21) becomes

$$\underline{\nabla} \times (\underline{\nabla} \times \underline{\omega}) = Re\underline{\nabla} \times (\underline{V} \times \underline{\omega}), \tag{2.1.23}$$

where the left hand side is the dimensionless viscous term and the right hand side is the inertia term. Equation (2.1.23) is required in order to be able to solve for the velocity of the flow.

We introduce the stream function in terms of the velocity of the incompressible fluids as the Stokes's stream function which is defined by ψ. The velocity components are

$$\underline{V} = V_r \, \underline{e}_r + V_\theta \, \underline{e}_\theta + V_\phi \, \underline{e}_\phi, \tag{2.1.24}$$

where $\underline{e}_r$, $\underline{e}_\theta$, $\underline{e}_\phi$ are unit base vectors in spherical coordinates. The flow is symmetric about the axis $\theta = 0$ and there is no flow in the ϕ direction.

Hence

$$V_r = V_r(r, \theta), \tag{2.1.25}$$
$$V_\theta = V_\theta(r, \theta), \tag{2.1.26}$$
$$V_\phi = 0. \tag{2.1.27}$$

The stream function in terms of the velocity components is defined as

$$V_r = \frac{1}{r^2 \sin\theta} \frac{\partial \psi}{\partial \theta}, \tag{2.1.28}$$
$$V_\theta = -\frac{1}{r \sin\theta} \frac{\partial \psi}{\partial r}. \tag{2.1.29}$$

Then

$$\underline{V} = \frac{1}{r^2 \sin\theta} \frac{\partial \psi}{\partial \theta} \, \underline{e}_r - \frac{1}{r \sin\theta} \frac{\partial \psi}{\partial r} \, \underline{e}_\theta. \tag{2.1.30}$$

The continuity equation is identically satisfied.

We now express the vorticity in terms of the stream function $\psi(r, \theta)$,

$$\underline{\omega} = \underline{\nabla} \times \underline{V}$$

$$= \frac{1}{r^2 \sin\theta} \begin{vmatrix} \underline{e}_r & r\ \underline{e}_\theta & r\sin\theta\ \underline{e}_\phi \\ \frac{\partial}{\partial r} & \frac{\partial}{\partial \theta} & \frac{\partial}{\partial \phi} \\ V_r(r,\theta) & r\ V_\theta(r,\theta) & 0 \end{vmatrix}$$

$$= \frac{1}{r^2 \sin\theta} \left(\frac{\partial}{\partial r}\left(r\ V_\theta\right) - \frac{\partial}{\partial \theta} V_r \right) r \sin\theta\ \underline{e}_\phi$$

$$= -\frac{1}{r\sin\theta} \left(\frac{\partial^2 \psi}{\partial r^2} + \frac{\sin\theta}{r^2} \frac{\partial}{\partial \theta} \left(\frac{1}{\sin\theta} \frac{\partial \psi}{\partial \theta} \right) \right) \underline{e}_\phi$$

$$\therefore\ \underline{\omega} = -\frac{1}{r\sin\theta} D^2 \psi\ \underline{e}_\phi, \tag{2.1.31}$$

where

$$D^2 = \frac{\partial^2}{\partial r^2} + \frac{\sin\theta}{r^2} \frac{\partial}{\partial \theta} \left(\frac{1}{\sin\theta} \frac{\partial}{\partial \theta} \right). \tag{2.1.32}$$

Now we express $\underline{\nabla} \times \underline{\omega}$ in terms of the stream function,

$$\underline{\nabla} \times \underline{\omega} = \frac{1}{r^2 \sin\theta} \begin{vmatrix} \underline{e}_r & r\ \underline{e}_\theta & r\sin\theta\ \underline{e}_\phi \\ \frac{\partial}{\partial r} & \frac{\partial}{\partial \theta} & \frac{\partial}{\partial \phi} \\ 0 & 0 & r\sin\theta\ \omega_\phi \end{vmatrix}$$

$$= \frac{1}{r^2 \sin\theta} \left(\frac{\partial}{\partial \theta}(r\sin\theta\ \omega_\phi)\ \underline{e}_r - \frac{\partial}{\partial r}(r\sin\theta \omega_\phi) r\ \underline{e}_\theta \right)$$

$$= \frac{1}{r\sin\theta} \frac{\partial}{\partial \theta}(-D^2\psi)\ \underline{e}_r - \frac{1}{r\sin\theta} \frac{\partial}{\partial r}(-D^2\psi)\ \underline{e}_\theta$$

Now $\underline{\nabla} \times (\underline{\nabla} \times \underline{\omega})$ can be expressed as

$$\underline{\nabla} \times (\underline{\nabla} \times \underline{\omega}) = \frac{1}{r \sin\theta} D^4 \psi \, \underline{e}_\phi. \tag{2.1.33}$$

We finally write

$$\underline{\nabla} \times (\underline{V} \times \underline{\omega}) = \frac{1}{r^2 \sin\theta} \begin{vmatrix} \underline{e}_r & r\,\underline{e}_\theta & r\sin\theta\,\underline{e}_\phi \\ \frac{\partial}{\partial r} & \frac{\partial}{\partial \theta} & \frac{\partial}{\partial \phi} \\ V_\theta\,\omega_\phi & -rV_r\,\omega_\phi & 0 \end{vmatrix}$$

$$= \frac{1}{r^2 \sin\theta} \left(\frac{\partial}{\partial r}(-rV_r\,\omega_\phi) - \frac{\partial}{\partial \theta}(V_\theta\,\omega_\phi) \right) r \sin\theta\,\underline{e}_\phi$$

$$= \frac{1}{r^3 \sin^2\theta} \left(\frac{\partial \psi}{\partial \theta}\frac{\partial}{\partial r} - \frac{\partial \psi}{\partial r}\frac{\partial}{\partial \theta} + 2\cot\theta \frac{\partial \psi}{\partial r} - \frac{2}{r}\frac{\partial \psi}{\partial \theta} \right) D^2 \psi \, \underline{e}_\phi$$

.

Then Navier-Stokes equation in terms of the stream function is given by

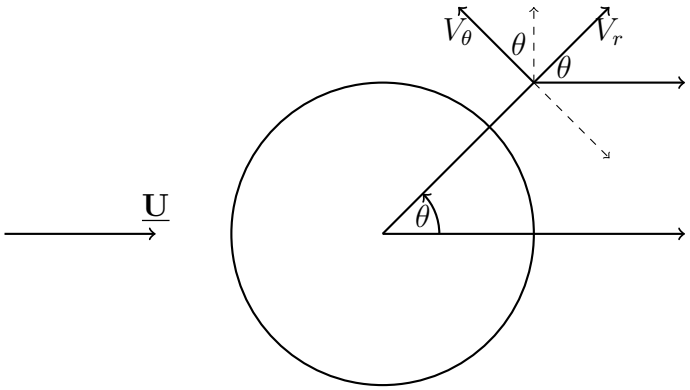
$$D^4 \psi = \frac{Re}{r^2 \sin\theta} \left(\frac{\partial \psi}{\partial \theta}\frac{\partial}{\partial r} - \frac{\partial \psi}{\partial r}\frac{\partial}{\partial \theta} + 2\cot\theta \frac{\partial \psi}{\partial r} - \frac{2}{r}\frac{\partial \psi}{\partial \theta} \right) D^2 \psi, \tag{2.1.34}$$

where

$$D^2 \psi = \frac{\partial^2 \psi}{\partial r^2} + \frac{\sin\theta}{r^2}\frac{\partial}{\partial \theta}\left(\frac{1}{\sin\theta}\frac{\partial \psi}{\partial \theta} \right). \tag{2.1.35}$$

We need to solve equation (2.1.34) to find the solution of ψ(r, θ).

2.1.2 Boundary Conditions



• The no slip boundary condition at the surface of the sphere at $r = 1$

$$V_\theta(1,\theta) = \frac{\partial \psi}{\partial r}(1,\theta) = 0. \tag{2.1.36}$$

• The no cavities form boundary condition at the surface of the sphere at $r = 1$

$$V_r(1,\theta) = \frac{\partial \psi}{\partial \theta}(1,\theta) = 0. \tag{2.1.37}$$

• Boundary condition far from the sphere as r $\to \infty$:

The free stream velocity $V = \underline{U}$ where $|\underline{U}| = 1$ in dimensionless variables.

The velocity components as $r \to \infty$ are

$$V_r = U\cos\theta, \tag{2.1.38}$$

$$V_\theta = -U\sin\theta. \tag{2.1.39}$$

Substitute (2.1.28) and (2.1.29) into (2.1.38) and (2.1.39)

$$\frac{\partial \psi}{\partial \theta} = r^2 \sin\theta\cos\theta, \tag{2.1.40}$$

$$\frac{\partial \psi}{\partial r} = r\sin^2\theta. \tag{2.1.41}$$

Integrating (2.1.41) with respect to r

$$\psi(r,\theta) = \frac{r^2}{2}\sin^2\theta + G(\theta). \tag{2.1.42}$$

Substitute (2.1.42) into (2.1.40)

$$r^2 \sin\theta \cos\theta + \frac{G(\theta)}{\partial\theta} = r^2 \sin\theta \cos\theta \tag{2.1.43}$$

We rearrange equation (2.1.43) to get

$$\frac{G(\theta)}{\partial\theta} = 0. \tag{2.1.44}$$

After integrating $G(\theta)$ with respect to θ

$$G(\theta) = C \tag{2.1.45}$$

where C is constant.

We choose $\psi(r,\theta) = 0$ because $\underline{V}$ depends only on the derivatives of ψ(r,θ) so that $C = 0$. Then

$$\psi(r,\theta) \to \frac{r^2}{2}\sin^2\theta \quad as\ r \to \infty. \tag{2.1.46}$$

2.1.3 Perturbation Expansion

We solve the Navier-Stokes equations (2.1.34) by expanding the solution in powers of Re where $Re << 1$. The expansion can be written as

$$\psi(r,\theta) = \psi_0(r,\theta) + Re\ \psi_1(r,\theta) + O(Re^2). \tag{2.1.47}$$

The Navier-Stokes equations (2.1.34) becomes

$$\begin{aligned} D^4\psi_0 + Re\ D^4\psi_1 + O(Re^2) = \frac{Re}{r^2\sin\theta}\left(\frac{\partial\psi_0}{\partial\theta}\frac{\partial}{\partial r} - \frac{\partial\psi_0}{\partial r}\frac{\partial}{\partial\theta}\right) D^2\psi_0 \\ + \frac{Re}{r^2\sin\theta}\left(2\cot\theta\frac{\partial\psi_0}{\partial r} - \frac{2}{r}\frac{\partial\psi_0}{\partial\theta}\right) D^2\psi_0 + O(Re^2). \end{aligned} \tag{2.1.48}$$

subject to boundary conditions

$$\frac{\partial\psi_0}{\partial\, r}(1,\theta) + Re\ \frac{\partial\psi_1}{\partial\, r}(1,\theta) + O(Re^2) = 0 \quad at\ r = 1, \tag{2.1.49}$$

$$\frac{\partial\psi_0}{\partial\, \theta}(1,\theta) + Re\ \frac{\partial\psi_1}{\partial\, \theta}(1,\theta) + O(Re^2) = 0 \quad at\ r = 1, \tag{2.1.50}$$

$$\begin{aligned} \psi_0(r,\theta) + Re\ \psi_1(r,\theta) + O(Re^2) = \frac{r^2}{2}\sin^2\theta \\ + Re\ O(r) \quad as\ r \to \infty. \end{aligned} \tag{2.1.51}$$

The expansion should be regarded as the expansion of the exact solution $\psi(r,\, \theta,\, Re)$ for small values of Re at a fixed value of r.

2.2 Oseen Approximation

Oseen [6] approximated the solution by linearising the inertia terms that were neglected completely by Stokes. Stokes approximation breaks down because the second approximation of the velocity remains finite at infinity and does not satisfy the boundary condition at infinity. The Navier-Stokes equations are given by (2.1.1).

Oseen [6] introduced the approximation

$$(\underline{V} \cdot \underline{\nabla})\,\underline{V} \simeq (\underline{\mathbf{U}} \cdot \underline{\nabla})\,\underline{V}, \tag{2.2.1}$$

where $\underline{\mathbf{U}}$ is the uniform stream velocity. Then equation (2.1.1) becomes

$$(\underline{\mathbf{U}} \cdot \underline{\nabla})\,\underline{V} = -\frac{1}{\rho}\underline{\nabla}P + \nu\nabla^2\underline{V}. \tag{2.2.2}$$

The Oseen's equation in dimensionless form is

$$(\underline{\mathbf{n}} \cdot \underline{\nabla})\,\underline{V} = -\underline{\nabla}P + \frac{1}{Re}\nabla^2\underline{V}, \tag{2.2.3}$$

where

$$\underline{\mathbf{n}} = \frac{\underline{\mathbf{U}}}{\mathbf{U}} = \cos\theta\underline{e}_r - \sin\theta\underline{e}_\theta, \tag{2.2.4}$$

where $\underline{\mathbf{n}}$ is a unit vector in a direction of the mainstream flow $\underline{U}$.

We write the Oseen equation in terms of the vorticity and velocity.
Using vector identities, $\underline{\nabla}(\underline{\mathbf{n}} \cdot \underline{V})$ can be expressed as

$$\underline{\nabla}(\underline{\mathbf{n}} \cdot \underline{V}) = (\underline{\mathbf{n}} \cdot \underline{\nabla})\underline{V} + (\underline{V} \cdot \underline{\nabla})\underline{\mathbf{n}} + \underline{\mathbf{n}} \times (\underline{\nabla} \times \underline{V}) + \underline{V} \times (\underline{\nabla} \times \underline{\mathbf{n}}) \tag{2.2.5}$$

and because $\underline{\mathbf{n}}$ is a constant vector then

$$(\underline{V} \cdot \underline{\nabla})\underline{\mathbf{n}} = 0, \tag{2.2.6}$$

$$\underline{\nabla} \times \underline{\mathbf{n}} = 0. \tag{2.2.7}$$

The vorticity of the flow is

$$\underline{\nabla} \times \underline{V} = \underline{\omega}. \tag{2.2.8}$$

By substituting (2.2.6), (2.2.7) and (2.2.8) into (2.2.5) we get

$$(\underline{\mathbf{n}} \cdot \underline{\nabla})\underline{V} = \underline{\nabla}(\underline{\mathbf{n}} \cdot \underline{V}) - \underline{\mathbf{n}} \times \underline{\omega}. \tag{2.2.9}$$

We use vector identities to define

$$\underline{\nabla} \times (\underline{\nabla} \times \underline{V}) = \underline{\nabla}(\underline{\nabla} \cdot \underline{V}) - \nabla^2 \underline{V}. \tag{2.2.10}$$

Since the fluid is incompressible (2.2.10) becomes

$$\nabla^2 \underline{V} = -\underline{\nabla} \times \underline{\omega}. \tag{2.2.11}$$

We substitute (2.2.9) and (2.2.11) into (2.2.3) to get

$$\underline{\nabla} \times \underline{\omega} = Re(\underline{\mathbf{n}} \times \underline{\omega} - \underline{\nabla}(\underline{\mathbf{n}} \cdot \underline{V} + P)). \tag{2.2.12}$$

We apply $\underline{\nabla}\times$ on (2.2.12) and use $\underline{\nabla} \times (\underline{\nabla} A) = 0$ to get

$$\underline{\nabla} \times (\underline{\nabla} \times \underline{\omega}) = Re \underline{\nabla} \times (\underline{\mathbf{n}} \times \underline{\omega}), \tag{2.2.13}$$

which is the Oseen equation in terms of the vorticity and velocity.

We introduce Oseen [6] variable

$$p = Re\ r, \tag{2.2.14}$$

and the stream function $\Phi(p,\theta)$. The velocity in terms of $\Phi(p,\theta)$ is given by

$$\underline{V} = \frac{Re^2}{p^2 \sin\theta}\frac{\partial \Phi}{\partial \theta}\,\underline{e}_\phi - \frac{Re^2}{p\sin\theta}\frac{\partial \Phi}{\partial p}\,\underline{e}_\theta \tag{2.2.15}$$

and the vorticity is given by

$$\underline{\omega} = -\frac{Re^3}{p\sin\theta} D^2\Phi\,\underline{e}_\phi. \tag{2.2.16}$$

We write

$$\underline{\nabla} \times (\underline{\nabla} \times \underline{\omega}) = -\frac{Re^5}{p\sin\theta} D^4\Phi\,\underline{e}_\phi, \tag{2.2.17}$$

$$\underline{n} \times \underline{\omega} = -\sin\theta\omega_\phi\,\underline{e}_p - \cos\theta\omega_\phi\,\underline{e}_\theta, \tag{2.2.18}$$

$$\underline{\nabla} \times (\underline{n} \times \underline{\omega}) = \frac{Re^4}{p\sin\theta}\left(\cos\theta\frac{\partial}{\partial p}(D^2\Phi) - \frac{\sin\theta}{p}\frac{\partial}{\partial\theta}(D^2\Phi)\right)\,\underline{e}_\phi. \tag{2.2.19}$$

Substituting (2.2.17) and (2.2.19) into (2.2.13) we get

$$D^4\Phi - \cos\theta\frac{\partial}{\partial p}(D^2\Phi) + \frac{\sin\theta}{p}\frac{\partial}{\partial p}(D^2\Phi) = 0, \tag{2.2.20}$$

which is the Oseen's equation in terms of Φ. We need to solve equation (2.2.20) to find the solution for $\Phi(p,\theta)$.

3 Analytical Method

In this section we investigate the analytical solution to the Stokes expansion version of the stream function equation.

3.1 Stokes Approximation

3.1.1 Stoke's solution for zero order problem

We derive the solution of the first order problem by solving equation (2.1.34) subject to the boundary conditions at the surface of the sphere and far away from the sphere. The zero order perturbation equation (2.1.34) becomes

$$D^4\psi_0 = 0 \tag{3.1.1}$$

and the boundary conditions (2.1.36), (2.1.37) and (2.1.46) are

$$\frac{\partial\psi_0}{\partial\, r}(1,\theta) = 0 \quad at\ r = 1, \tag{3.1.2}$$

$$\frac{\partial\psi_0}{\partial\, \theta}(1,\theta) = 0 \quad at\ r = 1, \tag{3.1.3}$$

$$\psi_0(r,\theta) \to \frac{r^2}{2}\sin^2\theta \quad as\ r \to \infty. \tag{3.1.4}$$

The boundary condition (3.1.4) suggest that solution will be of the form

$$\psi_0(r,\theta) = f(r)\sin^2\theta. \tag{3.1.5}$$

Then

$$\begin{aligned} D^2\psi_0 &= \frac{\partial^2\psi_0}{\partial r^2} + \frac{\sin\theta}{r^2}\frac{\partial}{\partial\theta}\left(\frac{1}{\sin\theta}\frac{\partial\psi_0}{\partial\theta}\right) \\ &= \frac{\partial^2(f(r)\sin^2\theta)}{\partial r^2} + \frac{\sin\theta}{r^2}\frac{\partial}{\partial\theta}\left(\frac{1}{\sin\theta}\frac{\partial(f(r)\sin^2\theta)}{\partial\theta}\right) \\ &= \sin^2\theta\frac{\partial^2 f(r)}{\partial r^2} - \frac{2\sin^2\theta}{r^2}f(r) \\ &= \sin^2\theta\left(\frac{\partial^2 f(r)}{\partial r^2} - \frac{2f(r)}{r^2}\right). \end{aligned}$$

Hence

$$D^2(D^2\psi_0) = \frac{\partial^2}{\partial r^2}\left(\sin^2\theta\left(\frac{\partial^2 f(r)}{\partial r^2} - \frac{2f(r)}{r^2}\right)\right)$$

$$+ \frac{\sin\theta}{r^2}\frac{\partial}{\partial\theta}\left(\frac{1}{\sin\theta}\frac{\partial}{\partial\theta}\left(\sin^2\theta\left(\frac{\partial^2 f(r)}{\partial r^2} - \frac{2f(r)}{r^2}\right)\right)\right) \quad .$$

$$= \left(\frac{\partial^4 f(r)}{\partial r^4} - \frac{4}{r^2}\frac{\partial^2 f(r)}{\partial r^2} + \frac{8}{r^3}\frac{\partial f(r)}{\partial r)} - \frac{8}{r^4}f(r)\right)\sin^2\theta\cos\theta$$

By substituting $D^4\psi_0$ into equation (3.1.1) we can write

$$\frac{\partial^4 f(r)}{\partial r^4} - \frac{4}{r^2}\frac{\partial^2 f(r)}{\partial r^2} + \frac{8}{r^3}\frac{\partial f(r)}{\partial r)} - \frac{8}{r^4}f(r) = 0, \tag{3.1.6}$$

this is an equidimensional equation which has a solution of the form

$$f(r) = r^\beta. \tag{3.1.7}$$

We write the derivatives of equation (3.1.7) as

$$\begin{aligned}
\frac{\partial f(r)}{\partial r} &= \beta\, r^{\beta-1} \\
\frac{\partial^2 f(r)}{\partial r^2} &= \beta(\beta-1)\, r^{\beta-2} \\
\frac{\partial^3 f(r)}{\partial r^3} &= \beta(\beta-1)(\beta-2)\, r^{\beta-3} \\
\frac{\partial^4 f(r)}{\partial r^4} &= \beta(\beta-1)(\beta-2)(\beta-3)\, r^{\beta-4}.
\end{aligned}$$

We substitute the derivatives of equation (3.1.7) into (3.1.6) then we get

$$(\beta-1)(\beta-2)(\beta-4)(\beta+1)\, r^{\beta-4} = 0 \tag{3.1.8}$$

$\therefore \beta = 1$, 2, 4 or -1. Then equation (3.1.7) becomes

$$f(r) = A\, r^4 + B\, r^2 + C\, r + \frac{D}{r} \tag{3.1.9}$$

where A, B, C,and D are constants.

We now use the boundary conditions to find the constants. By applying the boundary condition far from the sphere as $r \to \infty$

$$\psi(r,\theta) \to \frac{r^2}{2}\sin^2\theta \quad as\ r \to \infty \tag{3.1.10}$$

then we find that $A = 0$ and $B = 1/2$. We take the limit at infinity so that the solution is consistent with the boundary condition.

By applying the no slip boundary condition at the surface of the sphere

$$V_\theta(1,\theta) = \frac{\partial\psi}{\partial r}(1,\theta) = 0, \tag{3.1.11}$$

then C - D + $2B = 0$
$\therefore$ C - D= -1.

By applying the no cavities form boundary condition at the surface of the sphere

$$V_\theta(1,\theta) = \frac{\partial\psi}{\partial\theta}(1,\theta) = 0, \tag{3.1.12}$$

then $B + C + D = 0$,
$\therefore$ $D + C$ = -1/2.

$\therefore$ $A = 0$, $B = 1/2$, C= -3/4 and $D = 1/4$.

Hence

$$\psi_0 = \frac{1}{4}\left(2r^2 - 3r + \frac{1}{r}\right)\sin^2\theta. \tag{3.1.13}$$

The first term in (3.1.13) is the uniform stream $\underline{\mathbf{U}}$ because

$$V_r = \frac{1}{r^2\sin\theta}\frac{\partial}{\partial\theta}\left(\frac{1}{2}r^2\sin^2\theta\right) = \cos\theta, \tag{3.1.14}$$

$$V_\theta = -\frac{1}{r\sin\theta}\frac{\partial}{\partial r}\left(\frac{1}{2}r^2\sin^2\theta\right) = -\sin\theta, \tag{3.1.15}$$

$$\underline{V} = V_r \underline{e}_r + V_\theta \underline{e}_\theta = \cos\theta \underline{e}_r - \sin\theta \underline{e}_\theta = \underline{\mathbf{U}}. \tag{3.1.16}$$

The flow is irrotation and there are no vortices because $\underline{\omega} = 0$. The second term in (3.1.13) is called the Stokeslet because it contributes to the vorticity of the flow. The third term in (3.1.13) is called the doublet, it is at the centre of the sphere and $\underline{\omega} = 0$. Figures 1 shows the streamlines of the Stokes solution. For low Reynolds numbers, the streamlines distribution is symmetrical about the plane y = 0. The streamlines are uniform and straight in front of the sphere and they are deflected around the sphere.

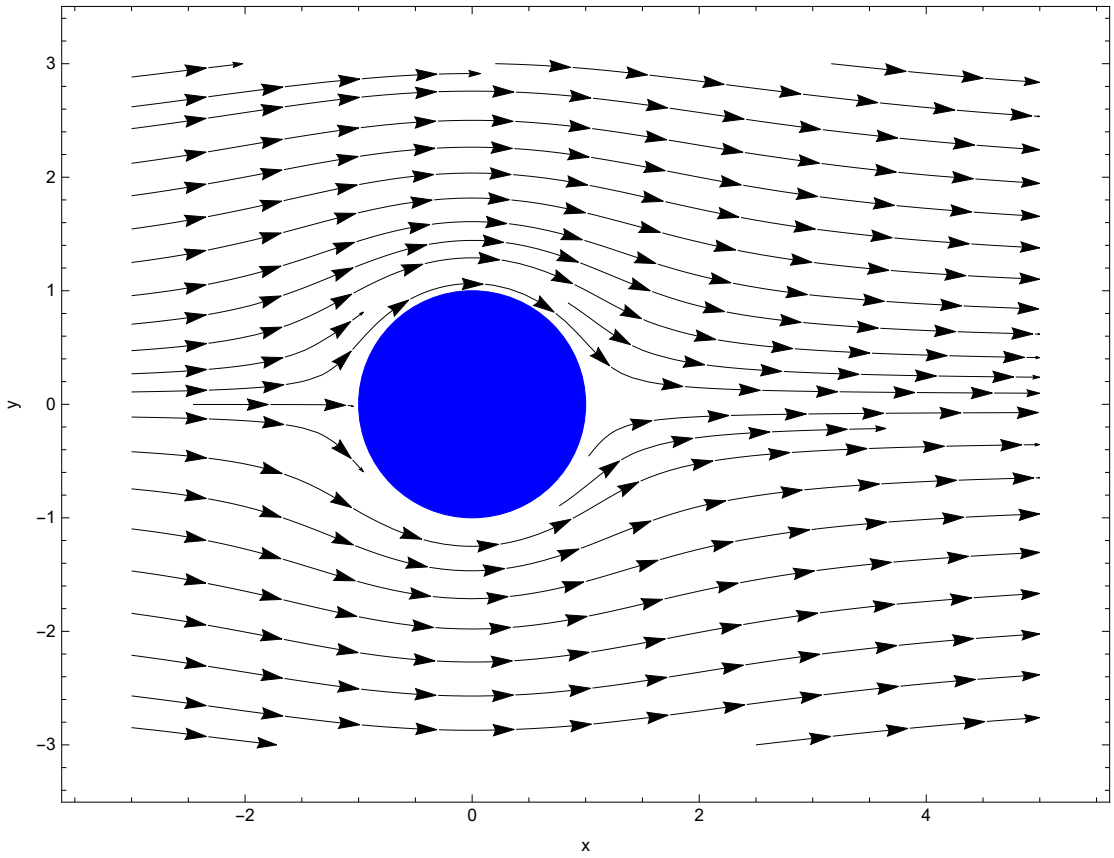


Figure 1: The streamlines illustrating the zeroth order flow of fluid around the sphere.

3.1.2 Solution of the first order problem

We now derive the solution of the second order problem by solving equation (2.1.34) subject to the boundary conditions at the surface of the sphere and far away from the sphere. The first order perturbation equation (2.1.34) becomes

$$D^4\psi_1 = \frac{Re}{r^2\sin\theta}\left(\frac{\partial\psi_0}{\partial\theta}\frac{\partial}{\partial r} - \frac{\partial\psi_0}{\partial r}\frac{\partial}{\partial\theta} + 2\cot\theta\frac{\partial\psi_0}{\partial r} - \frac{2}{r}\frac{\partial\psi_0}{\partial\theta}\right)D^2\psi_0, \quad (3.1.17)$$

subject to the boundary conditions below

$$\frac{\partial\psi_1}{\partial\, r}(1,\theta) = 0, \quad (3.1.18)$$

$$\frac{\partial\psi_1}{\partial\,\theta}(1,\theta) = 0, \quad (3.1.19)$$

$$\psi_1(r,\theta) = O(r) \quad as\ r\to\infty. \quad (3.1.20)$$

We first substitute ψ_0 from equation (3.1.13) into $D^2\psi_0$ to get

$$D^2\psi_0 = \frac{\partial^2}{\partial r^2}\left(\frac{1}{4}(2r^2 - 3r + \frac{1}{r})\sin^2\theta\right)$$

$$+ \frac{\sin\theta}{r^2}\frac{\partial}{\partial\theta}\left(\frac{1}{\sin\theta}\frac{\partial}{\partial\theta}\left(\frac{1}{4}(2r^2 - 3r + \frac{1}{r})\sin^2\theta\right)\right) \quad (3.1.21)$$

$$= \frac{3}{2\,r}\sin^2\theta.$$

The first derivatives of $\psi_0(r,\theta)$ with respect to r and θ are

$$\frac{\partial\psi_0}{\partial\, r} = \frac{1}{4}\left(4r - 3 - \frac{1}{r^2}\right)\sin^2\theta, \quad (3.1.22)$$

$$\frac{\partial\psi_0}{\partial\theta} = \frac{1}{2}\left(2r^2 - 3r + \frac{1}{r}\right)\sin\theta\cos\theta. \quad (3.1.23)$$

Substitute (3.1.21), (3.1.22) and (3.1.23) into (3.1.17) to get

$$D^4\psi_1 = \frac{9}{4}\left(-\frac{2}{r^2} + \frac{3}{r^3} - \frac{1}{r^5}\right)\sin^2\theta\cos\theta. \quad (3.1.24)$$

Now we look for the solution of the form

$$\psi_1(r,\theta) = g(r)\sin^2\theta\cos\theta. \tag{3.1.25}$$

Then

$$\begin{aligned} D^2\psi_1 &= \frac{\partial^2\psi_1}{\partial r^2} + \frac{\sin\theta}{r^2}\frac{\partial}{\partial\theta}\left(\frac{1}{\sin\theta}\frac{\partial\psi_1}{\partial\theta}\right) \\ &= \frac{\partial^2}{\partial r^2}\left(g(r)\sin^2\theta\cos\theta\right) + \frac{\sin\theta}{r^2}\frac{\partial}{\partial\theta}\left(\frac{1}{\sin\theta}\frac{\partial}{\partial\theta}\left(g(r)\sin^2\theta\cos\theta\right)\right) \\ &= \left(\frac{\partial^2 g(r)}{\partial r^2} - \frac{6}{r^2}g(r)\right)\sin^2\theta\cos\theta. \end{aligned}$$

Hence

$$\begin{aligned} D^2(D^2\psi_1) &= \frac{\partial^2}{\partial r^2}\left(\frac{\partial^2 g(r)}{\partial r^2} - \frac{6}{r^2}g(r)\right)\sin^2\theta\cos\theta \\ &\quad + \frac{\sin\theta}{r^2}\frac{\partial}{\partial\theta}\left(\frac{1}{\sin\theta}\frac{\partial}{\partial\theta}\left(\frac{\partial^2 g(r)}{\partial r^2} - \frac{6}{r^2}g(r)\right)\sin^2\theta\cos\theta\right) \\ &= \left(\frac{\partial^4 g(r)}{\partial r^4} - \frac{12}{r^2}\frac{\partial^2 g(r)}{\partial r^2} + \frac{24}{r^3}\frac{\partial g(r)}{\partial r}\right)\sin^2\theta\cos\theta. \end{aligned}$$

$$\therefore \quad D^4\psi_1 = \left(\frac{\partial^4 g(r)}{\partial r^4} - \frac{12}{r^2}\frac{\partial^2 g(r)}{\partial r^2} + \frac{24}{r^3}\frac{\partial g(r)}{\partial r}\right)\sin^2\theta\cos\theta. \tag{3.1.26}$$

Equating (3.1.24) and (3.1.26)

$$\left(\frac{\partial^4 g(r)}{\partial r^4} - \frac{12}{r^2}\frac{\partial^2 g(r)}{\partial r^2} + \frac{24}{r^3}\frac{\partial g(r)}{\partial r}\right) = \frac{9}{4}\left(-\frac{2}{r^2} + \frac{3}{r^3} - \frac{1}{r^5}\right). \tag{3.1.27}$$

We look for the homogeneous solution of the form

$$g(r) = r^\alpha. \tag{3.1.28}$$

We write the derivatives of equation (3.1.28) as

$$\begin{aligned}
\frac{\partial g(r)}{\partial r} &= \alpha\, r^{\alpha-1},\\
\frac{\partial^2 g(r)}{\partial r^2} &= \alpha(\alpha-1)\, r^{\alpha-2},\\
\frac{\partial^3 g(r)}{\partial r^3} &= \alpha(\alpha-1)(\alpha-2)\, r^{\alpha-3},\\
\frac{\partial^4 g(r)}{\partial r^4} &= \alpha(\alpha-1)(\alpha-2)(\alpha-3)\, r^{\alpha-4}.
\end{aligned}$$

Then by substituting the derivatives of (3.1.28) into equation (3.1.27), we get

$$\alpha(\alpha+2)(\alpha-3)(\alpha-5)r^{\alpha-4} = 0. \tag{3.1.29}$$

$\therefore$ α = -2, 0, 3, 5 then the complementary function is

$$CF = Ar^3 + Br^5 + \frac{C}{r^2} + D \tag{3.1.30}$$

and the particular solution is

$$g(r) = -\frac{3}{16}r^2 + \frac{9}{32}r + \frac{3}{32r}. \tag{3.1.31}$$

The general solution is

$$g(r) = Ar^3 + Br^5 + \frac{C}{r^2} + D - \frac{3}{16}r^2 + \frac{9}{32}r + \frac{3}{32r}. \tag{3.1.32}$$

Hence

$$\begin{aligned}
\psi_1(r,\theta) = &\left(Ar^3 + Br^5 + \frac{C}{r^2} + D\right)\sin^2\theta\cos\theta\\
&+ \left(-\frac{3}{16}r^2 + \frac{9}{32}r + \frac{3}{32r}\right)\sin^2\theta\cos\theta.
\end{aligned} \tag{3.1.33}$$

By applying the boundary condition far from the sphere

$$\psi_1(r,\theta) = O(r) \quad as \;\; r \;\rightarrow\; \infty, \tag{3.1.34}$$

then $A = 0$ and $B = 0$.

We apply the boundary conditions at the surface of the sphere

$$\frac{\partial \psi_1}{\partial \theta} = 0. \tag{3.1.35}$$

$$\therefore \;\; g(1) = 0, \tag{3.1.36}$$

then $C + D + 3/16 = 0$.

$$\frac{\partial \psi_1}{\partial r} = 0, \tag{3.1.37}$$

$$\therefore \;\; \frac{\partial g(r)}{\partial r} = 0 \qquad at \;\; r = 1, \tag{3.1.38}$$

then $2\,C + 3/16 = 0$.

$\therefore C =$ - 3/32 and $D =$ - 3/32.

$$\therefore \psi_1(r,\theta) = -\frac{3}{32}\left(2r^2 - 3r + 1 - \frac{1}{r} + \frac{1}{r^2}\right)\sin^2\theta\cos\theta. \tag{3.1.39}$$

Thus

$$\begin{aligned}\psi(r,\theta) = {} & \frac{1}{4}\left(2r^2 - 3r + \frac{1}{r}\right)\sin^2\theta \\ & - Re\frac{3}{32}\left(2r^2 - 3r + 1 - \frac{1}{r} + \frac{1}{r^2}\right)\sin^2\theta\cos\theta + O(Re^2).\end{aligned} \tag{3.1.40}$$

Figures 2 and 3 shows the streamlines for the solution of ψ up to ψ_1 at Re = 0.50 and 3.00. For Re = 0.50, the streamlines are symmetrical from front to back but as we increase the Reynolds number to 3.00, the flow pattern breaks because the analytical solutions are effectively limited to Re < 1.

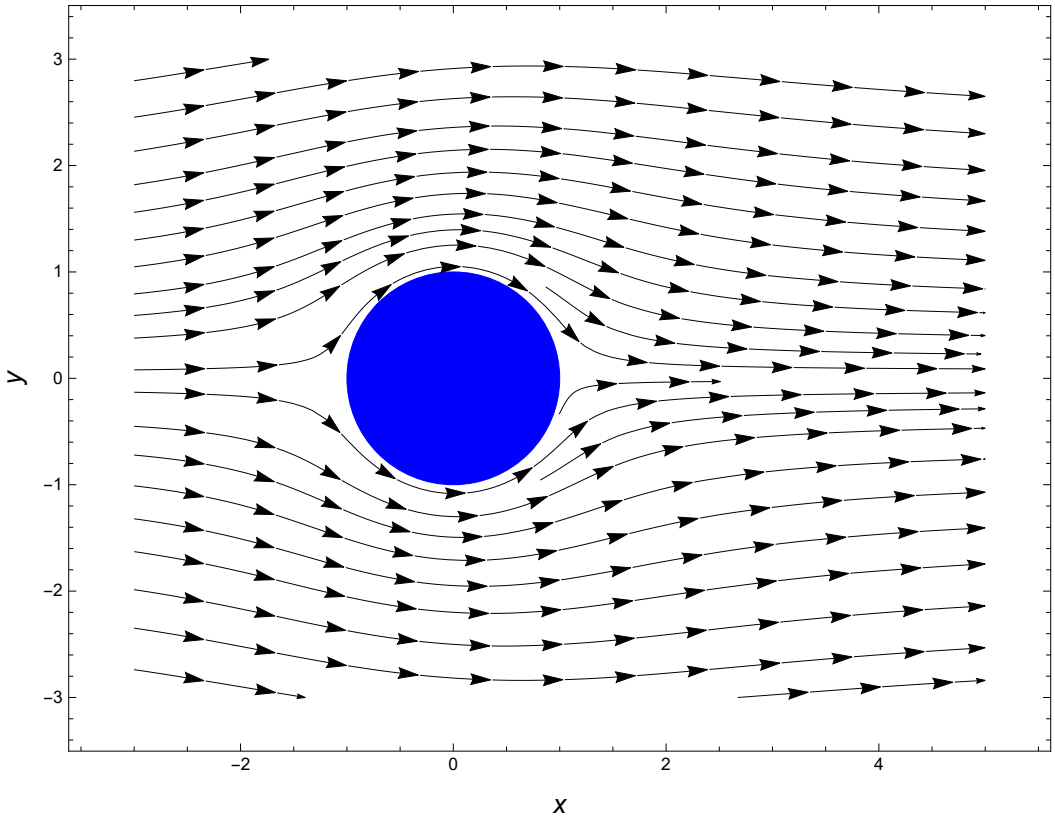


Figure 2: The streamlines illustrating the flow of fluid around the sphere for ψ up to ψ_1 at Re = 0.50

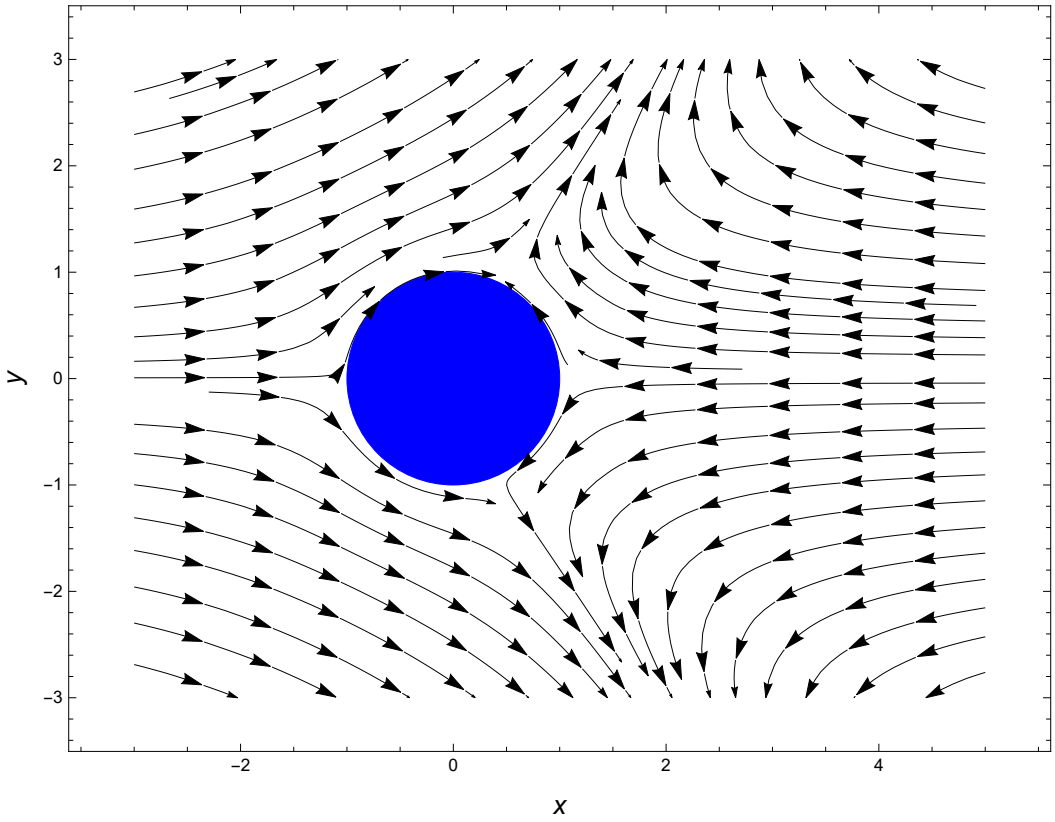


Figure 3: The streamlines illustrating the flow of fluid around the sphere for ψ up to ψ_1 at Re = 3.00

3.1.3 Whitehead Paradox

The Stokes expansion breaks down because the equation (3.1.39) does not satisfy the boundary condition as $r \to \infty$. It does satisfy the boundary condition at the surface of the sphere. The boundary condition requires that the solution must be of $O(r)$ at infinity but it behaves like $O(r^2)$. There is no choice of a constant that can be used to ensure that the solution behave like $O(r)$ at infinity. Thus giving rise to an incorrect expression for the velocity at infinity; this is the Whitehead paradox.

The Whitehead paradox is the non-existence of a second order approximation to Stokes solution for unbounded flow past any body. This is a singular perturbation problem. However the paradox was resolved by the Oseen approximations which we discuss in section 3.2.

3.1.4 Solution of second order problem

We now derive the solution of the second order problem by solving equation (2.1.34) subject to the boundary conditions at the surface of the sphere and far away from the sphere. The first order perturbation equation (2.1.34) becomes

$$D^4\psi_2 = \frac{Re}{r^2\sin\theta}\left(\frac{\partial\psi_1}{\partial\theta}\frac{\partial}{\partial r} - \frac{\partial\psi_1}{\partial r}\frac{\partial}{\partial\theta} + 2\cot\theta\frac{\partial\psi_1}{\partial r} - \frac{2}{r}\frac{\partial\psi_1}{\partial\theta}\right)D^2\psi_1 \quad (3.1.41)$$

subject to boundary conditions

$$\frac{\partial\psi_2}{\partial\, r}(1,\theta) = 0 \quad at\ r = 1, \quad (3.1.42)$$

$$\frac{\partial\psi_2}{\partial\,\theta}(1,\theta) = 0 \quad at\ r = 1, \quad (3.1.43)$$

$$\psi_2(r,\theta) = O(r) \quad as\ \ r \to\ \infty. \quad (3.1.44)$$

We first substitute ψ_1 from equation (3.1.39) into $D^2\psi_1$ to get

$$D^2\psi_1 = \frac{\partial^2}{\partial r^2}\left(-\frac{3}{32}\left(2r^2 - 3r + 1 - \frac{1}{r} + \frac{1}{r^2}\right)\sin^2\theta\cos\theta\right)$$

$$+\frac{\sin\theta}{r^2}\frac{\partial}{\partial\theta}\left(-\frac{3}{32}\left(2r^2 - 3r + 1 - \frac{1}{r} + \frac{1}{r^2}\right)\sin^2\theta\cos\theta\right).$$

$$\therefore D^2\psi_1 = \left(\frac{3}{4} - \frac{3}{8r^3} + \frac{9}{16r^2} - \frac{27}{16r}\right)\sin^2\theta\cos\theta. \tag{3.1.45}$$

The first derivatives of $\psi_1(r,\theta)$ with respect to r and θ are

$$\frac{\partial\psi_1}{\partial\, r} = -\frac{3}{32}\left(-3 - \frac{2}{r^3} + \frac{1}{r^2} + 4r\right)\sin^2\theta\cos\theta, \tag{3.1.46}$$

$$\begin{aligned}\frac{\partial\psi_1}{\partial\theta} = &-\frac{3}{16}\left(1 + \frac{1}{r^2} - \frac{1}{r} - 3r + 2r^2\right)\sin^2\theta\cos\theta \\ &+ \frac{3}{32}\left(1 + \frac{1}{r^2} - \frac{1}{r} - 3r + 2r^2\right)\sin^3\theta.\end{aligned} \tag{3.1.47}$$

Substitute (3.1.45), (3.1.46) and (3.1.47) into (3.1.41) to get

$$\begin{aligned}D^4\psi_2 = &\, Re^2\left(\frac{33}{64\, r^8} - \frac{27}{64\, r^7} + \frac{63}{32\, r^5} - \frac{297}{64\, r^4} + \frac{189}{64\, r^3} - \frac{3}{8\, r^2}\right)\sin^2\theta \\ &+ Re\left(-\frac{9}{4\, r^6} + \frac{27}{4\, r^4} - \frac{9}{2\, r^3}\right)\cos\theta\sin^2\theta \\ &+ Re^2\left(\frac{27}{64\, r^8} + \frac{9}{64\, r^7} - \frac{9}{8\, r^6} + \frac{27}{8\, r^5}\right)\cos(2\,\theta)\sin^2\theta \\ &+ Re^2\left(-\frac{495}{64\, r^4} + \frac{387}{64\, r^3} - \frac{9}{8\, r^2}\right)\cos(2\,\theta)\sin^2\theta.\end{aligned} \tag{3.1.48}$$

Now we look for the solution of the form

$$\psi_2(r,\theta) = h(r)\sin^2\theta + j(r)\cos\theta\sin^2\theta + k(r)\cos(2\theta)\sin^2\theta. \tag{3.1.49}$$

Then

$$
\begin{aligned}
D^4\psi_2 = Re^2 &\left(-\frac{8h(r)}{r^5} + \frac{48k(r)}{r^5} + \frac{8}{r^4}\frac{\partial h(r)}{\partial r} + \frac{24}{r^4}\frac{\partial k(r)}{\partial r}\right)\sin^2\theta \\
&+ Re^2\left(-\frac{4}{r^3}\frac{\partial^2 h(r)}{\partial r^2} - \frac{12}{r^3}\frac{\partial^2 k(r)}{\partial r^2} + \frac{1}{r}\frac{\partial^4 h(r)}{\partial r^4}\right)\sin^2\theta \\
&+ Re\left(-\frac{9}{4r^6} + \frac{27}{4r^4} - \frac{9}{2r^3}\right)\cos\theta\sin^2\theta \\
&+ Re^2\left(\frac{24}{r^4}\frac{\partial j(r)}{\partial r} - \frac{12}{r^3}\frac{\partial^2 j(r)}{\partial r^2} + \frac{1}{r}\frac{\partial^4 j(r)}{\partial r^4}\right)\cos\theta\sin^2\theta \\
&+ Re^2\left(\frac{72k(r)}{r^5} + \frac{48}{r^4}\frac{\partial k(r)}{\partial r}\right)\cos(2\,\theta)\sin^2\theta \\
&+ Re^2\left(-\frac{24}{r^3}\frac{\partial^2 k(r)}{\partial r^2} + \frac{1}{r}\frac{\partial^4 k(r)}{\partial r^4}\right)\cos(2\,\theta)\sin^2\theta.
\end{aligned}
\tag{3.1.50}
$$

We equate equation (3.1.48) and (3.1.50)

$$
\begin{aligned}
Re^2\left(-\frac{8h(r)}{r^5}+\frac{48k(r)}{r^5}+\frac{8}{r^4}\frac{\partial h(r)}{\partial r}+\frac{24}{r^4}\frac{\partial k(r)}{\partial r}-\frac{4}{r^3}\frac{\partial^2 h(r)}{\partial r^2}-\frac{12}{r^3}\frac{\partial^2 k(r)}{\partial r^2}\right)\sin^2\theta \\
+Re^2\left(\frac{1}{r}\frac{\partial^4 h(r)}{\partial r^4}\right)\sin^2\theta+\left(-\frac{9Re}{4r^6}+\frac{27Re}{4r^4}-\frac{9Re}{2r^3}+\frac{24Re^2}{r^4}\frac{\partial j(r)}{\partial r}\right)\cos\theta\sin^2\theta \\
+\left(-\frac{12Re^2}{r^3}\frac{\partial^2 j(r)}{\partial r^2}+\frac{1Re^2}{r}\frac{\partial^4 j(r)}{\partial r^4}\right)\cos\theta\sin^2\theta \\
+Re^2\left(\frac{72k(r)}{r^5}+\frac{48}{r^4}\frac{\partial k(r)}{\partial r}-\frac{24}{r^3}\frac{\partial^2 k(r)}{\partial r^2}+\frac{1}{r}\frac{\partial^4 k(r)}{\partial r^4}\right)\cos(2\,\theta)\sin^2\theta= \\
Re^2\left(\frac{33}{64\,r^8}-\frac{27}{64\,r^7}+\frac{63}{32\,r^5}-\frac{297}{64\,r^4}+\frac{189}{64\,r^3}-\frac{3}{8\,r^2}\right)\sin^2\theta \\
+Re\left(-\frac{9}{4\,r^6}+\frac{27}{4\,r^4}-\frac{9}{2\,r^3}\right)\cos\theta\sin^2\theta \\
+Re^2\left(\frac{27}{64\,r^8}+\frac{9}{64\,r^7}-\frac{9}{8\,r^6}+\frac{27}{8\,r^5}\right)\cos(2\,\theta)\sin^2\theta \\
+Re^2\left(-\frac{495}{64\,r^4}+\frac{387}{64\,r^3}-\frac{9}{8\,r^2}\right)\cos(2\,\theta)\sin^2\theta.
\end{aligned}
$$

The coefficients of $\cos(2\,\theta)\sin^2\theta$,

$$
\begin{aligned}
\frac{72k(r)}{r^5}+\frac{48}{r^4}\frac{\partial k(r)}{\partial r}-\frac{24}{r^3}\frac{\partial^2 k(r)}{\partial r^2}+\frac{1}{r}\frac{\partial^4 k(r)}{\partial r^4}= \\
\frac{27}{64\,r^8}+\frac{9}{64\,r^7}-\frac{9}{8\,r^6}+\frac{27}{8\,r^5}.
\end{aligned}
$$

The solution to the differential equation is

$$
\begin{aligned}
k(r)=\frac{C_1}{r^3}+\frac{C_2}{r}+r^4C_3+r^6C_4+\left(\frac{-9500-11025r+9504r^2}{3763200r^3}\right) \\
+\left(\frac{176400r^3-242550r^4+189630r^5-58800r^6}{3763200r^3}\right) \\
+\left(\frac{-12600\log r-60480r^2\log r}{3763200r^3}\right).
\end{aligned}
$$

The coefficients of $\cos\theta\sin^2\theta$,

$$
\frac{24Re^2}{r^4}\frac{\partial j(r)}{\partial r}-\frac{12Re^2}{r^3}\frac{\partial^2 j(r)}{\partial r^2}+\frac{Re^2}{r}\frac{\partial^4 j(r)}{\partial r^4}=0.
$$

The solution to the differential equation is

$$j(r) = \frac{9}{128r} + \frac{27r}{128} - \frac{9r^2}{64} - \frac{C_5}{2r^2} + \frac{1}{3}r^3 C_6 + \frac{1}{5}r^5 C_7 + C_8.$$

The coefficients of $\sin^2\theta$,

$$-\frac{8h(r)}{r^5} + \frac{48k(r)}{r^5} + \frac{8}{r^4}\frac{\partial h(r)}{\partial r} + \frac{24}{r^4}\frac{\partial k(r)}{\partial r} = \frac{33}{64\,r^8} - \frac{27}{64\,r^7} + \frac{63}{32\,r^5} - \frac{297}{64\,r^4} + \frac{189}{64\,r^3} - \frac{3}{8\,r^2}.$$

The solution to the differential equation is

$$\begin{aligned} h(r) = {} & \frac{C_9}{r} + C_{10}r + C_{11}r^2 + C_{12}r^4 + \left(\frac{-724 - 11025r - 41664r^2}{1254400r^3}\right) \\ & + \left(\frac{44100r^3 - 117600r^5 - 58800r^6 + 752640C_{13} + 752640C_{14}r^9}{1254400r^3}\right) \\ & + \left(\frac{141120r^5\log r - 2520\log r - 40320r^2\log r}{1254400r^3}\right). \end{aligned}$$

$$
\begin{aligned}
\therefore\ \psi_2(r,\theta) = &\left(\frac{C_9}{r} + C_{10}r + C_{11}r^2 + C_{12}r^4\right)\sin^2\theta \\
&+ \left(\frac{-724 - 11025r - 41664r^2}{1254400r^3}\right)\sin^2\theta \\
&+ \left(\frac{44100r^3 - 117600r^5 - 58800r^6}{1254400r^3}\right)\sin^2\theta \\
&+ \left(\frac{752640C_{13} + 752640C_{14}r^9}{1254400r^3}\right)\sin^2\theta \\
&+ \left(\frac{141120r^5\log r - 2520\log r - 40320r^2\log r}{1254400r^3}\right)\sin^2\theta \\
&+ \left(\frac{9}{128r} + \frac{27r}{128} - \frac{9r^2}{64} - \frac{C_5}{2r^2}\right)cos\theta\sin^2\theta \\
&+ \left(\frac{1}{3}r^3C_6 + \frac{1}{5}r^5C_7 + C_8\right)cos\theta\sin^2\theta \\
&+ \left(\frac{C_1}{r^3} + \frac{C_2}{r} + r^4C_3 + r^6C_4\right)\cos(2\theta)\sin\theta \\
&+ \left(\frac{-9500 - 11025r + 9504r^2}{3763200r^3}\right)\cos(2\theta)\sin\theta \\
&+ \left(\frac{176400r^3 - 242550r^4}{(3763200r^3}\right)\cos(2\theta)\sin\theta \\
&+ \left(\frac{189630r^5 - 58800r^6}{(3763200r^3}\right)\cos(2\theta)\sin\theta \\
&+ \left(\frac{-12600\log r - 60480r^2\log r}{3763200r^3}\right)\cos(2\theta)\sin\theta.
\end{aligned}
$$

We could not find the constants that will satisfy the boundary conditions. The terms that include the $\log r$ makes it difficult to determine the constants. Proudman and Pearson [5] were able to find the solution of the second order problem by using the matching procedure. We discuss the solution in section 3.3.

3.2 Oseen Approximation

3.2.1 Leading term of Oseen expansion

The Oseen expansion is as follows as $Re \to 0$

$$\Phi(p,\theta) = \frac{1}{Re^2}\Phi_0(p,\theta) + \frac{1}{Re}\Phi_1(p,\theta) + ... \tag{3.2.1}$$

where

$$\Phi_0(p,\theta) = \frac{1}{2}p^2 \sin^2\theta, \tag{3.2.2}$$

which is the uniform stream.

3.2.2 Second term of Oseen expansion

We derive the second term of the Oseen expansion by substituting equation (3.2.1) into the Oseen differential equation (2.2.20) to get

$$D^4\Phi_1 = \cos\theta\frac{\partial}{\partial p}\left(D^2\Phi_1\right) - \sin\theta\frac{\partial}{\partial\theta}\left(D^2\Phi_1\right) \tag{3.2.3}$$

We assume

$$D^2\Phi_1 = e^{\frac{1}{2}p\cos\theta}\Phi_1 \tag{3.2.4}$$

then equation (3.2.3) becomes

$$D^2\Phi_1 - \frac{1}{4}\Phi_1 = 0 \tag{3.2.5}$$

We look for the solution of the form

$$\Phi_1 = f(p)\sin^2\theta \tag{3.2.6}$$

Substitute equation (3.2.6) into (3.2.5)

$$\frac{\partial^2 f(p)}{\partial p^2} - \frac{2f(p)}{p^2} - \frac{1}{4}f(p) = 0 \tag{3.2.7}$$

$$\therefore f(p) = A_1 \left(1 + \frac{2}{p}\right) e^{-\frac{1}{2}p} \tag{3.2.8}$$

Then equation (3.2.4) becomes

$$D^2\Phi_1 = A_1 \left(1 + \frac{2}{p}\right) e^{-\frac{1}{2}p(1-\cos\theta)} \sin^2\theta \tag{3.2.9}$$

The particular integral of less than order unity in the Stokes region is

$$\Phi_1(p,\theta) = -2A_1(1+\cos\theta)\left(1 - e^{-\frac{1}{2}p(1-\cos\theta)}\right). \tag{3.2.10}$$

When p is of order unity equation (3.2.9) becomes

$$\Phi_1(p,\theta) = -A_1 p \sin^2\theta \tag{3.2.11}$$

Then Oseen expansion (3.2.1) is

$$\Phi(p,\theta) = \frac{1}{2}\frac{p^2}{Re^2}\sin^2\theta - A_1\frac{p}{Re}\sin^2\theta \tag{3.2.12}$$

The dominating terms of the Stokes solution (3.1.1) in terms of Oseen variables are

$$\psi_0(p,\theta) = \frac{1}{2}\frac{p^2}{Re^2}\sin^2\theta - \frac{3}{4}\frac{p}{Re}\sin^2\theta \tag{3.2.13}$$

By comparing the coefficients of the second terms of equations (3.2.12) and

(3.2.13) then $A_1 = 3/4$.

Then the stream function Φ solution becomes

$$\Phi(p,\theta) = \frac{1}{2}p^2\sin^2\theta - \frac{3}{2}\frac{1}{Re}(1+\cos\theta)\left(1 - e^{-\frac{1}{2}p(1-\cos\theta)}\right). \qquad (3.2.14)$$

The Oseen solution satisfies all the boundary conditions. The Oseen expansion is uniformly valid over the whole field of flow. We can use the Oseen expansion to find a finite number of terms which will give a uniform accurate approximation to the solution [5]. Figure 4 shows the streamlines for flow past the sphere for Oseen solution at low Reynolds number (Re = 0.30). The streamlines are in agreement with results obtained in J. R. Grace and M. E. Weber [63].

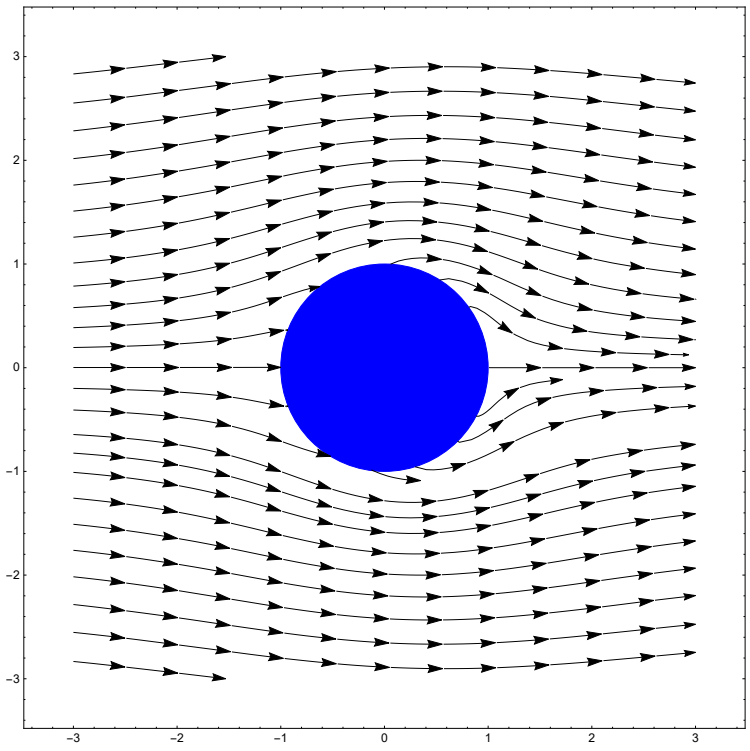


Figure 4: Streamlines for flow around the sphere for Oseen solution at Re = 0.30

3.3 Improved Approximation

In this section we use the matched asymptotic expansion to improve the second and third term of the Stokes expansion. We match the Stokes second term with the Oseen second term to find the constant.

3.3.1 Improved solution of the first order problem

We write the Oseen expansion (3.2.15) in terms of Stokes variables as

$$\Phi(r,\theta) = \frac{1}{4}(2r^2 - 3r)\sin^2\theta + \frac{3}{16}Rer^2(1-\cos\theta)\sin^2\theta \tag{3.3.1}$$

Now the Stokes expansion must have the form

$$\psi(r,\theta) = \frac{1}{4}\left(2r^2 - 3r + \frac{1}{r}\right) + Re\psi_1(r,\theta) + ... \tag{3.3.2}$$

in order to match the Oseen expansion form.

Thus

$$\begin{aligned}\psi_1(r,\theta) = A_2&\left(2r^2 - 3r + \frac{1}{r}\right)\sin^2\theta \\ &- \frac{3}{32}\left(2r^2 - 3r + 1 - \frac{1}{r} + \frac{1}{r^2}\right)\sin^2\theta\cos\theta.\end{aligned} \tag{3.3.3}$$

Now the Stokes expansion in terms of Oseen variables is

$$\psi(p,\theta) = \frac{1}{2}\frac{1}{Re^2}p^2\sin^2\theta - \frac{1}{Re}\left(2A_2p^2 - \frac{3}{16}p^2\cos\theta - \frac{3}{4}p\right)\sin^2\theta. \tag{3.3.4}$$

Comparing equation (3.3.1) and (3.3.5) gives $A_2 = 3/32$.

Thus the Stokes expansion becomes

$$\psi(r,\theta) = \frac{1}{4}\left(2r^2 - 3r + \frac{1}{r}\right)\sin^2\theta + \frac{3}{32}\left(2r^2 - 3r + \frac{1}{r}\right)\sin^2\theta \\ - \frac{3}{32}\left(2r^2 - 3r + 1 - \frac{1}{r} + \frac{1}{r^2}\right)\sin^2\theta\cos\theta. \tag{3.3.5}$$

The streamlines of the improved solution of the first order problem are illustrated in figures 5 and 6. Figure 5 shows the flow pattern of the improved solution at $Re = 0.50$ which is comparable to the Stokes solution for low Reynolds number.

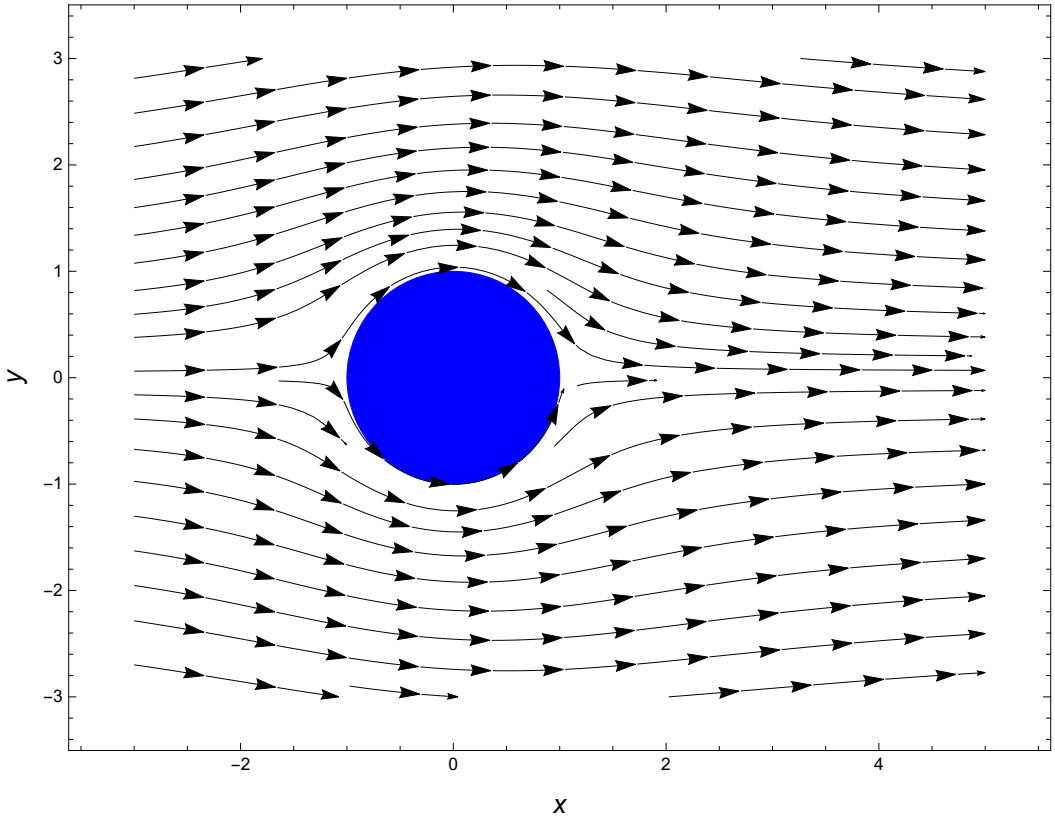


Figure 5: Streamlines illustrating the flow past a sphere for the improved solution of ψ up to ψ_1 at Re = 0.50.

Figure 6 shows the streamlines for the improved solution at Re = 3.00, we note that the flow pattern does not break when the Reynolds number increases. The streamlines in Figure 5 provides an improved solution compared to the streamlines of the first order solution in figure 3. The flow patterns at $Re = 3.00$ shows great improvement as compared to the flow pattern in figure 3.

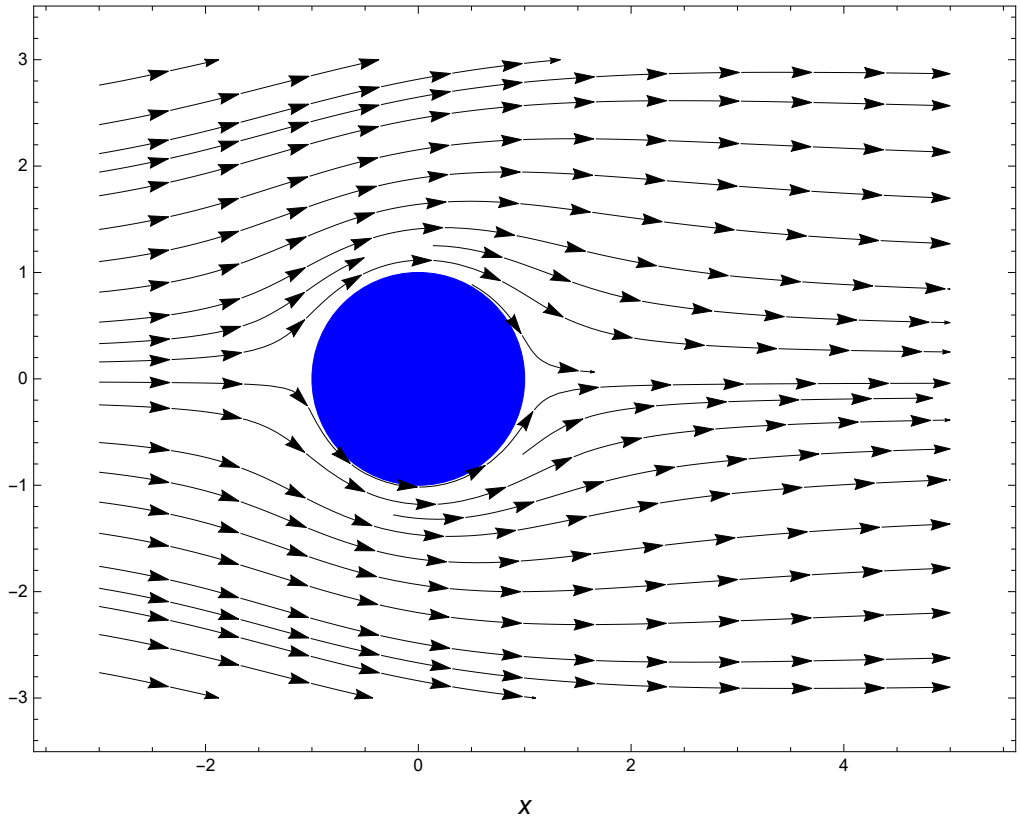


Figure 6: Streamlines illustrating the flow past a sphere for the improved solution of ψ up to ψ_1 at Re = 3.00.

3.3.2 Improved solution of the second order problem

The solution of the second order problem was found by Proudman and Pearson [5]. The arbitrary constants of the third term of the Stokes expansion are found using the Van Dyke matching principle. Re^2 is replaced by $Re^2 \log r$ on the third term of the Stokes expansion. The solution as in Proudman and Pearson [5] is

$$\psi_2(r,\theta) = \frac{9}{160}\left(2r^2 - 3r + \frac{1}{r}\right)\sin^2\theta. \tag{3.3.6}$$

Figure 7 shows the streamlines for improved solution of ψ up to ψ_2 at $Re = 0.5$. The streamlines are in agreement with the condition for $Re < 1$.

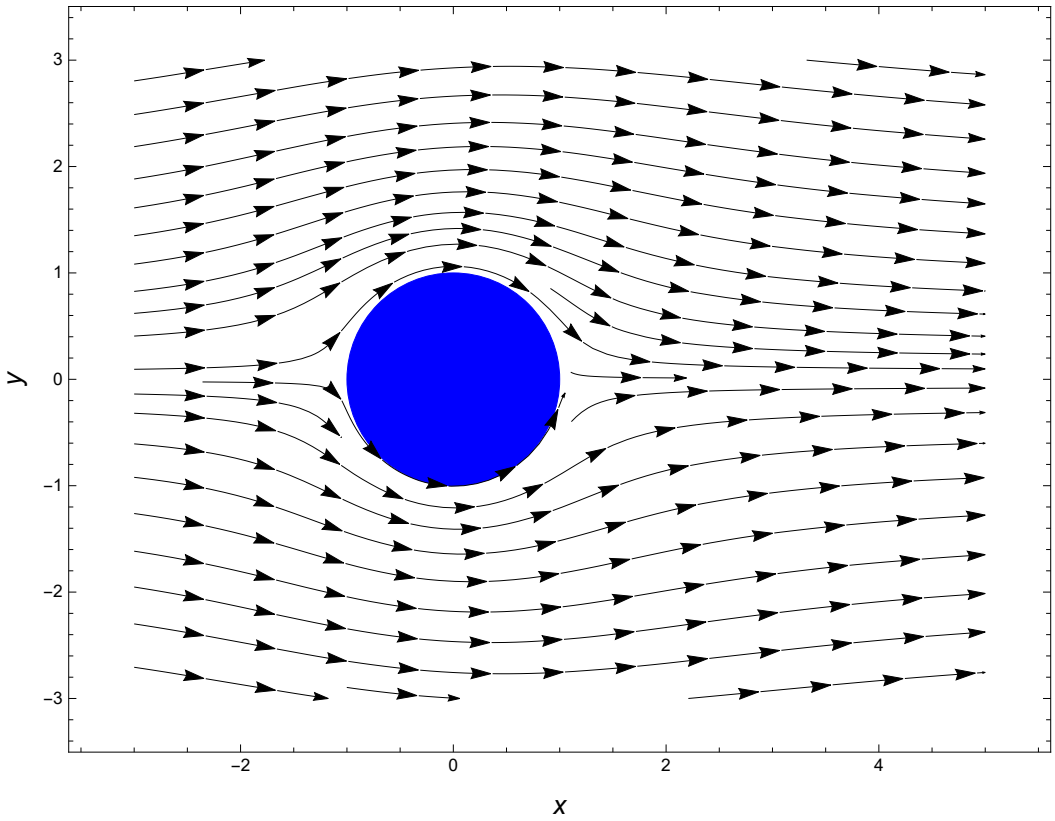


Figure 7: Streamlines illustrating the flow past a sphere for the improved solution of ψ up to ψ_2 at Re = 0.50

3.4 Conclusion

We have reproduced the analytical solutions that were obtained by Stokes [3] and Oseen [6] for incompressible flow past a sphere. We first solved the zero order problem by neglecting the inertia of the fluid to obtain the Stokes solution. We then derived the first order solution when the Reynolds number is not negligibly small. The first order solution does not satisfy the boundary condition at infinity because $\psi_1(r, \theta)$ behaves like $O(r^2)$ as $r \to \infty$. We also attempted to find the solution of the second order problem. We were able to find the form of the second order solution but we could not determine the constants of integration because of the logarithms terms. We also tried to write an algorithm to obtain higher approximations of the flow but the trigonometry terms on the $D^4\psi$ expression made it difficult for us to find the form of the nth term of ψ.

We derived the second term of the Oseen expansion that was obtained by S. Goldstein [64]. The Stokes solution was improved by using the method of matched asymptotic expansions. We improved the first order solution by matching it to the Oseen expansion. We were able to find a free constant that will ensure that the solution satisfies the boundary condition far from the sphere thus resolving the Whitehead paradox. Proudman and Pearson [5] found that constants of the second order problem must be multiple of $\log r$ in order to satisfy the no-slip condition on the sphere. The Re^2 in the second term of the Stokes expansion is replaced by $Re^2 \log r$.

The attempt to create an algorithm that will formally produce the nth term of the Stokes expansion using the stream function analytical method was unsuccessful. However we were able to use Mathematica to solve the Navier-Stokes equations using the Stream function approach for the first three terms of the Stokes expansion. The breakdown of the expansion leads us to try and solve the problem using a numerical method. We will use the finite difference method to approximate the nth ψ numerically in the next section.

4 Numerical Method

In this section we use the finite difference method (FDM) to accurately approximate the solution of the stream function equation. We use Mathematica to generate code to numerically solve the stream function equation and plot solutions.

4.1 Finite Difference Method

4.1.1 Navier-Stokes Equations

We approximate the solutions for the stream function using the finite difference method. The coordinates are transformed from (r, θ) to (ξ, μ). We define ξ and μ as

$$\xi = 1 - e^{1-r}, \tag{4.1.1}$$

$$\mu = \cos\theta. \tag{4.1.2}$$

We transformed the coordinates because we cannot take r to infinity. We chose

$$r = (1 - \log(1 - \xi)) \tag{4.1.3}$$

so that we can get arbitrarily close to infinity. By using ξ we can create a grid for ξ that starts from 0 to 1. The main disadvantage of the coordinate system is that r gets to infinity quickly, the graph below shows how ξ gets to 1 quickly.

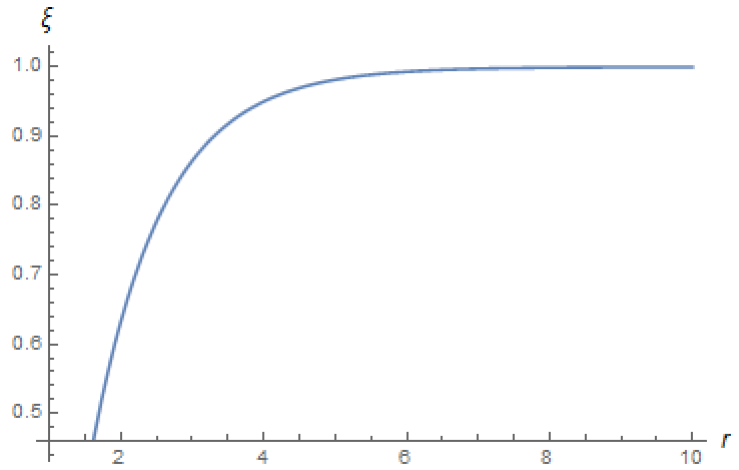


Figure 8: The graph shows that ξ gets to 1 quickly. ξ gets closer to 1 before r gets to 10.

The first derivatives of the stream function in terms of the new coordinates are

$$\frac{\partial \Psi(r,\theta)}{\partial r} = (1-\xi)\frac{\partial \Psi(\xi,\mu)}{\partial \xi},$$
$$\frac{\partial \Psi(r,\theta)}{\partial \theta} = -\sqrt{1-\mu^2}\frac{\partial \Psi(\xi,\mu)}{\partial \mu}.$$

The Navier-Stokes equation (2.1.34) in terms of the new coordinates is

$$D^4\Psi_{n+1} = \lambda D^2\Psi_n, \quad 0 \le \xi \le 1, \quad -1 \le \mu \le 1, \tag{4.1.4}$$

where

$$
\begin{aligned}
D^4\Psi_{n+1} = &\left[\frac{4\ \mu\ (\mu^2-1)}{(\log(1-\xi)-1)^3}\frac{\partial^3\Psi(\xi,\mu)}{\partial\mu^3} - \frac{4\ (\mu^2-1)}{(\log(1-\xi)-1)^3}\frac{\partial^2\Psi(\xi,\mu)}{\partial\mu^2}\right] \\
&+ \left[\frac{(\mu^2-1)^2}{(\log(1-\xi)-1)^4}\frac{\partial^4\Psi(\xi,\mu)}{\partial\mu^4} + (\xi-1)\frac{\partial\Psi(\xi,\mu)}{\partial\mu}\right] \\
&+ \left[7\ (\xi-1)^2\frac{\partial^2\Psi(\xi,\mu)}{\partial\xi^2} - \frac{2\ (\mu^2-1)(\xi-1)(\log(1-\xi)-3)}{(\log(1-\xi)-1)^3}\frac{\partial^3\Psi(\xi,\mu)}{\partial\xi\partial\mu^2}\right] \\
&+ \left[6\ (\xi-1)^3\frac{\partial^3\Psi(\xi,\mu)}{\partial\xi^3} + (\xi-1)^4\frac{\partial^4\Psi(\xi,\mu)}{\partial\xi^4} - \frac{2\ (\mu^2-1)(\xi-1)^2}{(\log(1-\xi)-1)^2}\frac{\partial^4\Psi(\xi,\mu)}{\partial\xi^2\partial\mu^2}\right]
\end{aligned}
\tag{4.1.5}
$$

and

$$
\begin{aligned}
\lambda D^2\Psi_n = &\left[\frac{4\ \ (\mu^2-1)}{(\log(1-\xi)-1)^5}\frac{\partial\Psi(\xi,\mu)}{\partial\mu}\frac{\partial^2\Psi(\xi,\mu)}{\partial\mu^2}\right] \\
&+ \left[\frac{(\xi-1)(\log(1-\xi)-3)}{(\log(1-\xi)-1)^3}\frac{\partial\Psi(\xi,\mu)}{\partial\mu}\frac{\partial\Psi(\xi,\mu)}{\partial\xi}\right] \\
&+ \left[\frac{(\mu^2-1)(\xi-1)}{(\log(1-\xi)-1)^4}\frac{\partial^3\Psi(\xi,\mu)}{\partial\mu^3}\frac{\partial\Psi(\xi,\mu)}{\partial\xi}\right] \\
&+ \left[\frac{2\ \ \mu(\xi-1)^2}{(\mu^2-1)(\log(1-\xi)-1)^2}(\frac{\partial\Psi(\xi,\mu)}{\partial\xi})^2\right] \\
&+ \left[\frac{(2\xi-\xi^2-1)}{(\log(1-\xi)-1)^2}\frac{\partial\Psi(\xi,\mu)}{\partial\xi}\frac{\partial^2\Psi(\xi,\mu)}{\partial\xi\partial\mu}\right] \\
&+ \left[\frac{(1-\mu^2)(\xi-1)}{(\log(1-\xi)-1)^4}\frac{\partial\Psi(\xi,\mu)}{\partial\mu}\frac{\partial^3\Psi(\xi,\mu)}{\partial\xi\partial\mu^2}\right] \\
&+ \left[\frac{(\xi-1)^2(3\log(1-\xi)-5)}{(\log(1-\xi)-1)^3}\frac{\partial\Psi(\xi,\mu)}{\partial\mu}\frac{\partial^2\Psi(\xi,\mu)}{\partial\xi^2}\right] \\
&+ \left[\frac{2\ \ \mu\ (\xi-1)^3}{(\mu^2-1)(\log(1-\xi)-1)^2}\frac{\partial\Psi(\xi,\mu)}{\partial\xi}\frac{\partial^2\Psi(\xi,\mu)}{\partial\xi^2}\right] \\
&+ \left[\frac{(\xi-1)^3}{(1-\mu^2)(\log(1-\xi)-1)^2}\frac{\partial\Psi(\xi,\mu)}{\partial\xi}\frac{\partial^3\Psi(\xi,\mu)}{\partial\xi^2\partial\mu}\right] \\
&+ \left[\frac{(\xi-1)^3}{(\log(1-\xi)-1)^2}\frac{\partial\Psi(\xi,\mu)}{\partial\mu}\frac{\partial^3\Psi(\xi,\mu)}{\partial\xi^3\partial\xi}\right].
\end{aligned}
\tag{4.1.6}
$$

4.1.2 Method

We replace the derivatives in equation (4.1.4) with the finite difference approximations and use the steps below to solve the equation:

• We choose $\delta\xi$ and $\delta\mu$ as step sizes.

• Create a ξ grid by dividing [0,0.9] into (Nξ+2) equal subintervals, the endpoints are at

$$\xi_i = a + (i-2)\delta\xi, \quad i = 2, 3.....(N\xi + 1), \quad \delta\xi = \frac{b-a}{(N\xi - 1)}. \tag{4.1.7}$$

• i = 1 and i = $N\xi + 2$ are ghost points.

• We choose 0.9 and 0.99 for the end point of the ξ and μ grids respectively because we cannot get to 1 due to the singularity of the Navier-Stokes equation.

• Create a μ grid by dividing [-0.99,0.99] into (Nμ+1) equal subintervals, the endpoints are at

$$\mu_j = c + (j-2)\delta\mu, \quad j = 2, 3.....(N\mu + 1), \quad \delta\mu = \frac{d-c}{(N\mu - 1)}. \tag{4.1.8}$$

• j = 1 and j = $N\mu + 2$ are ghost points.

• Replace the derivatives in the stream function equation with the below finite difference approximations. We use the explicit central difference scheme to second order accuracy.

$$\left(\frac{\partial \Psi}{\partial \xi}\right)_{i,j} = \frac{\Psi_{i+1,j} - \Psi_{i-1,j}}{2\delta\xi}$$

$$\left(\frac{\partial \Psi}{\partial \mu}\right)_{i,j} = \frac{\Psi_{i,j+1} - \Psi_{i,j-1}}{2\delta\mu}$$

$$\left(\frac{\partial^2 \Psi}{\partial \xi^2}\right)_{i,j} = \frac{\Psi_{i+1,j} - 2\Psi_{i,j} + \Psi_{i-1,j}}{(\delta\xi)^2}$$

$$\left(\frac{\partial^2 \Psi}{\partial \mu^2}\right)_{i,j} = \frac{\Psi_{i,j+1} - 2\Psi_{i,j} + \Psi_{i,j-1}}{(\delta\mu)^2}$$

$$\left(\frac{\partial^3 \Psi}{\partial \xi^3}\right)_{i,j} = \frac{-\Psi_{i-2,j} + 2\Psi_{i-1,j} - 2\Psi_{i+1,j} + \Psi_{i+2,j}}{2(\delta\xi)^3}$$

$$\left(\frac{\partial^3 \Psi}{\partial \mu^3}\right)_{i,j} = \frac{-\Psi_{i,j-2} + 2\Psi_{i,j-1} - 2\Psi_{i,j+1} + \Psi_{i,j+2}}{2(\delta\mu)^3}$$

$$\left(\frac{\partial^4 \Psi}{\partial \xi^4}\right)_{i,j} = \frac{\Psi_{i-2,j} - 4\Psi_{i-1,j} + 6\Psi_{i,j} - 4\Psi_{i+1,j} + \Psi_{i+2,j}}{(\delta\xi)^4}$$

$$\left(\frac{\partial^4 \Psi}{\partial \mu^4}\right)_{i,j} = \frac{\Psi_{i,j-2} - 4\Psi_{i,j-1} + 6\Psi_{i,j} - 4\Psi_{i,j+1} + \Psi_{i,j+2}}{(\delta\mu)^4}$$

$$\left(\frac{\partial^2 \Psi}{\partial \xi \partial \mu}\right)_{i,j} = \frac{\Psi_{i+1,j+1} - \Psi_{i-1,j+1}}{4\ \delta\xi\ \delta\mu} - \frac{\Psi_{i+1,j-1} - \Psi_{i-1,j-1}}{4\ \delta\xi\ \delta\mu}$$

$$\left(\frac{\partial^3 \Psi}{\partial \xi^2 \partial \mu}\right)_{i,j} = \frac{\Psi_{i+2,j+1} - \Psi_{i,j+1}}{8\ (\delta\xi)^2\ \delta\mu} - \frac{\Psi_{i+2,j-1} - \Psi_{i,j-1}}{8\ (\delta\xi)^2\ \delta\mu} - \frac{\Psi_{i,j+1} - \Psi_{i-2,j+1}}{8\ (\delta\xi)^2\ \delta\mu} + \frac{\Psi_{i,j-1} - \Psi_{i-2,j-1}}{8\ (\delta\xi)^2\ \delta\mu}$$

$$\left(\frac{\partial^3 \Psi}{\partial \xi \partial \mu^2}\right)_{i,j} = \frac{\Psi_{i+1,j+2} - \Psi_{i-1,j+2}}{8\ \delta\xi\ (\delta\mu)^2} - \frac{\Psi_{i+1,j} - \Psi_{i-1,j}}{8\ \delta\xi\ (\delta\mu)^2} - \frac{\Psi_{i+1,j} - \Psi_{i-1,j}}{8\ \delta\xi\ (\delta\mu)^2} + \frac{\Psi_{i+1,j-2} - \Psi_{i-1,j-2}}{8\ \delta\xi\ (\delta\mu)^2}$$

$$\left(\frac{\partial^4 \Psi}{\partial \xi^2 \partial \mu^2}\right)_{i,j} = \frac{\Psi_{i+1,j+1} - 2\ \Psi_{i+1,j} + \Psi_{i+1,j-1}}{(\delta\xi)^2\ (\delta\mu)^2} - 2\ \frac{\Psi_{i,j+1} - 2\ \Psi_{i,j} + \Psi_{i,j-1}}{(\delta\xi)^2\ (\delta\mu)^2} + \frac{\Psi_{i-1,j+1} - 2\ \Psi_{i-1,j} + \Psi_{i-1,j-1}}{(\delta\xi)^2\ (\delta\mu)^2}$$

• The Dirichlet boundary condition at the surface of the sphere is

$$\Psi_{2,j} = 0, \quad j = 2, 3, 4.....(N\mu + 1). \tag{4.1.9}$$

• The Neumann boundary condition at the surface of the sphere is

$$\left(\frac{\partial \Psi}{\partial \xi}\right)_{2,j} = \frac{\Psi_{3,j} - \Psi_{1,j}}{2\ \delta\xi} = 0, \quad j =, 3, 4, ...(N\mu), \tag{4.1.10}$$

then

$$\Psi_{1,j} = \Psi_{3,j}, \quad j = 3, 4.....(N\mu). \tag{4.1.11}$$

• The boundary condition far from the sphere is

$$\Psi_{N\xi+1,j} = 0, \quad j = 2, 3.....(N\mu + 1). \tag{4.1.12}$$

• We add a ghost point on the ξ grid far from the sphere

$$\Psi_{N\xi+2,j} = \Psi_{N\xi,j} + (1 - \mu_j^2), \ j = 3, 4.....(N\mu). \tag{4.1.13}$$

• We add a ghost point on the μ grid on each end point.

$$\Psi_{i,1} = -\Psi_{i,N\mu}, \quad i = 2, 3.....(N\xi + 1). \tag{4.1.14}$$

$$\Psi_{i,N\mu+2} = -\Psi_{i,3}, \quad i = 2, 3.....(N\xi + 1). \tag{4.1.15}$$

• The solution of Ψ_{n+1} is approximated by using the known solution of Ψ_n. The first term of Stokes solution will be used as the known solution to approximate the second term of the Stokes expansion.

Using matrix notation:

$$\begin{bmatrix} A_{1,1} & A_{1,2} & A_{1,3} & ... & A_{1,m} \\ A_{2,1} & A_{2,2} & A_{2,3} & ... & A_{2,m} \\ A_{3,1} & A_{3,2} & A_{3,3} & ... & A_{3,m} \\ . & . & . & ... & . \\ . & . & . & ... & . \\ . & . & . & ... & . \\ A_{m,1} & A_{m,2} & A_{m,3} & ... & A_{m,m} \end{bmatrix} \vec{\Psi}_{n+1} = \vec{B}_n$$

A is the finite difference approximation and is a matrix of order (m × m). B is equal to $\lambda D^2 \Psi_n$ and is a (m × 1) column matrix.

4.2 Numerical Methodology for Direct Simulation of the Navier-Stokes equations

We now solve the full Navier-Stokes equations for incompressible fluid flow past a sphere using a direct numerical simulation (DNS) method that uses a projection step, an implicit viscosity step, discretization on a staggered grid and the visualization of the solution over time. B. Seibold [65] used the method to the Navier-Stokes equations.

4.2.1 Navier-Stokes Equations

The Navier-Stokes equations in dimensionless form are given by

$$\underline{\nabla} \cdot \underline{V} = 0, \tag{4.2.1}$$

$$\frac{\partial \underline{V}}{\partial t} + (\underline{V} \cdot \underline{\nabla})\,\underline{V} = -\underline{\nabla} P + \frac{1}{Re}\nabla^2 \underline{V}. \tag{4.2.2}$$

subject to boundary conditions,

- The no slip boundary condition at the surface of the sphere

$$V_r(t, 1, \theta) = 0. \tag{4.2.3}$$

- The no cavities form boundary condition at the surface of the sphere

$$V_\theta(t, 1, \theta) = 0. \tag{4.2.4}$$

- Symmetry boundary condition

$$\frac{\partial}{\partial \theta}\left(V_\theta(t, r, 0)\right) = 0 \tag{4.2.5}$$

and

$$\frac{\partial}{\partial \theta}\left(V_\theta(t, r, \pi)\right) = 0. \tag{4.2.6}$$

- The boundary condition far from the sphere

$$V_r(t, r_\infty, \theta) = \frac{1}{r^2 \sin\theta}\frac{\partial \psi_0}{\partial \theta} \tag{4.2.7}$$

and

$$V_\theta(t, r_\infty, \theta) = -\frac{1}{r \sin\theta}\frac{\partial \psi_0}{\partial r}, \tag{4.2.8}$$

where r_∞ is the boundary for DNS, it correspond to $\xi = 0.9$.
The Navier-Stokes equations in spherical coordinates are

$$\frac{1}{r^2}\frac{\partial}{\partial r}\left(r^2 V_r\right) + \frac{1}{r\sin\theta}\frac{\partial}{\partial\theta}\left(V_\theta \sin\theta\right) = 0, \tag{4.2.9}$$

$$\frac{\partial V_r}{\partial t} + \left(V_r\frac{\partial V_r}{\partial r} + \frac{V_\theta}{r}\frac{\partial V_r}{\partial\theta} - \frac{V_\theta^2}{r}\right) = -\frac{\partial P}{\partial r}$$

$$+\frac{1}{Re}\left(\frac{1}{r^2}\frac{\partial^2}{\partial r^2}\left(r^2 V_r\right) + \frac{1}{r^2\sin\theta}\frac{\partial}{\partial\theta}\left(\sin\theta\frac{\partial V_r}{\partial\theta}\right)\right), \tag{4.2.10}$$

$$\frac{\partial V_\theta}{\partial t} + \left(V_r\frac{\partial V_\theta}{\partial r} + \frac{V_\theta}{r}\frac{\partial V_\theta}{\partial\theta}\right) = -\frac{\partial P}{\partial r}$$

$$+\frac{1}{Re}\left(\frac{1}{r^2}\frac{\partial}{\partial r}\left(r^2\frac{\partial V_\theta}{\partial r}\right)\right)$$

$$+\frac{1}{Re}\left(\frac{1}{r^2}\frac{\partial}{\partial\theta}\left(\frac{1}{\sin\theta}\frac{\partial}{\partial\theta}\left(V_\theta\sin\theta\right)\right) + \frac{2}{r^2}\frac{\partial V_r}{\partial\theta}\right). \tag{4.2.11}$$

4.2.2 Method

We define the velocity field at the n^{th} time step (t) as $\underline{V^n}$. We approximate the solution of the Navier-Stokes equations at the $(n+1)^{st}$ time step $(t+\triangle t)$ where $\triangle\ t$ is the step size. We use the steps below to approximate the solution:

- We approximate the nonlinear terms explicitly,

$$V_r^* = (V_r)^m - \triangle t\left((V_r)^m\frac{\partial(V_\theta)^m}{\partial r} + \frac{(V_\theta)^m}{r}\frac{\partial(V_r)^m}{\partial\theta} - \frac{(V_\theta^m)^2}{r}\right), \tag{4.2.12}$$

$$V_\theta^* = (V_r)^m - \triangle t\left((V_r)^m\frac{\partial(V_\theta)^m}{\partial r} + \frac{(V_\theta)^m}{r}\frac{\partial(V_\theta)^m}{\partial\theta}\right). \tag{4.2.13}$$

- We approximate the viscosity terms implicitly,

$$V_r^{**} = V_r^* - \frac{\triangle t}{Re}\left(\frac{1}{r^2}\frac{\partial^2}{\partial r^2}\left(r^2(V_r)^{**}\right) + \frac{1}{r^2\sin\theta}\frac{\partial}{\partial\theta}\left(\sin\theta\frac{\partial(V_r)^{**}}{\partial\theta}\right)\right) \tag{4.2.14}$$

and

$$V_\theta^{**} = V_\theta^* - \frac{\triangle t}{Re}\left(\frac{1}{r^2}\frac{\partial}{\partial r}\left(r^2\frac{\partial (V_\theta)^{**}}{\partial r}\right)\right) + \frac{\triangle t}{Re}\left(\frac{1}{r^2}\frac{\partial}{\partial \theta}\left(\frac{1}{\sin\theta}\frac{\partial}{\partial \theta}\left((V_\theta)^{**}\sin\theta\right)\right) + \frac{2}{r^2}\frac{\partial (V_r)^{**}}{\partial \theta}\right). \tag{4.2.15}$$

• We also approximate pressure implicitly,

$$\frac{\underline{V}^{m+1} - \underline{V}^{**}}{\triangle t} = -\nabla P^{m+1}. \tag{4.2.16}$$

By applying the divergence on both sides of equation (4.2.16) to enforce incompressibility we get

$$\frac{\nabla \cdot \underline{V}^{m+1} - \nabla \cdot \underline{V}^{**}}{\triangle t} = -\nabla^2 P^{m+1} \tag{4.2.17}$$

Then by using the incompressibility condition ($\underline{\nabla} \cdot \underline{V} = 0$), equation (4.2.17) becomes

$$\frac{\nabla \cdot \underline{V}^{**}}{\triangle t} = \nabla^2 P^{m+1}. \tag{4.2.18}$$

We use equation (4.2.19) to update the velocity.

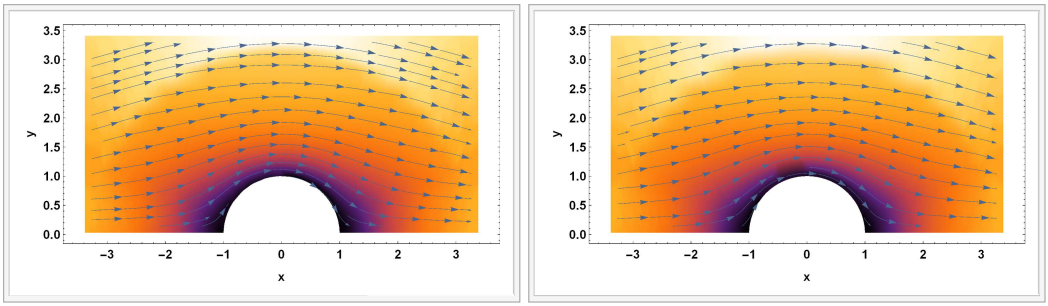
$$\frac{\nabla \cdot \underline{V}^{m+1}}{\triangle t} = \nabla P^{m+1}. \tag{4.2.19}$$

5 Numerical Results

5.1 Results

The numerical results of the stream function are generated using the second-order finite difference method (FDM). Figure 9 shows the streamlines for the first two terms of the stream function (Ψ) at $Re = 0.01$, 1.00, 10.00 and 50.00. We used 40×40 grid points to approximate the solution of the second term of Ψ. The vortex does not form at $Re = 0.01$, 1.00 and 10.00, it forms at $Re = 50.00$.

(a) $Re = 0.01$ (b) $Re = 1.00$



(c) $Re = 10.00$ (d) $Re = 50.00$

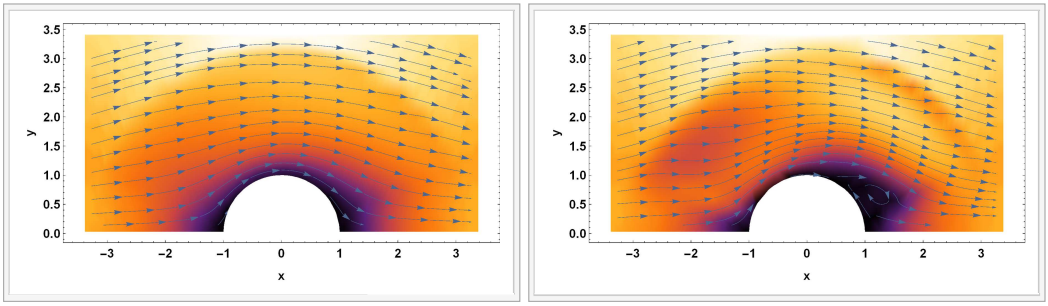
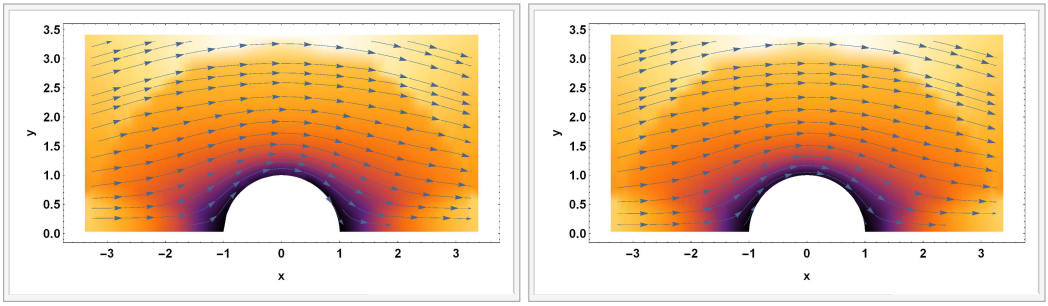


Figure 9: Streamlines for Ψ up to Ψ_1 for various values of Reynolds numbers using 40×40 grid points for r interval [1, 3.30259] (ξ interval [0, 0.9]).

In figure 10, we have approximated the solution for the first two terms of Ψ using 80×80 grid points at various Reynolds numbers. The results are in good agreement with the approximation of 40×40 grid points in figure 9.

(a) $Re = 0.01$ (b) $Re = 1.00$



(c) $Re = 10.00$ (d) $Re = 50.00$

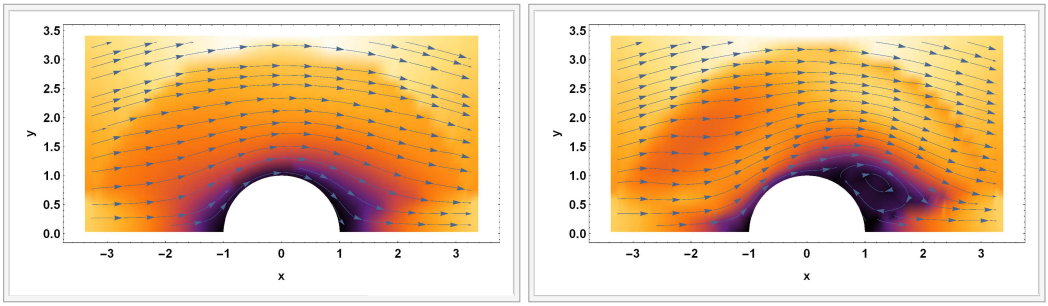
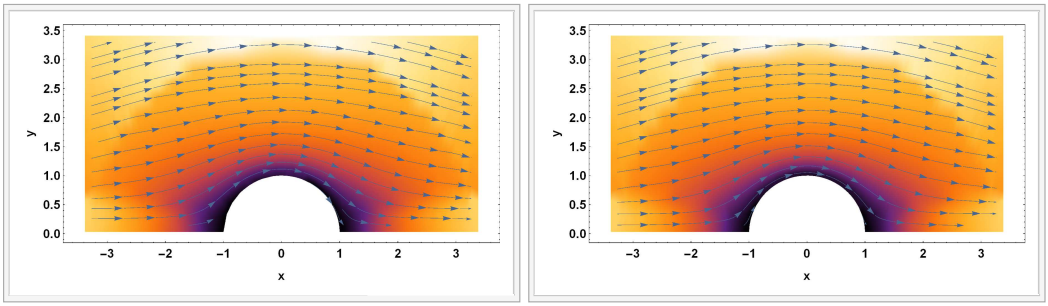


Figure 10: Streamlines for Ψ up to Ψ_1 using 80×80 grid points for r interval [1, 3.30259] (ξ interval [0, 0.9]).

Figure 11 shows the streamlines for the first six terms of Ψ using 80×80 grid points. The vortex also does not from at $Re = 0.01$, 1.00 and 10.00 but it forms at $Re = 50.00$.

(a) $Re = 0.01$ (b) $Re = 1.00$



(c) $Re = 10.00$ (d) $Re = 50.00$

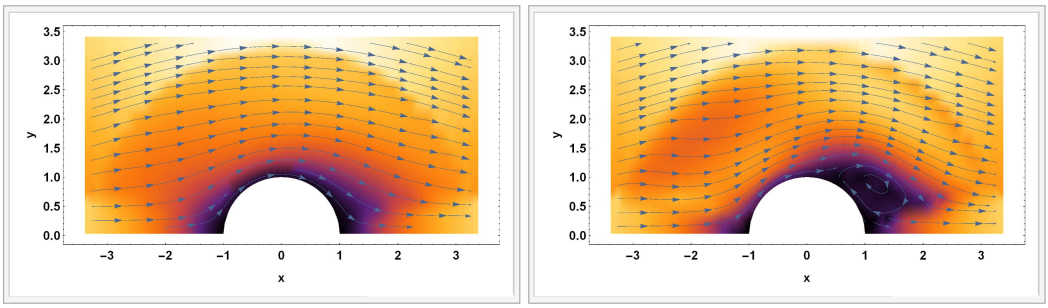
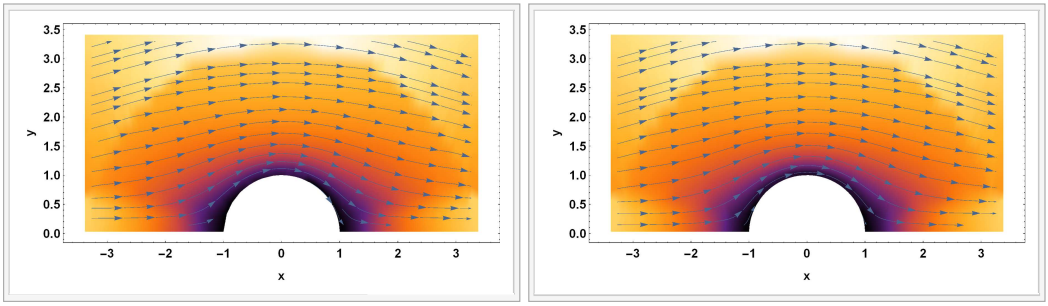


Figure 11: Streamlines for Ψ up to Ψ_5 for various values of Reynolds numbers using 80×80 grid points for r interval [1, 3.30259] (ξ interval [0, 0.9]).

Figure 12 shows the streamlines for the first eleven terms of Ψ at different values of Reynolds number. The vortex also does not from at $Re = 0.01$, 1.00 and 10.00 but it forms at $Re = 50.00$.

(a) $Re = 0.01$ (b) $Re = 1.00$



(c) $Re = 10.00$ (d) $Re = 50.00$

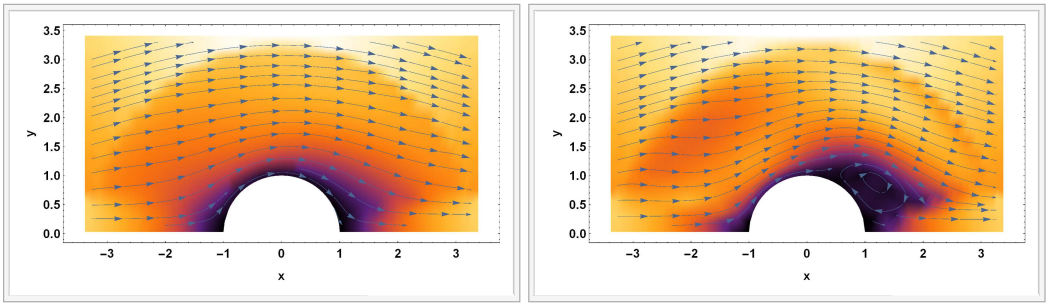
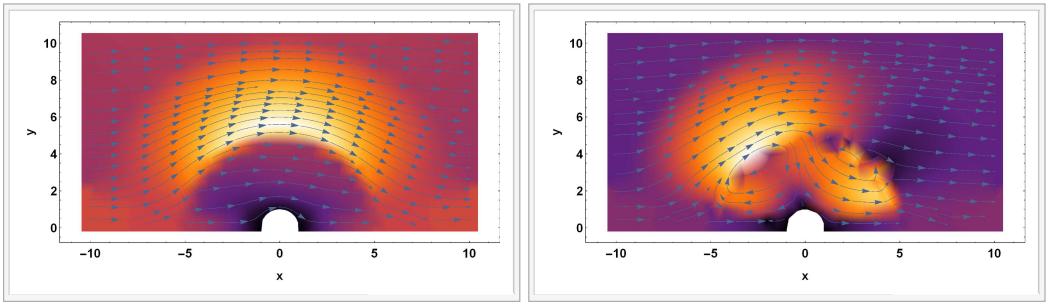


Figure 12: Streamlines for Ψ up to Ψ_{10} for various values of Reynolds numbers using 80×80 grid points for r interval [1, 3.30259] (ξ interval [0, 0.9]).

Figure 13 shows the streamlines of the first two terms of Ψ using 80×80 grid points for r interval [1, 10.2103] (ξ interval [0, 0.9999]) at $Re = 0.01$, 0.50, 10.00 and 50.00. The streamlines indicates that the solution is not in good agreement with solution for the first two term of Ψ for r interval [1, 3.30259] (ξ interval [0, 0.9]) in figure 10. The difference between the two solutions in figure 10 and 13 is the r interval. The r interval in figure 13 is further from the sphere as compared to the r interval in figure 10. The vortex forms early at $Re = 0.5$ which is not in agreement with the results obtained in figure 10. The vortex is expected to form at Re greater than 1 for stream function expansion. It looks like it is due to the Whitehead paradox affecting the solution for large r.

(a) $Re = 0.01$ (b) $Re = 0.50$



(c) $Re = 10.00$ (d) $Re = 50.00$

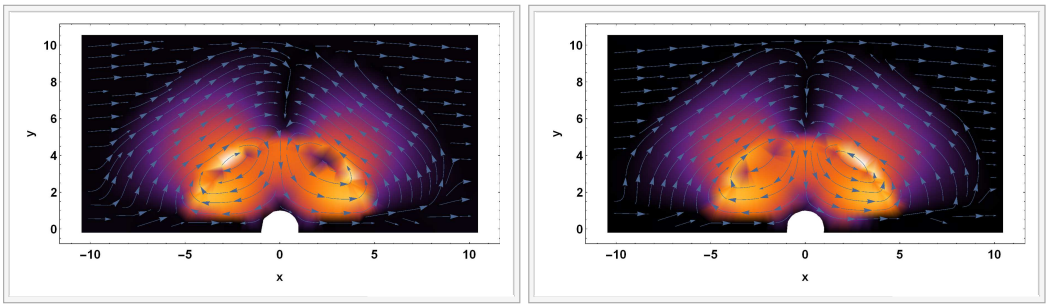


Figure 13: Streamlines for Ψ up to Ψ_{10} for various values of Reynolds numbers using 80×80 grid points for$r$ interval [1, 10.2103] (ξ interval [0, 0.9999])

5.2 Comparison of the Analytical and Numerical Results of the stream function

In this section we compare the analytical results with the numerical results of the stream function for the first two terms. We generated the analytical stream function values from the exact solution ($\psi_0 + Re\ \psi_1$) and the numerical stream function ($\Psi_0 + Re\ \Psi_1$) from the finite difference method (FDM). We used 40×40 data points to generate the values and created a table with r values on the top row and the θ values on the first column. The values in bold represents the analytical solution of the stream function and the values in normal font represents the numerical solution of the stream function.

Table 1 shows the analytical and numerical values of the stream functions for $Re = 0.01$. The values in table 1 indicates that the analytical results are in agreement with the numerical results. We then generated the analytical and numerical values for $Re = 1.00$ in Table 2. The analytical results are still in agreement with the numerical results. Table 3 shows the analytical and numerical results for $Re = 10.00$. The results are slight different but still in agreement because the difference is small. The analytical values changes the sign to negative from $\theta = 0.141539$ to 1.340300. We also note the increase of the analytical values from $\theta = 1.443530$ to 3.000050. The numerical values remains almost the same for $Re = 10.00$. The results in table 4 are for $Re = 50.00$, the analytical values are now negative from 0.141539 to 1.494570. Also the analytical values increases from $\theta = 1.545410$ to 3.000050. The numerical values does not change much from the values for $Re = 10.00$. We note that the numerical values are in good agreement with the analytical values for $Re \leq 1$.

θ \ r	1.07174		1.57708		2.9231	
0.141539	**0.0000747**	0.0000751	**0.0043454**	0.0043640	**0.0429244**	0.0430924
0.350414	**0.0004427**	0.0004446	**0.0257384**	0.0258372	**0.2542450**	0.2551930
0.476814	**0.0007916**	0.0007947	**0.0460147**	0.0461821	**0.4545260**	0.4561340
0.577752	**0.0011212**	0.0011254	**0.0651735**	0.0653978	**0.6437610**	0.6459120
0.664990	**0.0014316**	0.0014366	**0.0832141**	0.0834838	**0.8219440**	0.8245250
0.743426	**0.0017227**	0.0017284	**0.1001360**	0.1004400	**0.9890680**	0.9919730
0.815665	**0.0019946**	0.0020008	**0.1159380**	0.1162660	**1.1451300**	1.1482600
0.883286	**0.0022473**	0.0022537	**0.1306190**	0.1309620	**1.2901100**	1.2933800
0.947338	**0.0024806**	0.0024872	**0.1441800**	0.1445280	**1.4240200**	1.4273300
1.008560	**0.0026947**	0.0027012	**0.1566180**	0.1569640	**1.5468400**	1.5501300
1.067510	**0.0028895**	0.0028958	**0.1679340**	0.1682690	**1.6585600**	1.6617500
1.124600	**0.0030649**	0.0030709	**0.1781260**	0.1784450	**1.7591900**	1.7622200
1.180170	**0.0032211**	0.0032266	**0.1871940**	0.1874900	**1.8487100**	1.8515200
1.234490	**0.0033578**	0.0033629	**0.1951380**	0.1954040	**1.9271200**	1.9296600
1.287800	**0.0034753**	0.0034796	**0.2019550**	0.2021890	**1.9944100**	1.9966300
1.340300	**0.0035733**	0.0035770	**0.2076460**	0.2078430	**2.0505800**	2.0524400
1.392160	**0.0036519**	0.0036549	**0.2122110**	0.2123670	**2.0956100**	2.0970900
1.443530	**0.0037112**	0.0037133	**0.2156470**	0.2157600	**2.1295000**	2.1305800
1.494570	**0.0037510**	0.0037523	**0.2179540**	0.2180230	**2.1522400**	2.1529000
1.545410	**0.0037714**	0.0037718	**0.2191320**	0.2191560	**2.1638400**	2.1640500
1.596180	**0.0037723**	0.0037719	**0.2191810**	0.2191580	**2.1642700**	2.1640500
1.647020	**0.0037538**	0.0037525	**0.2180980**	0.2180290	**2.1535300**	2.1528800
1.698060	**0.0037157**	0.0037136	**0.2158830**	0.2157700	**2.1316300**	2.1305500
1.749440	**0.0036582**	0.0036553	**0.2125370**	0.2123800	**2.0985400**	2.0970600
1.801290	**0.0035812**	0.0035775	**0.2080570**	0.2078600	**2.0542700**	2.0524000
1.853790	**0.0034847**	0.0034803	**0.2024430**	0.2022100	**1.9988000**	1.9965800
1.907100	**0.0033686**	0.0033636	**0.1956950**	0.1954280	**1.9321400**	1.9296000
1.961420	**0.0032330**	0.0032275	**0.1878120**	0.1875160	**1.8542700**	1.8514600
2.016990	**0.0030778**	0.0030719	**0.1787920**	0.1784730	**1.7651800**	1.7621500
2.074080	**0.0029031**	0.0028968	**0.1686350**	0.1683000	**1.6648800**	1.6616900
2.133030	**0.0027087**	0.0027022	**0.1573410**	0.1569960	**1.5533400**	1.5500500
2.194250	**0.0024948**	0.0024882	**0.1449090**	0.1445610	**1.4305800**	1.4272600
2.258310	**0.0022612**	0.0022548	**0.1313380**	0.1309950	**1.2965700**	1.2933100
2.325930	**0.0020080**	0.0020018	**0.1166270**	0.1162980	**1.1513200**	1.1481900
2.398170	**0.0017351**	0.0017294	**0.1007750**	0.1004710	**0.9948180**	0.9919130
2.476600	**0.0014426**	0.0014375	**0.0837821**	0.0835124	**0.8270530**	0.8244730
2.563840	**0.0011303**	0.0011261	**0.0656472**	0.0654228	**0.6480220**	0.6458710
2.664780	**0.0007984**	0.0007953	**0.0463694**	0.0462020	**0.4577170**	0.4561090
2.791180	**0.0004468**	0.0004450	**0.0259482**	0.0258494	**0.2561320**	0.2551840
3.000050	**0.0000755**	0.0000751	**0.0043827**	0.0043640	**0.0432604**	0.0430924

Table 1: Comparison of the analytical ($\psi_0+Re\psi_1$) and numerical ($\Psi_0+Re\Psi_1$) results of the stream function for $Re = 0.01$. The analytical values are in bold font and numerical values in normal font. The vertical and horizontal values represents θ and r respectively.

θ \ r	1.07174		1.57708		2.9231	
0.141539	**0.0000389**	0.0000751	**0.0024966**	0.0043640	**0.0262949**	0.0430924
0.350414	**0.0002416**	0.0004253	**0.0153516**	0.0252309	**0.1608170**	0.2556160
0.476814	**0.0004515**	0.0007643	**0.0284530**	0.0452003	**0.2965600**	0.4574130
0.577752	**0.0006671**	0.0010869	**0.0417263**	0.0641600	**0.4328560**	0.6479100
0.664990	**0.0008871**	0.0013924	**0.0550971**	0.0820690	**0.5690340**	0.8270850
0.743426	**0.0011100**	0.0016802	**0.0684910**	0.0989074	**0.7044260**	0.9949550
0.815665	**0.0013342**	0.0019500	**0.0818336**	0.1146640	**0.8383620**	1.1515300
0.883286	**0.0015585**	0.0022018	**0.0950504**	0.1293310	**0.9701720**	1.2968400
0.947338	**0.0017814**	0.0024353	**0.1080670**	0.1429040	**1.0991900**	1.4308800
1.008560	**0.0020013**	0.0026504	**0.1208090**	0.1553780	**1.2247400**	1.5536600
1.067510	**0.0022170**	0.0028470	**0.1332020**	0.1667500	**1.3461500**	1.6651900
1.124600	**0.0024268**	0.0030250	**0.1451710**	0.1770180	**1.4627700**	1.7654900
1.180170	**0.0026295**	0.0031843	**0.1566430**	0.1861780	**1.5739100**	1.8545600
1.234490	**0.0028235**	0.0033248	**0.1675420**	0.1942270	**1.6789100**	1.9324100
1.287800	**0.0030074**	0.0034465	**0.1777950**	0.2011640	**1.7770900**	1.9990400
1.340300	**0.0031798**	0.0035492	**0.1873260**	0.2069840	**1.8678000**	2.0544700
1.392160	**0.0033392**	0.0036328	**0.1960620**	0.2116860	**1.9503500**	2.0987100
1.443530	**0.0034842**	0.0036973	**0.2039280**	0.2152670	**2.0240900**	2.1317500
1.494570	**0.0036134**	0.0037426	**0.2108490**	0.2177250	**2.0883400**	2.1536100
1.545410	**0.0037253**	0.0037686	**0.2167520**	0.2190560	**2.1424200**	2.1642900
1.596180	**0.0038184**	0.0037751	**0.2215610**	0.2192570	**2.1856800**	2.1638100
1.647020	**0.0038913**	0.0037621	**0.2252030**	0.2183270	**2.2174400**	2.1521700
1.698060	**0.0039427**	0.0037296	**0.2276020**	0.2162630	**2.2370400**	2.1293800
1.749440	**0.0039709**	0.0036774	**0.2286850**	0.2130610	**2.2438000**	2.0954400
1.801290	**0.0039747**	0.0036054	**0.2283770**	0.2087190	**2.2370500**	2.0503700
1.853790	**0.0039525**	0.0035135	**0.2266040**	0.2032350	**2.2161200**	1.9941700
1.907100	**0.0039030**	0.0034017	**0.2232900**	0.1966050	**2.1803500**	1.9268500
1.961420	**0.0038246**	0.0032698	**0.2183630**	0.1888280	**2.1290700**	1.8484200
2.016990	**0.0037160**	0.0031178	**0.2117470**	0.1799000	**2.0616100**	1.7588800
2.074080	**0.0035756**	0.0029456	**0.2033670**	0.1698190	**1.9772900**	1.6582500
2.133030	**0.0034021**	0.0027531	**0.1931510**	0.1585820	**1.8754400**	1.5465200
2.194250	**0.0031940**	0.0025401	**0.1810220**	0.1461850	**1.7554100**	1.4237200
2.258310	**0.0029499**	0.0023067	**0.1669070**	0.1326260	**1.6165100**	1.2898500
2.325930	**0.0026683**	0.0020526	**0.1507310**	0.1179010	**1.4580900**	1.1449100
2.398170	**0.0023478**	0.0017776	**0.1324200**	0.1020030	**1.2794600**	0.9889310
2.476600	**0.0019870**	0.0014817	**0.1118990**	0.0849272	**1.0799600**	0.8219120
2.563840	**0.0015844**	0.0011646	**0.0890943**	0.0666607	**0.8589270**	0.6438730
2.664780	**0.0011385**	0.0008257	**0.0639311**	0.0471838	**0.6156830**	0.4548300
2.791180	**0.0006479**	0.0004642	**0.0363349**	0.0264557	**0.3495600**	0.2547610
3.000050	**0.0001113**	0.0000751	**0.0062315**	0.0043640	**0.0598899**	0.0430924

Table 2: Comparison of the analytical ($\psi_0+Re\psi_1$) and numerical ($\Psi_0+Re\Psi_1$) results of the stream function for $Re = 1.00$. The analytical values are in bold font and numerical values in normal font. The vertical and horizontal values represents θ and r respectively.

θ \ r	1.07174		1.57708		2.9231	
0.141539	**-0.0002865**	0.0000751	**-0.0143104**	0.0043640	**-0.1248820**	0.0430924
0.350414	**-0.0015868**	0.0002503	**-0.0790734**	0.0197191	**-0.6885280**	0.2594670
0.476814	**-0.0026399**	0.0004878	**-0.1311980**	0.0362749	**-1.1394900**	0.4690320
0.577752	**-0.0034603**	0.0007375	**-0.1714300**	0.0529069	**-1.4844600**	0.6660790
0.664990	**-0.0040624**	0.0009902	**-0.2005120**	0.0692071	**-1.7301500**	0.8503660
0.743426	**-0.0044605**	0.0012415	**-0.2191890**	0.0849757	**-1.8832300**	1.0220600
0.815665	**-0.0046692**	0.0014887	**-0.2282040**	0.1000990	**-1.9504000**	1.1813200
0.883286	**-0.0047027**	0.0017298	**-0.2283030**	0.1145030	**-1.9383700**	1.3282900
0.947338	**-0.0045756**	0.0019634	**-0.2202300**	0.1281370	**-1.8538100**	1.4630700
1.008560	**-0.0043022**	0.0021881	**-0.2047280**	0.1409610	**-1.7034400**	1.5857600
1.067510	**-0.0038970**	0.0024030	**-0.1825430**	0.1529420	**-1.4939400**	1.6964600
1.124600	**-0.0033743**	0.0026071	**-0.1544170**	0.1640480	**-1.2320000**	1.7952500
1.180170	**-0.0027485**	0.0027993	**-0.1210960**	0.1742510	**-0.9243300**	1.8822100
1.234490	**-0.0020342**	0.0029789	**-0.0833237**	0.1835250	**-0.5776110**	1.9574200
1.287800	**-0.0012456**	0.0031448	**-0.0418443**	0.1918430	**-0.1985420**	2.0209700
1.340300	**-0.0003972**	0.0032963	**0.0025979**	0.1991770	**0.2061830**	2.0729300
1.392160	**0.0004966**	0.0034323	**0.0492587**	0.2055010	**0.6298700**	2.1133900
1.443530	**0.0014214**	0.0035521	**0.0973938**	0.2107890	**1.0658200**	2.1424100
1.494570	**0.0023627**	0.0036546	**0.1462590**	0.2150140	**1.5073500**	2.1600700
1.545410	**0.0033062**	0.0037391	**0.1951100**	0.2181480	**1.9477600**	2.1664600
1.596180	**0.0042374**	0.0038046	**0.2432030**	0.2201650	**2.3803500**	2.1616500
1.647020	**0.0051420**	0.0038501	**0.2897930**	0.2210390	**2.7984300**	2.1457100
1.698060	**0.0060055**	0.0038748	**0.3341360**	0.2207410	**3.1953000**	2.1187200
1.749440	**0.0068136**	0.0038778	**0.3754890**	0.2192460	**3.5642800**	2.0807600
1.801290	**0.0075517**	0.0038582	**0.4131050**	0.2165260	**3.8986600**	2.0319100
1.853790	**0.0082055**	0.0038151	**0.4462430**	0.2125560	**4.1917600**	1.9722400
1.907100	**0.0087606**	0.0037476	**0.4741560**	0.2073070	**4.4368700**	1.9018400
1.961420	**0.0092026**	0.0036548	**0.4961020**	0.2007540	**4.6273100**	1.8207700
2.016990	**0.0095170**	0.0035357	**0.5113350**	0.1928700	**4.7563800**	1.7291300
2.074080	**0.0096895**	0.0033896	**0.5191120**	0.1836280	**4.8173800**	1.6269800
2.133030	**0.0097057**	0.0032153	**0.5186880**	0.1729980	**4.8036200**	1.5144200
2.194250	**0.0095510**	0.0030121	**0.5093190**	0.1609520	**4.7084100**	1.3915300
2.258310	**0.0092112**	0.0027786	**0.4902600**	0.1474540	**4.5250500**	1.2583900
2.325930	**0.0086718**	0.0025139	**0.4607690**	0.1324660	**4.2468500**	1.1151200
2.398170	**0.0079183**	0.0022163	**0.4200990**	0.1159350	**3.8671100**	0.9618250
2.476600	**0.0069365**	0.0018839	**0.3675080**	0.0977891	**3.3791400**	0.7986310
2.563840	**0.0057118**	0.0015140	**0.3022500**	0.0779137	**2.7762500**	0.6257040
2.664780	**0.0042299**	0.0011021	**0.2235830**	0.0561092	**2.0517300**	0.4432110
2.791180	**0.0024763**	0.0006393	**0.1307600**	0.0319675	**1.1989000**	0.2509100
3.000050	**0.0004367**	0.0000751	**0.0230385**	0.0043640	**0.2110670**	0.0430924

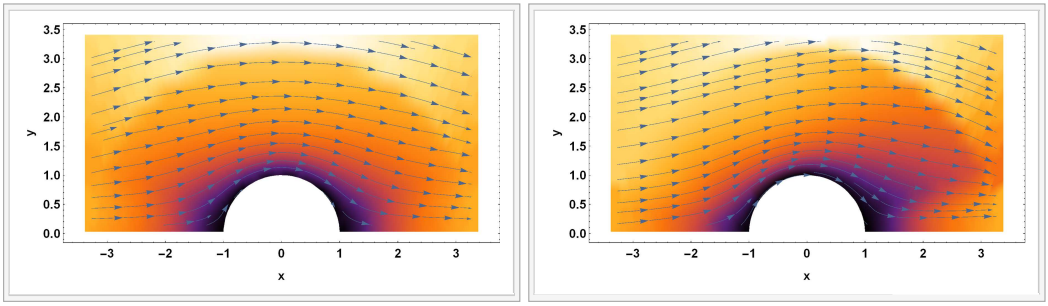
Table 3: Comparison of the analytical ($\psi_0+Re\psi_1$) and numerical ($\Psi_0+Re\Psi_1$) results of the stream function for $Re = 10.00$. The analytical values are in bold font and numerical values in normal font. The vertical and horizontal values represents θ and r respectively.

θ \ r	1.07174		1.57708		2.9231	
0.141539	**-0.0017329**	0.0000751	**-0.0890081**	0.0043640	**-0.7967810**	0.0430924
0.350414	**-0.0097130**	-0.0005279	**-0.4987400**	-0.0047777	**-4.4633900**	0.2765800
0.476814	**-0.0163795**	-0.0007407	**-0.8407600**	-0.0033936	**-7.5219400**	0.5206740
0.577752	**-0.0218045**	-0.0008155	**-1.1187900**	0.0028933	**-10.0059000**	0.7468280
0.664990	**-0.0260601**	-0.0007972	**-1.3365500**	0.0120432	**-11.9487000**	0.9538370
0.743426	**-0.0292182**	-0.0007080	**-1.4977600**	0.0230567	**-13.3839000**	1.1425300
0.815665	**-0.0313510**	-0.0005616	**-1.6061500**	0.0353639	**-14.3449000**	1.3137300
0.883286	**-0.0325305**	-0.0003679	**-1.6654300**	0.0486006	**-14.8652000**	1.4680800
0.947338	**-0.0328288**	-0.0001341	**-1.6793300**	0.0625088	**-14.9783000**	1.6061600
1.008560	**-0.0323179**	0.0001336	**-1.6515600**	0.0768881	**-14.7176000**	1.7284500
1.067510	**-0.0310699**	0.0004299	**-1.5858500**	0.0915697	**-14.1166000**	1.8354200
1.124600	**-0.0291568**	0.0007497	**-1.4859200**	0.1064030	**-13.2088000**	1.9274900
1.180170	**-0.0266507**	0.0010884	**-1.3554900**	0.1212450	**-12.0276000**	2.0050800
1.234490	**-0.0236237**	0.0014414	**-1.1982800**	0.1359620	**-10.6066000**	2.0685900
1.287800	**-0.0201477**	0.0018042	**-1.0180200**	0.1504170	**-8.9791400**	2.1184300
1.340300	**-0.0162949**	0.0021723	**-0.8184170**	0.1644780	**-7.1787700**	2.1549800
1.392160	**-0.0121373**	0.0025413	**-0.6032010**	0.1780120	**-5.2389500**	2.1786300
1.443530	**-0.0077470**	0.0029066	**-0.3760910**	0.1908850	**-3.1931300**	2.1897800
1.494570	**-0.0031959**	0.0032637	**-0.1408090**	0.2029630	**-1.0748000**	2.1888000
1.545410	**0.0014437**	0.0036082	**0.0989247**	0.2141130	**1.0825800**	2.1760900
1.596180	**0.0060999**	0.0039355	**0.3393880**	0.2242000	**3.2455300**	2.1520200
1.647020	**0.0107007**	0.0042410	**0.5768610**	0.2330890	**5.3805800**	2.1169800
1.698060	**0.0151739**	0.0045203	**0.8076210**	0.2406450	**7.4542600**	2.0713500
1.749440	**0.0194475**	0.0047689	**1.0279500**	0.2467360	**9.4331000**	2.0155200
1.801290	**0.0234494**	0.0049822	**1.2341200**	0.2512250	**11.2836000**	1.9498700
1.853790	**0.0271077**	0.0051558	**1.4224200**	0.2539820	**12.9724000**	1.8747900
1.907100	**0.0303501**	0.0052851	**1.5891200**	0.2548710	**14.4658000**	1.7906700
1.961420	**0.0331048**	0.0053657	**1.7305000**	0.2537600	**15.7306000**	1.6979000
2.016990	**0.0352996**	0.0053931	**1.8428400**	0.2505150	**16.7331000**	1.5968800
2.074080	**0.0368625**	0.0053627	**1.9224200**	0.2450000	**17.4400000**	1.4880200
2.133030	**0.0377214**	0.0052698	**1.9655200**	0.2370710	**17.8177000**	1.3717300
2.194250	**0.0378042**	0.0051095	**1.9684200**	0.2265800	**17.8329000**	1.2484400
2.258310	**0.0370390**	0.0048763	**1.9273900**	0.2133570	**17.4519000**	1.1186000
2.325930	**0.0353536**	0.0045642	**1.8387100**	0.1972010	**16.6414000**	0.9827230
2.398170	**0.0326760**	0.0041658	**1.6986800**	0.1778540	**15.3678000**	0.8413540
2.476600	**0.0289342**	0.0036713	**1.5035500**	0.1549530	**13.5977000**	0.6951600
2.563840	**0.0240560**	0.0030670	**1.2496100**	0.1279270	**11.2977000**	0.5449550
2.664780	**0.0179695**	0.0023307	**0.9331450**	0.0957777	**8.4341800**	0.3915690
2.791180	**0.0106025**	0.0014174	**0.5504270**	0.0564642	**4.9737700**	0.2337970
3.000050	**0.0018831**	0.0000751	**0.0977361**	0.0043640	**0.8829660**	0.0430924

Table 4: Comparison of the analytical ($\psi_0+Re\psi_1$) and numerical ($\Psi_0+Re\Psi_1$) results of the stream function for $Re = 50.00$. The analytical values are in bold font and numerical values in normal font. The vertical and horizontal values represents θ and r respectively.

Figure 14 shows the streamlines of the analytical solution of the stream function at $Re = 0.01$, 1.00, 10.00 and 50.00. The vortex does not form at $Re = 0.01$ and 1.00. The flow pattern breaks at $Re = 10.00$ and 50.00 because analytical solutions are valid for $Re \leq 1$. Figure 15 shows the streamlines of the numerical solution of the stream function at $Re = 0.01$, 1.00, 10.00 and 50.00. The streamlines of the analytical and numerical solution of the stream function are in good agreement at $Re = 0.01$ and 1.00. The flow pattern of the numerical solution does not change at $Re = 10.00$ and the vortex forms at $Re = 50.00$. The two solutions are not in agreement at $Re > 1$. This is because the analytical solution breaks for $Re > 1$, the breaking of the solution is called the Whitehead paradox.

(a) $Re = 0.01$ (b) $Re = 1.00$



(c) $Re = 10.00$ (d) $Re = 50.00$

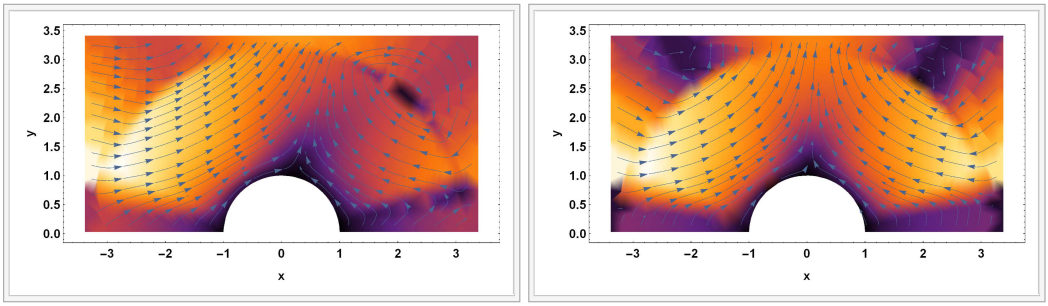
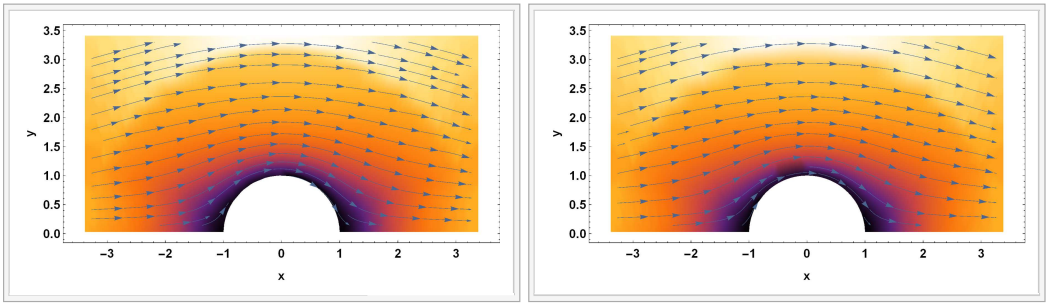


Figure 14: Streamlines of the analytical results for various values of Reynolds numbers using 40×40 grid points.

(a) $Re = 0.01$ (b) $Re = 1.00$



(c) $Re = 10.00$ (d) $Re = 50.00$

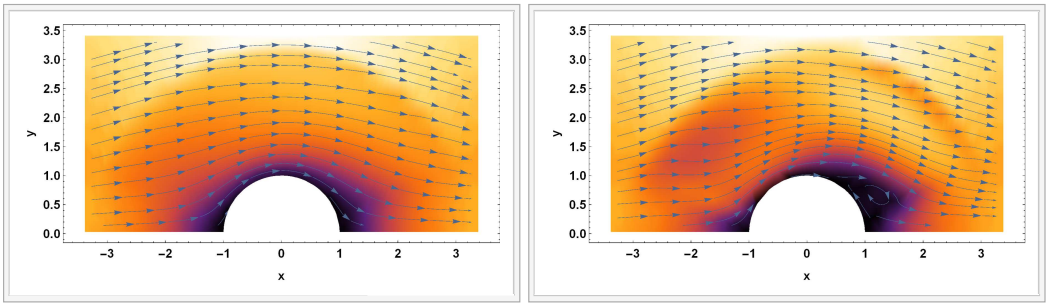


Figure 15: Streamlines of the numerical results for various values of Reynolds numbers using 40×40 grid points.

5.3 Comparison of the numerical results of the direct numerical simulation (DNS) and finite difference method (FDM)

In this section we compare the numerical solution of the full Navier-Stokes equations and the stream function in terms of the radial velocity (V_r) and tangential velocity (V_θ). The stream function solution is generated using the finite difference method (FDM) in section 4.1 and the numerical solution of the full Navier-Stokes solution is simulated using the direct numerical simulation (DNS) in section 4.2. We generated tables 5, 6, 7, 8, 9, 10, 11 and 12 with r values on the top row and the θ values on the first column. The numerical values of the DNS solution are in bold font and the numerical values of the FDM solution are in normal font. We used 40×40 data points to generate both solutions.

Table 5 shows the numerical values of the DNS and the FDM solutions in terms of the radial velocity (V_r) at $Re = 0.01$. We note that the numerical values of the DNS solution are in good agreement with numerical values of the FDM solution in terms of the radial velocity (V_r). Also the numerical values of the FDM solution in terms of the tangential velocity (V_θ) in table 6 are in agreement with the numerical values of the DNS solution at $Re = 0.01$. We also noted the slight difference in the values especially for $r = 1.07174$.

At $Re = 1.00$ in table 7 and 8, the numerical values of the DNS solution are still in good agreement with numerical values of the FDM solution in terms of V_r and V_θ respectively. We increased the value of Re to 10.00 in tables 9 and 10 and we can see that the values of the FDM solution are still in agreement with the values of the DNS solution. Also in tables 11 and 12, we increased Re to 50.00 and the numerical values of the FDM solution and the DNS solution are in agreement with a slight difference but it is within the order of magnitude.

θ \ r	1.07174		1.57708		2.9231	
0.141539	**0.0182819**	0.0076271	**0.1641437**	0.2046640	**0.4342778**	0.5882670
0.350414	**0.0165550**	0.0061697	**0.1587805**	0.1655880	**0.4302208**	0.4760770
0.476814	**0.0146964**	0.0058371	**0.1502572**	0.1566490	**0.4159874**	0.4503480
0.577752	**0.0142848**	0.0055039	**0.1434394**	0.1477040	**0.3944165**	0.4246110
0.664990	**0.0136589**	0.0051706	**0.1358396**	0.1387570	**0.3712948**	0.3988750
0.743426	**0.0129304**	0.0048372	**0.1277837**	0.1298090	**0.3477107**	0.3731380
0.815665	**0.0121420**	0.0045038	**0.1194458**	0.1208590	**0.3239342**	0.3474030
0.883286	**0.0113151**	0.0041704	**0.1109244**	0.1119090	**0.3000605**	0.3216670
0.947338	**0.0104616**	0.0038370	**0.1022791**	0.1029590	**0.2761316**	0.2959320
1.008560	**0.0095892**	0.0035035	**0.0935475**	0.0940089	**0.2521691**	0.2701960
1.067510	**0.0087030**	0.0031700	**0.0847547**	0.0850582	**0.2281852**	0.2444620
1.124600	**0.0078064**	0.0028365	**0.0759176**	0.0761073	**0.2041873**	0.2187270
1.180170	**0.0069020**	0.0025030	**0.0670480**	0.0671562	**0.1801801**	0.1929920
1.234490	**0.0059917**	0.0021695	**0.0581544**	0.0582048	**0.1561667**	0.1672580
1.287800	**0.0050768**	0.0018359	**0.0492428**	0.0492533	**0.1321492**	0.1415240
1.340300	**0.0041585**	0.0015024	**0.0403177**	0.0403015	**0.1081288**	0.1157900
1.392160	**0.0032377**	0.0011688	**0.0313826**	0.0313495	**0.0841066**	0.0900559
1.443530	**0.0023149**	0.0008352	**0.0224401**	0.0223974	**0.0600832**	0.0643223
1.494570	**0.0013908**	0.0005016	**0.0134924**	0.0134450	**0.0360590**	0.0385888
1.545410	**0.0004660**	0.0001679	**0.0045412**	0.0044923	**0.0120344**	0.0128555
1.596180	**-0.0004592**	-0.0001657	**-0.0044119**	-0.0044605	**-0.0119905**	-0.0128776
1.647020	**-0.0013841**	-0.0004994	**-0.0133652**	-0.0134135	**-0.0360155**	-0.0386105
1.698060	**-0.0023084**	-0.0008330	**-0.0223173**	-0.0223668	**-0.0600404**	-0.0643433
1.749440	**-0.0032316**	-0.0011667	**-0.0312662**	-0.0313203	**-0.0840648**	-0.0900759
1.801290	**-0.0041529**	-0.0015004	**-0.0402098**	-0.0402739	**-0.1080884**	-0.1158080
1.853790	**-0.0050718**	-0.0018341	**-0.0491456**	-0.0492278	**-0.1321106**	-0.1415410
1.907100	**-0.0059874**	-0.0021679	**-0.0580699**	-0.0581819	**-0.1561302**	-0.1672730
1.961420	**-0.0068985**	-0.0025016	**-0.0669784**	-0.0671362	**-0.1801459**	-0.1930040
2.016990	**-0.0078038**	-0.0028354	**-0.0758648**	-0.0760908	**-0.2041557**	-0.2187360
2.074080	**-0.0087013**	-0.0031692	**-0.0847207**	-0.0850455	**-0.2281565**	-0.2444680
2.133030	**-0.0095886**	-0.0035030	**-0.0935343**	-0.0940005	**-0.2521435**	-0.2701990
2.194250	**-0.0104621**	-0.0038368	**-0.1022884**	-0.1029560	**-0.2761093**	-0.2959300
2.258310	**-0.0113167**	-0.0041706	**-0.1109580**	-0.1119110	**-0.3000415**	-0.3216610
2.325930	**-0.0121448**	-0.0045045	**-0.1195051**	-0.1208670	**-0.3239185**	-0.3473910
2.398170	**-0.0129342**	-0.0048384	**-0.1278700**	-0.1298240	**-0.3476981**	-0.3731220
2.476600	**-0.0136637**	-0.0051723	**-0.1359537**	-0.1387810	**-0.3712850**	-0.3988520
2.563840	**-0.0142903**	-0.0055063	**-0.1435812**	-0.1477390	**-0.3944092**	-0.4245810
2.664780	**-0.0147024**	-0.0058404	**-0.1504254**	-0.1567000	**-0.4159727**	-0.4503110
2.791180	**-0.0165688**	-0.0061750	**-0.1589953**	-0.1656670	**-0.4302083**	-0.4760480
3.000050	**-0.0183034**	-0.0076271	**-0.1643926**	-0.2046640	**-0.4342761**	-0.5882670

Table 5: Comparison of the direct numerical simulation (DNS) and finite difference method (FDM) results of the radial velocity (V_r) for $Re = 0.01$. The DNS values are in bold font and FDM values in normal font. The vertical and horizontal values represents θ and r respectively.

θ \ r	1.07174		1.57708		2.9231	
0.141539	**-0.0246469**	-0.0137457	**-0.0671936**	-0.0651056	**-0.1186507**	-0.1049560
0.350414	**-0.0432363**	-0.0334363	**-0.1129280**	-0.1584100	**-0.1975803**	-0.2554220
0.476814	**-0.0694307**	-0.0447040	**-0.1760151**	-0.2117890	**-0.3088930**	-0.3414740
0.577752	**-0.0834345**	-0.0531989	**-0.2097160**	-0.2520290	**-0.3706880**	-0.4063420
0.664990	**-0.0952385**	-0.0601079	**-0.2397471**	-0.2847560	**-0.4241804**	-0.4590970
0.743426	**-0.1052999**	-0.0659314	**-0.2651197**	-0.3123390	**-0.4685999**	-0.5035600
0.815665	**-0.1140131**	-0.0709370	**-0.2869292**	-0.3360470	**-0.5064320**	-0.5417760
0.883286	**-0.1216269**	-0.0752881	**-0.3058768**	-0.3566540	**-0.5391237**	-0.5749940
0.947338	**-0.1283099**	-0.0790926	**-0.3224333**	-0.3746710	**-0.5675935**	-0.6040370
1.008560	**-0.1341824**	-0.0824263	**-0.3369304**	-0.3904580	**-0.5924662**	-0.6294830
1.067510	**-0.1393336**	-0.0853443	**-0.3496113**	-0.4042750	**-0.6141881**	-0.6517550
1.124600	**-0.1438313**	-0.0878880	**-0.3606587**	-0.4163190	**-0.6330890**	-0.6711690
1.180170	**-0.1477281**	-0.0900890	**-0.3702130**	-0.4267400	**-0.6494191**	-0.6879650
1.234490	**-0.1510651**	-0.0919721	**-0.3783833**	-0.4356540	**-0.6633706**	-0.7023330
1.287800	**-0.1538747**	-0.0935563	**-0.3852547**	-0.4431530	**-0.6750929**	-0.7144180
1.340300	**-0.1561823**	-0.0948565	**-0.3908937**	-0.4493060	**-0.6847018**	-0.7243350
1.392160	**-0.1580076**	-0.0958844	**-0.3953516**	-0.4541690	**-0.6922865**	-0.7321720
1.443530	**-0.1593655**	-0.0966486	**-0.3986668**	-0.4577830	**-0.6979138**	-0.7379950
1.494570	**-0.1602666**	-0.0971553	**-0.4008670**	-0.4601780	**-0.7016316**	-0.7418520
1.545410	**-0.1607179**	-0.0974085	**-0.4019699**	-0.4613710	**-0.7034708**	-0.7437730
1.596180	**-0.1607227**	-0.0974101	**-0.4019841**	-0.4613730	**-0.7034466**	-0.7437730
1.647020	**-0.1602810**	-0.0971602	**-0.4009095**	-0.4601840	**-0.7015591**	-0.7418530
1.698060	**-0.1593893**	-0.0966567	**-0.3987372**	-0.4577940	**-0.6977937**	-0.7379960
1.749440	**-0.1580406**	-0.0958956	**-0.3954492**	-0.4541840	**-0.6921196**	-0.7321740
1.801290	**-0.1562242**	-0.0948708	**-0.3910178**	-0.4493250	**-0.6844896**	-0.7243370
1.853790	**-0.1539251**	-0.0935736	**-0.3854040**	-0.4431750	**-0.6748372**	-0.7144200
1.907100	**-0.1511235**	-0.0919923	**-0.3785565**	-0.4356800	**-0.6630738**	-0.7023350
1.961420	**-0.1477938**	-0.0901120	**-0.3704083**	-0.4267700	**-0.6490839**	-0.6879680
2.016990	**-0.1439037**	-0.0879135	**-0.3608740**	-0.4163520	**-0.6327188**	-0.6711710
2.074080	**-0.1394118**	-0.0853722	**-0.3498443**	-0.4043120	**-0.6137868**	-0.6517580
2.133030	**-0.1342655**	-0.0824564	**-0.3371782**	-0.3904980	**-0.5920387**	-0.6294860
2.194250	**-0.1283968**	-0.0791246	**-0.3226925**	-0.3747140	**-0.5671453**	-0.6040380
2.258310	**-0.1217164**	-0.0753217	**-0.3061436**	-0.3567000	**-0.5386615**	-0.5749950
2.325930	**-0.1141039**	-0.0709719	**-0.2871989**	-0.3360950	**-0.5059640**	-0.5417760
2.398170	**-0.1053905**	-0.0659671	**-0.2653870**	-0.3123900	**-0.4681363**	-0.5035570
2.476600	**-0.0953273**	-0.0601438	**-0.2400057**	-0.2848090	**-0.4237345**	-0.4590910
2.563840	**-0.0835202**	-0.0532341	**-0.2099592**	-0.2520830	**-0.3702814**	-0.4063320
2.664780	**-0.0695152**	-0.0447370	**-0.1762485**	-0.2118420	**-0.3085728**	-0.3414570
2.791180	**-0.0432985**	-0.0334638	**-0.1131016**	-0.1584570	**-0.1974035**	-0.2553970
3.000050	**-0.0246863**	-0.0137457	**-0.0673079**	-0.0651056	**-0.1185576**	-0.1049560

Table 6: Comparison of the direct numerical simulation (DNS) and finite difference method (FDM) results of the tangential velocity (V_θ) for $Re = 0.01$. The DNS values are in bold font and FDM values in normal font. The vertical and horizontal values represents θ and r respectively.

θ \ r	1.07174		1.57708		2.9231	
0.141539	**0.0069692**	0.0076271	**0.1227939**	0.2046640	**0.4029158**	0.5882670
0.350414	**0.0060466**	0.0059090	**0.1207574**	0.1617000	**0.4005590**	0.4775510
0.476814	**0.0055026**	0.0056726	**0.1177369**	0.1541480	**0.3894476**	0.4521630
0.577752	**0.0060248**	0.0053853	**0.1151469**	0.1459900	**0.3715371**	0.4260900
0.664990	**0.0062102**	0.0050864	**0.1115450**	0.1375900	**0.3529156**	0.4000080
0.743426	**0.0062376**	0.0047814	**0.1072933**	0.1290670	**0.3337833**	0.3739640
0.815665	**0.0061726**	0.0044724	**0.1025876**	0.1204690	**0.3142820**	0.3479540
0.883286	**0.0060457**	0.0041604	**0.0975325**	0.1118220	**0.2944588**	0.3219720
0.947338	**0.0058725**	0.0038461	**0.0921867**	0.1031390	**0.2743333**	0.2960140
1.008560	**0.0056620**	0.0035299	**0.0865846**	0.0944261	**0.2539137**	0.2700790
1.067510	**0.0054192**	0.0032118	**0.0807466**	0.0856882	**0.2332028**	0.2441630
1.124600	**0.0051471**	0.0028922	**0.0746843**	0.0769272	**0.2122006**	0.2182680
1.180170	**0.0048474**	0.0025709	**0.0684041**	0.0681442	**0.1909056**	0.1923910
1.234490	**0.0045209**	0.0022480	**0.0619087**	0.0593397	**0.1693151**	0.1665330
1.287800	**0.0041680**	0.0019237	**0.0551986**	0.0505141	**0.1474255**	0.1406930
1.340300	**0.0037887**	0.0015978	**0.0482726**	0.0416673	**0.1252323**	0.1148710
1.392160	**0.0033827**	0.0012703	**0.0411285**	0.0327995	**0.1027304**	0.0890668
1.443530	**0.0029499**	0.0009413	**0.0337635**	0.0239105	**0.0799128**	0.0632806
1.494570	**0.0024895**	0.0006108	**0.0261741**	0.0150002	**0.0567712**	0.0375121
1.545410	**0.0020013**	0.0002787	**0.0183568**	0.0060687	**0.0332943**	0.0117613
1.596180	**0.0014846**	-0.0000550	**0.0103079**	-0.0028841	**0.0094690**	-0.0139718
1.647020	**0.0009390**	-0.0003902	**0.0020238**	-0.0118583	**-0.0147159**	-0.0396873
1.698060	**0.0003641**	-0.0007269	**-0.0064988**	-0.0208537	**-0.0392644**	-0.0653850
1.749440	**-0.0002405**	-0.0010652	**-0.0152629**	-0.0298703	**-0.0641758**	-0.0910649
1.801290	**-0.0008749**	-0.0014050	**-0.0242703**	-0.0389081	**-0.0894474**	-0.1167270
1.853790	**-0.0015391**	-0.0017464	**-0.0335219**	-0.0479670	**-0.1150764**	-0.1423710
1.907100	**-0.0022330**	-0.0020893	**-0.0430173**	-0.0570470	**-0.1410592**	-0.1679980
1.961420	**-0.0029561**	-0.0024337	**-0.0527540**	-0.0661482	**-0.1673921**	-0.1936060
2.016990	**-0.0037071**	-0.0027798	**-0.0627270**	-0.0752709	**-0.1940705**	-0.2191950
2.074080	**-0.0044841**	-0.0031273	**-0.0729276**	-0.0844155	**-0.2210891**	-0.2447660
2.133030	**-0.0052839**	-0.0034766	**-0.0833418**	-0.0935833	**-0.2484413**	-0.2703170
2.194250	**-0.0061011**	-0.0038276	**-0.0939476**	-0.1027760	**-0.2761186**	-0.2958470
2.258310	**-0.0069272**	-0.0041806	**-0.1047106**	-0.1119990	**-0.3041094**	-0.3213560
2.325930	**-0.0077482**	-0.0045359	**-0.1155756**	-0.1212580	**-0.3323975**	-0.3468400
2.398170	**-0.0085399**	-0.0048942	**-0.1264523**	-0.1305650	**-0.3609590**	-0.3722960
2.476600	**-0.0092580**	-0.0052564	**-0.1371856**	-0.1399470	**-0.3897591**	-0.3977190
2.563840	**-0.0098115**	-0.0056249	**-0.1474892**	-0.1494540	**-0.4187294**	-0.4231030
2.664780	**-0.0099867**	-0.0060048	**-0.1567891**	-0.1592000	**-0.4468505**	-0.4484960
2.791180	**-0.0120297**	-0.0064357	**-0.1688931**	-0.1695540	**-0.4697725**	-0.4745740
3.000050	**-0.0141175**	-0.0076271	**-0.1766949**	-0.2046640	**-0.4790892**	-0.5882670

Table 7: Comparison of the direct numerical simulation (DNS) and finite difference method (FDM) results of the radial velocity (V_r) for $Re = 1.00$. The DNS values are in bold font and FDM values in normal font. The vertical and horizontal values represents θ and r respectively.

θ \ r	1.07174		1.57708		2.9231	
0.141539	**-0.0136479**	-0.0137457	**-0.0622291**	-0.0651056	**-0.1254564**	-0.1049560
0.350414	**-0.0225484**	-0.0320730	**-0.1002271**	-0.1560860	**-0.1997403**	-0.2566390
0.476814	**-0.0346653**	-0.0430701	**-0.1530676**	-0.2091500	**-0.3054506**	-0.3422920
0.577752	**-0.0415277**	-0.0514572	**-0.1829551**	-0.2493550	**-0.3660374**	-0.4068240
0.664990	**-0.0485177**	-0.0583316	**-0.2108751**	-0.2821370	**-0.4190684**	-0.4593530
0.743426	**-0.0549247**	-0.0641641	**-0.2350172**	-0.3098150	**-0.4632251**	-0.5036670
0.815665	**-0.0608071**	-0.0692091	**-0.2562953**	-0.3336380	**-0.5010814**	-0.5417860
0.883286	**-0.0662343**	-0.0736224	**-0.2752875**	-0.3543750	**-0.5340305**	-0.5749390
0.947338	**-0.0712625**	-0.0775072	**-0.2923747**	-0.3725330	**-0.5629431**	-0.6039410
1.008560	**-0.0759349**	-0.0809363	**-0.3078193**	-0.3884710	**-0.5884091**	-0.6293640
1.067510	**-0.0802836**	-0.0839623	**-0.3218085**	-0.4024490	**-0.6108482**	-0.6516230
1.124600	**-0.0843326**	-0.0866248	**-0.3344788**	-0.4146610	**-0.6305697**	-0.6710330
1.180170	**-0.0880990**	-0.0889540	**-0.3459307**	-0.4252590	**-0.6478065**	-0.6878330
1.234490	**-0.0915946**	-0.0909730	**-0.3562380**	-0.4343560	**-0.6627368**	-0.7022090
1.287800	**-0.0948267**	-0.0926999	**-0.3654543**	-0.4420440	**-0.6754977**	-0.7143080
1.340300	**-0.0977989**	-0.0941485	**-0.3736170**	-0.4483920	**-0.6861943**	-0.7242410
1.392160	**-0.1005115**	-0.0953291	**-0.3807498**	-0.4534540	**-0.6949062**	-0.7320960
1.443530	**-0.1029617**	-0.0962495	**-0.3868652**	-0.4572700	**-0.7016919**	-0.7379400
1.494570	**-0.1051440**	-0.0969149	**-0.3919655**	-0.4598690	**-0.7065911**	-0.7418180
1.545410	**-0.1070502**	-0.0973282	**-0.3960433**	-0.4612680	**-0.7096263**	-0.7437620
1.596180	**-0.1086692**	-0.0974904	**-0.3990823**	-0.4614770	**-0.7108025**	-0.7437850
1.647020	**-0.1099874**	-0.0974006	**-0.4010574**	-0.4604930	**-0.7101050**	-0.7418860
1.698060	**-0.1109883**	-0.0970558	**-0.4019340**	-0.4583070	**-0.7075016**	-0.7380510
1.749440	**-0.1116519**	-0.0964509	**-0.4016671**	-0.4548990	**-0.7029472**	-0.7322490
1.801290	**-0.1119550**	-0.0955789	**-0.4002009**	-0.4502390	**-0.6963829**	-0.7244310
1.853790	**-0.1118698**	-0.0944299	**-0.3974670**	-0.4442840	**-0.6877314**	-0.7145300
1.907100	**-0.1113642**	-0.0929913	**-0.3933826**	-0.4369780	**-0.6768934**	-0.7024590
1.961420	**-0.1104001**	-0.0912470	**-0.3878466**	-0.4282510	**-0.6637426**	-0.6881000
2.016990	**-0.1089327**	-0.0891766	**-0.3807362**	-0.4180100	**-0.6481187**	-0.6713070
2.074080	**-0.1069084**	-0.0867542	**-0.3718999**	-0.4061380	**-0.6298181**	-0.6518900
2.133030	**-0.1042631**	-0.0839464	**-0.3611490**	-0.3924840	**-0.6085781**	-0.6296060
2.194250	**-0.1009187**	-0.0807100	**-0.3482433**	-0.3768520	**-0.5840553**	-0.6041340
2.258310	**-0.0967787**	-0.0769875	**-0.3328706**	-0.3589780	**-0.5557877**	-0.5750490
2.325930	**-0.0917222**	-0.0726999	**-0.3146112**	-0.3385040	**-0.5231316**	-0.5417660
2.398170	**-0.0855950**	-0.0677344	**-0.2928781**	-0.3149140	**-0.4851397**	-0.5034500
2.476600	**-0.0781995**	-0.0619202	**-0.2668088**	-0.2874270	**-0.4402946**	-0.4588350
2.563840	**-0.0693059**	-0.0549758	**-0.2351599**	-0.2547570	**-0.3860713**	-0.4058500
2.664780	**-0.0594710**	-0.0463710	**-0.2000323**	-0.2144820	**-0.3238079**	-0.3406390
2.791180	**-0.0389023**	-0.0348271	**-0.1325268**	-0.1607810	**-0.2119666**	-0.2541800
3.000050	**-0.0233174**	-0.0137457	**-0.0827482**	-0.0651056	**-0.1325381**	-0.1049560

Table 8: Comparison of the direct numerical simulation (DNS) and finite difference method (FDM) results of the tangential velocity (V_θ) for $Re = 1.00$. The DNS values are in bold font and FDM values in normal font. The vertical and horizontal values represents θ and r respectively.

θ \ r	1.07174		1.57708		2.9231	
0.141539	**-0.0001550**	0.0076271	**0.0467133**	0.2046640	**0.3165739**	0.5882670
0.350414	**-0.0001443**	0.0035389	**0.0495880**	0.1263580	**0.3143289**	0.4909430
0.476814	**0.0002370**	0.0041778	**0.0557994**	0.1314150	**0.3093430**	0.4686660
0.577752	**0.0008141**	0.0043073	**0.0619972**	0.1304020	**0.3045416**	0.4395310
0.664990	**0.0012059**	0.0043215	**0.0674796**	0.1269830	**0.2998598**	0.4103090
0.743426	**0.0015702**	0.0042741	**0.0725378**	0.1223220	**0.2943048**	0.3814660
0.815665	**0.0019260**	0.0041865	**0.0772344**	0.1169200	**0.2880539**	0.3529640
0.883286	**0.0022780**	0.0040696	**0.0815638**	0.1110260	**0.2809890**	0.3247440
0.947338	**0.0026267**	0.0039295	**0.0854876**	0.1047680	**0.2730123**	0.2967660
1.008560	**0.0029705**	0.0037696	**0.0889490**	0.0982184	**0.2640251**	0.2690080
1.067510	**0.0033064**	0.0035921	**0.0918795**	0.0914155	**0.2539337**	0.2414540
1.124600	**0.0036307**	0.0033980	**0.0942032**	0.0843808	**0.2426507**	0.2140950
1.180170	**0.0039390**	0.0031880	**0.0958393**	0.0771259	**0.2300950**	0.1869260
1.234490	**0.0042260**	0.0029624	**0.0967036**	0.0696567	**0.2161916**	0.1599410
1.287800	**0.0044860**	0.0027214	**0.0967111**	0.0619758	**0.2008701**	0.1331390
1.340300	**0.0047129**	0.0024651	**0.0957762**	0.0540838	**0.1840630**	0.1065180
1.392160	**0.0049000**	0.0021933	**0.0938149**	0.0459808	**0.1657035**	0.0800753
1.443530	**0.0050398**	0.0019061	**0.0907460**	0.0376660	**0.1457222**	0.0538108
1.494570	**0.0051248**	0.0016035	**0.0864920**	0.0291390	**0.1240444**	0.0277238
1.545410	**0.0051467**	0.0012854	**0.0809806**	0.0203992	**0.1005890**	0.0018139
1.596180	**0.0050968**	0.0009517	**0.0741455**	0.0114464	**0.0752732**	-0.0239193
1.647020	**0.0049658**	0.0006026	**0.0659272**	0.0022805	**0.0480417**	-0.0494755
1.698060	**0.0047441**	0.0002379	**0.0562734**	-0.0070981	**0.0189552**	-0.0748547
1.749440	**0.0044213**	-0.0001422	**0.0451394**	-0.0166890	**-0.0116961**	-0.1000570
1.801290	**0.0039866**	-0.0005377	**0.0324873**	-0.0264916	**-0.0436342**	-0.1250800
1.853790	**0.0034285**	-0.0009486	**0.0182865**	-0.0365053	**-0.0767359**	-0.1499250
1.907100	**0.0027350**	-0.0013749	**0.0025108**	-0.0467300	**-0.1108765**	-0.1745890
1.961420	**0.0018941**	-0.0018166	**-0.0148527**	-0.0571665	**-0.1459351**	-0.1990710
2.016990	**0.0008942**	-0.0022739	**-0.0337967**	-0.0678173	**-0.1818093**	-0.2233680
2.074080	**-0.0002757**	-0.0027471	**-0.0542988**	-0.0786883	**-0.2184133**	-0.2474750
2.133030	**-0.0016282**	-0.0032368	**-0.0763235**	-0.0897910	**-0.2556751**	-0.2713880
2.194250	**-0.0031755**	-0.0037443	**-0.0998226**	-0.1011470	**-0.2935347**	-0.2950950
2.258310	**-0.0049260**	-0.0042714	**-0.1247306**	-0.1127950	**-0.3319438**	-0.3185840
2.325930	**-0.0068823**	-0.0048218	**-0.1509557**	-0.1248060	**-0.3708644**	-0.3418300
2.398170	**-0.0090329**	-0.0054015	**-0.1783658**	-0.1373110	**-0.4102637**	-0.3647940
2.476600	**-0.0113162**	-0.0060214	**-0.2067574**	-0.1505540	**-0.4501539**	-0.3874170
2.563840	**-0.0134529**	-0.0067029	**-0.2356941**	-0.1650410	**-0.4909774**	-0.4096620
2.664780	**-0.0144092**	-0.0074996	**-0.2632110**	-0.1819340	**-0.5323627**	-0.4319930
2.791180	**-0.0162002**	-0.0088059	**-0.2904858**	-0.2048960	**-0.5823315**	-0.4611820
3.000050	**-0.0180093**	-0.0076271	**-0.3047704**	-0.2046640	**-0.6116635**	-0.5882670

Table 9: Comparison of the direct numerical simulation (DNS) and finite difference method (FDM) results of the radial velocity (V_r) for $Re = 10.00$. The DNS values are in bold font and FDM values in normal font. The vertical and horizontal values represents θ and r respectively.

θ \ r	1.07174		1.57708		2.9231	
0.141539	**-0.0020462**	-0.0137457	**-0.0355153**	-0.0651056	**-0.1472043**	-0.1049560
0.350414	**-0.0027398**	-0.0196793	**-0.0530162**	-0.1349590	**-0.2028866**	-0.2677060
0.476814	**-0.0040905**	-0.0282161	**-0.0807612**	-0.1851560	**-0.2897760**	-0.3497320
0.577752	**-0.0060979**	-0.0356239	**-0.1023292**	-0.2250480	**-0.3485482**	-0.4112080
0.664990	**-0.0089217**	-0.0421825	**-0.1242249**	-0.2583350	**-0.3984280**	-0.4616830
0.743426	**-0.0120032**	-0.0480978	**-0.1451847**	-0.2868690	**-0.4399972**	-0.5046470
0.815665	**-0.0153513**	-0.0535008	**-0.1658937**	-0.3117410	**-0.4760667**	-0.5418760
0.883286	**-0.0189645**	-0.0584794	**-0.1865349**	-0.3336570	**-0.5077274**	-0.5744450
0.947338	**-0.0228438**	-0.0630948	**-0.2072058**	-0.3530990	**-0.5357600**	-0.6030740
1.008560	**-0.0269901**	-0.0673907	**-0.2279478**	-0.3704110	**-0.5606953**	-0.6282740
1.067510	**-0.0314024**	-0.0713987	**-0.2487635**	-0.3858460	**-0.5829171**	-0.6504200
1.124600	**-0.0360778**	-0.0751415	**-0.2696257**	-0.3995920	**-0.6027119**	-0.6697990
1.180170	**-0.0410105**	-0.0786352	**-0.2904839**	-0.4117920	**-0.6203004**	-0.6866320
1.234490	**-0.0461916**	-0.0818908	**-0.3112675**	-0.4225550	**-0.6358554**	-0.7010890
1.287800	**-0.0516089**	-0.0849151	**-0.3318882**	-0.4319630	**-0.6495149**	-0.7133050
1.340300	**-0.0572466**	-0.0877116	**-0.3522414**	-0.4400790	**-0.6613889**	-0.7233850
1.392160	**-0.0630846**	-0.0902810	**-0.3722078**	-0.4469470	**-0.6715654**	-0.7314100
1.443530	**-0.0690986**	-0.0926215	**-0.3916541**	-0.4526010	**-0.6801118**	-0.7374390
1.494570	**-0.0752591**	-0.0947292	**-0.4104341**	-0.4570580	**-0.6870741**	-0.7415130
1.545410	**-0.0815310**	-0.0965982	**-0.4283892**	-0.4603300	**-0.6924695**	-0.7436590
1.596180	**-0.0878733**	-0.0982204	**-0.4453490**	-0.4624150	**-0.6962629**	-0.7438870
1.647020	**-0.0942378**	-0.0995863	**-0.4611318**	-0.4633040	**-0.6983185**	-0.7421910
1.698060	**-0.1005684**	-0.1006840	**-0.4755449**	-0.4629770	**-0.6983694**	-0.7385530
1.749440	**-0.1068002**	-0.1014990	**-0.4883837**	-0.4614060	**-0.6961537**	-0.7329360
1.801290	**-0.1128572**	-0.1020160	**-0.4994307**	-0.4585520	**-0.6915240**	-0.7252870
1.853790	**-0.1186511**	-0.1022150	**-0.5084533**	-0.4543640	**-0.6844048**	-0.7155330
1.907100	**-0.1240787**	-0.1020740	**-0.5152060**	-0.4487790	**-0.6747372**	-0.7035790
1.961420	**-0.1290186**	-0.1015660	**-0.5194123**	-0.4417170	**-0.6624381**	-0.6893010
2.016990	**-0.1333283**	-0.1006600	**-0.5207750**	-0.4330790	**-0.6473927**	-0.6725410
2.074080	**-0.1368399**	-0.0993178	**-0.5189783**	-0.4227410	**-0.6294428**	-0.6530930
2.133030	**-0.1393444**	-0.0974920	**-0.5136558**	-0.4105440	**-0.6083704**	-0.6306950
2.194250	**-0.1405824**	-0.0951224	**-0.5043721**	-0.3962860	**-0.5838759**	-0.6050010
2.258310	**-0.1402329**	-0.0921304	**-0.4905890**	-0.3796960	**-0.5555436**	-0.5755430
2.325930	**-0.1378814**	-0.0884082	**-0.4716047**	-0.3604010	**-0.5227905**	-0.5416770
2.398170	**-0.1329733**	-0.0838007	**-0.4464205**	-0.3378590	**-0.4847615**	-0.5024700
2.476600	**-0.1247316**	-0.0780692	**-0.4134310**	-0.3112290	**-0.4399808**	-0.4565050
2.563840	**-0.1121517**	-0.0708091	**-0.3701457**	-0.2790650	**-0.3856776**	-0.4014660
2.664780	**-0.0962958**	-0.0612249	**-0.3158673**	-0.2384750	**-0.3225200**	-0.3331990
2.791180	**-0.0662778**	-0.0472209	**-0.2283845**	-0.1819090	**-0.2230728**	-0.2431130
3.000050	**-0.0446044**	-0.0137457	**-0.1705929**	-0.0651056	**-0.1567988**	-0.1049560

Table 10: Comparison of the direct numerical simulation (DNS) and finite difference method (FDM) results of the tangential velocity (V_θ) for $Re = 10.00$. The DNS values are in bold font and FDM values in normal font. The vertical and horizontal values represents θ and r respectively.

θ \ r	1.07174		1.57708		2.9231	
0.141539	**-0.0067984**	0.0076271	**-0.0678828**	0.2046640	**0.2489047**	0.5882670
0.350414	**-0.0051561**	-0.0069951	**-0.0500541**	-0.0307181	**0.2535690**	0.5504670
0.476814	**-0.0032915**	-0.0024659	**-0.0193979**	0.0303748	**0.2655633**	0.5420140
0.577752	**-0.0024516**	-0.0004838	**0.0051116**	0.0611254	**0.2781489**	0.4992690
0.664990	**-0.0014751**	0.0009216	**0.0275520**	0.0798414	**0.2873104**	0.4560940
0.743426	**-0.0008017**	0.0020195	**0.0484791**	0.0923435	**0.2934423**	0.4148120
0.815665	**-0.0001972**	0.0029161	**0.0683975**	0.1011470	**0.2963402**	0.3752320
0.883286	**0.0003892**	0.0036661	**0.0875388**	0.1074860	**0.2961548**	0.3370620
0.947338	**0.0010089**	0.0042999	**0.1059344**	0.1120110	**0.2929983**	0.3001080
1.008560	**0.0016938**	0.0048352	**0.1234406**	0.1150730	**0.2870634**	0.2642480
1.067510	**0.0024593**	0.0052820	**0.1397743**	0.1168700	**0.2785764**	0.2294110
1.124600	**0.0033068**	0.0056461	**0.1545702**	0.1175080	**0.2677833**	0.1955500
1.180170	**0.0042220**	0.0059307	**0.1674270**	0.1170450	**0.2549230**	0.1626350
1.234490	**0.0051823**	0.0061374	**0.1779459**	0.1155100	**0.2402038**	0.1306460
1.287800	**0.0061728**	0.0062671	**0.1857592**	0.1129170	**0.2237825**	0.0995686
1.340300	**0.0071825**	0.0063198	**0.1905506**	0.1092680	**0.2057492**	0.0693931
1.392160	**0.0081933**	0.0062956	**0.1920688**	0.1045640	**0.1861191**	0.0401128
1.443530	**0.0091796**	0.0061943	**0.1901351**	0.0988018	**0.1648315**	0.0117230
1.494570	**0.0101110**	0.0060157	**0.1846474**	0.0919780	**0.1417576**	-0.0157796
1.545410	**0.0109542**	0.0057596	**0.1755792**	0.0840904	**0.1167212**	-0.0423969
1.596180	**0.0116734**	0.0054260	**0.1629761**	0.0751376	**0.0895365**	-0.0681301
1.647020	**0.0122303**	0.0050148	**0.1469493**	0.0651196	**0.0600761**	-0.0929789
1.698060	**0.0125856**	0.0045261	**0.1276661**	0.0540377	**0.0284031**	-0.1169430
1.749440	**0.0126982**	0.0039601	**0.1053391**	0.0418944	**-0.0049972**	-0.1400190
1.801290	**0.0125267**	0.0033170	**0.0802137**	0.0286928	**-0.0394225**	-0.1622050
1.853790	**0.0120291**	0.0025970	**0.0525551**	0.0144356	**-0.0749475**	-0.1834960
1.907100	**0.0111629**	0.0018001	**0.0226351**	-0.0008766	**-0.1117853**	-0.2038840
1.961420	**0.0098845**	0.0009260	**-0.0092545**	-0.0172476	**-0.1495921**	-0.2233610
2.016990	**0.0081497**	-0.0000258	**-0.0427027**	-0.0346904	**-0.1880988**	-0.2419120
2.074080	**0.0059145**	-0.0010572	**-0.0773819**	-0.0532339	**-0.2271339**	-0.2595180
2.133030	**0.0031412**	-0.0021713	**-0.1131631**	-0.0729360	**-0.2665890**	-0.2761470
2.194250	**-0.0002172**	-0.0033738	**-0.1499619**	-0.0939044	**-0.3063953**	-0.2917540
2.258310	**-0.0042375**	-0.0046750	**-0.1877556**	-0.1163340	**-0.3465107**	-0.3062650
2.325930	**-0.0089867**	-0.0060923	**-0.2266087**	-0.1405800	**-0.3869168**	-0.3195620
2.398170	**-0.0144785**	-0.0076561	**-0.2666928**	-0.1672890	**-0.4276197**	-0.3314490
2.476600	**-0.0207744**	-0.0094213	**-0.3081567**	-0.1976960	**-0.4686301**	-0.3416330
2.563840	**-0.0284125**	-0.0114940	**-0.3512160**	-0.2343180	**-0.5103205**	-0.3499230
2.664780	**-0.0378086**	-0.0141433	**-0.4018702**	-0.2829740	**-0.5521870**	-0.3586450
2.791180	**-0.0362550**	-0.0193399	**-0.4501485**	-0.3619730	**-0.6116061**	-0.4016580
3.000050	**-0.0295772**	-0.0076271	**-0.4697461**	-0.2046640	**-0.6502667**	-0.5882670

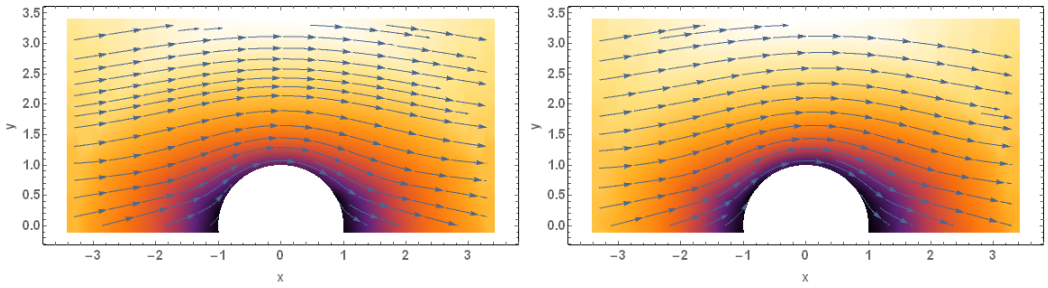
Table 11: Comparison of the direct numerical simulation (DNS) and finite difference method (FDM) results of the radial velocity (V_r) for $Re = 50.00$. The DNS values are in bold font and FDM values in normal font. The vertical and horizontal values represents θ and r respectively.

θ \ r	1.07174		1.57708		2.9231	
0.141539	**0.0201518**	-0.0137457	**0.0162823**	-0.0651056	**-0.1797531**	-0.1049560
0.350414	**0.0264501**	0.0354040	**0.0184379**	-0.0410589	**-0.2221507**	-0.3168920
0.476814	**0.0323974**	0.0378015	**0.0115575**	-0.0785170	**-0.2961229**	-0.3828000
0.577752	**0.0327191**	0.0347464	**-0.0064501**	-0.1170150	**-0.3504173**	-0.4306910
0.664990	**0.0328255**	0.0295909	**-0.0278552**	-0.1525480	**-0.3916220**	-0.4720380
0.743426	**0.0313751**	0.0233080	**-0.0540839**	-0.1848910	**-0.4250934**	-0.5090000
0.815665	**0.0292468**	0.0163138	**-0.0833551**	-0.2144230	**-0.4525700**	-0.5422740
0.883286	**0.0264198**	0.0088225	**-0.1156602**	-0.2415780	**-0.4755635**	-0.5722490
0.947338	**0.0228864**	0.0009605	**-0.1504977**	-0.2667230	**-0.4950155**	-0.5992220
1.008560	**0.0185714**	-0.0071882	**-0.1874541**	-0.2901440	**-0.5116918**	-0.6234310
1.067510	**0.0133762**	-0.0155605	**-0.2260294**	-0.3120560	**-0.5262074**	-0.6450750
1.124600	**0.0071966**	-0.0241045	**-0.2656808**	-0.3326180	**-0.5390796**	-0.6643170
1.180170	**-0.0000440**	-0.0327740	**-0.3058320**	-0.3519430	**-0.5507439**	-0.6812920
1.234490	**-0.0083839**	-0.0415253	**-0.3458911**	-0.3701080	**-0.5615634**	-0.6961070
1.287800	**-0.0178603**	-0.0503159	**-0.3852678**	-0.3871620	**-0.5718326**	-0.7088480
1.340300	**-0.0285127**	-0.0591033	**-0.4233901**	-0.4031330	**-0.5817798**	-0.7195820
1.392160	**-0.0403632**	-0.0678448	**-0.4597184**	-0.4180310	**-0.5915671**	-0.7283580
1.443530	**-0.0534104**	-0.0764969	**-0.4937584**	-0.4318480	**-0.6012872**	-0.7352100
1.494570	**-0.0676273**	-0.0850151	**-0.5250703**	-0.4445680	**-0.6109537**	-0.7401570
1.545410	**-0.0829594**	-0.0933536	**-0.5532773**	-0.4561600	**-0.6204835**	-0.7432040
1.596180	**-0.0993227**	-0.1014650	**-0.5780696**	-0.4665850	**-0.6296616**	-0.7443420
1.647020	**-0.1166024**	-0.1093000	**-0.5992065**	-0.4757940	**-0.6380602**	-0.7435480
1.698060	**-0.1346508**	-0.1168080	**-0.6165154**	-0.4837290	**-0.6449227**	-0.7407820
1.749440	**-0.1532858**	-0.1239350	**-0.6298873**	-0.4903230	**-0.6492763**	-0.7359880
1.801290	**-0.1722889**	-0.1306240	**-0.6392680**	-0.4954970	**-0.6504417**	-0.7290900
1.853790	**-0.1914025**	-0.1368140	**-0.6446453**	-0.4991650	**-0.6481619**	-0.7199900
1.907100	**-0.2103259**	-0.1424390	**-0.6460366**	-0.5012260	**-0.6423914**	-0.7085610
1.961420	**-0.2287094**	-0.1474270	**-0.6434950**	-0.5015660	**-0.6331871**	-0.6946410
2.016990	**-0.2461459**	-0.1516970	**-0.6371627**	-0.5000530	**-0.6205923**	-0.6780230
2.074080	**-0.2621588**	-0.1551560	**-0.6271343**	-0.4965300	**-0.6046034**	-0.6584390
2.133030	**-0.2761904**	-0.1576950	**-0.6133351**	-0.4908120	**-0.5851347**	-0.6355390
2.194250	**-0.2876082**	-0.1591780	**-0.5955770**	-0.4826620	**-0.5619945**	-0.6088530
2.258310	**-0.2955190**	-0.1594320	**-0.5735327**	-0.4717750	**-0.5348500**	-0.5777390
2.325930	**-0.2987307**	-0.1582230	**-0.5466719**	-0.4577190	**-0.5031717**	-0.5412790
2.398170	**-0.2957784**	-0.1552070	**-0.5142146**	-0.4398380	**-0.4661646**	-0.4981170
2.476600	**-0.2846158**	-0.1498430	**-0.4752319**	-0.4170160	**-0.4225747**	-0.4461500
2.563840	**-0.2612827**	-0.1411790	**-0.4277935**	-0.3870980	**-0.3694473**	-0.3819830
2.664780	**-0.2134136**	-0.1272430	**-0.3606467**	-0.3451140	**-0.3052671**	-0.3001310
2.791180	**-0.1408861**	-0.1023040	**-0.2831347**	-0.2758090	**-0.2122288**	-0.1939270
3.000050	**-0.1008314**	-0.0137457	**-0.2465727**	-0.0651056	**-0.1538793**	-0.1049560

Table 12: Comparison of the direct numerical simulation (DNS) and finite difference method (FDM) results of the tangential velocity (V_θ) for $Re = 50.00$. The DNS values are in bold font and FDM values in normal font. The vertical and horizontal values represents θ and r respectively.

Figure 16 shows the streamlines of the DNS solution at $Re = 0.01$, 1.00, 10.00 and 50.00. The vortex does not form at $Re = 0.01$, 1.00 and 10.00 but it forms at $Re = 50.00$. The streamlines of the DNS solution are in agreement with streamlines of the FDM solution in figure 17. The vortex forms at the same value of $Re = 50.00$.

(a) $Re = 0.01$ (b) $Re = 1.00$



(c) $Re = 10.00$ (d) $Re = 50.00$

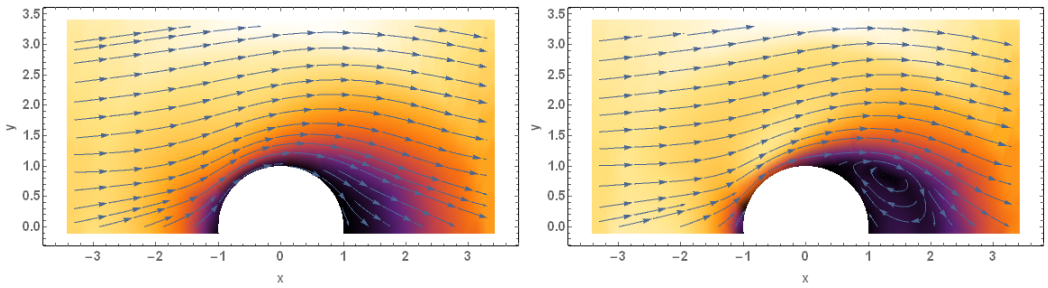
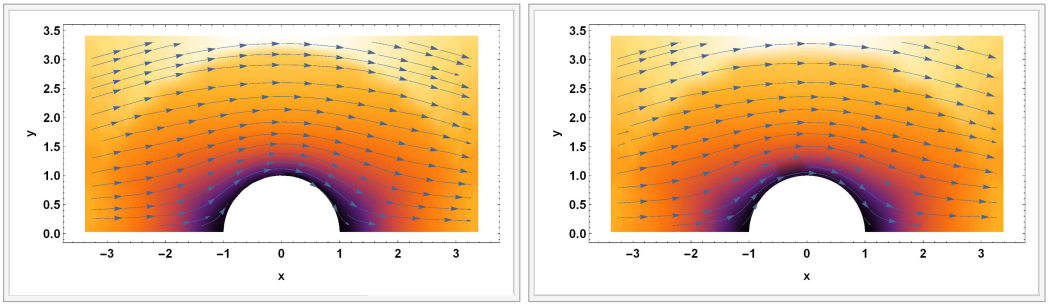


Figure 16: Streamlines of the direct numerical simulation (DNS) results for various values of Reynolds numbers using 40×40 grid points for $r = 3.30259$.

(a) $Re = 0.01$ (b) $Re = 1.00$



(c) $Re = 10.00$ (d) $Re = 50.00$

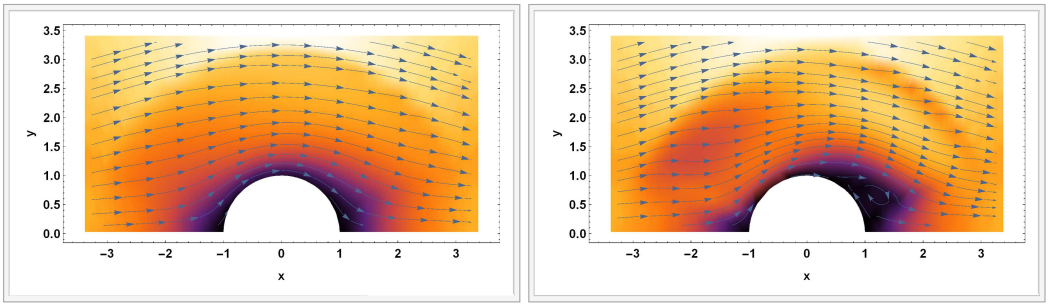


Figure 17: Streamlines of the finite difference method (FDM)results for various values of Reynolds numbers using 80×80 grid points for $r = 3.30259$

5.4 Conclusion

We solved the stream function equation numerically using the finite difference method. We transformed the coordinates from (r,θ) to (ξ,μ) to allow us to get arbitrarily close to infinity. The transformation does not solve the singularity of the problem. We produced a Mathematica code to solve the stream function equation numerically using the finite difference method to approximate the stream function solutions. We compared the analytical results with the numerical results for the first two terms of the stream function solution at various Reynolds numbers. The numerical results are in agreement with the analytical results for $Re <= 1$. For $Re = 10.00$, the analytical and numerical results are not in agreement because the analytical results are limited to $Re <= 1$. We compared the solution of the stream function equation with the solution of the full Navier-Stokes equations. The numerical results of the full Navier-Stokes equations are in good agreement with the numerical results of the stream function. The vortex forms at $Re = 50$ in both solutions.

6 Stability Analysis

6.1 Von Neumann Stability Analysis

The Von Neumann stability analysis is used to check the stability of the finite difference method (FDM). FDM refers to the finite difference method. The stream function equation in terms of ξ and μ coordinates is given by

$$D^4\Psi_{n+1} = \lambda D^2\Psi_n, \quad 0 \leq \xi \leq 1, \quad -1 \leq \mu \leq 1, \tag{6.1.1}$$

where

$$\begin{aligned} D^4\Psi_{n+1} = & \left[\frac{4\,\mu\,(\mu^2-1)}{(\log(1-\xi)-1)^3}\frac{\partial^3\Psi(\xi,\mu)}{\partial\mu^3} - \frac{4\,(\mu^2-1)}{(\log(1-\xi)-1)^3}\frac{\partial^2\Psi(\xi,\mu)}{\partial\mu^2}\right] \\ & + \left[\frac{(\mu^2-1)^2}{(\log(1-\xi)-1)^4}\frac{\partial^4\Psi(\xi,\mu)}{\partial\mu^4} + (\xi-1)\frac{\partial\Psi(\xi,\mu)}{\partial\mu}\right] \\ & + \left[7\,(\xi-1)^2\frac{\partial^2\Psi(\xi,\mu)}{\partial\xi^2} - \frac{2\,(\mu^2-1)(\xi-1)(\log(1-\xi)-3)}{(\log(1-\xi)-1)^3}\frac{\partial^3\Psi(\xi,\mu)}{\partial\xi\partial\mu^2}\right] \\ & + \left[6\,(\xi-1)^3\frac{\partial^3\Psi(\xi,\mu)}{\partial\xi^3} + (\xi-1)^4\frac{\partial^4\Psi(\xi,\mu)}{\partial\xi^4} - \frac{2\,(\mu^2-1)(\xi-1)^2}{(\log(1-\xi)-1)^2}\frac{\partial^4\Psi(\xi,\mu)}{\partial\xi^2\partial\mu^2}\right] \end{aligned} \tag{6.1.2}$$

and

$$
\begin{aligned}
\lambda D^2\Psi_n = &\left[\frac{4\ \ (\mu^2-1)}{(\log(1-\xi)-1)^5}\frac{\partial\Psi(\xi,\mu)}{\partial\mu}\frac{\partial^2\Psi(\xi,\mu)}{\partial\mu^2}\right] \\
&+\left[\frac{(\xi-1)(\log(1-\xi)-3)}{(\log(1-\xi)-1)^3}\frac{\partial\Psi(\xi,\mu)}{\partial\mu}\frac{\partial\Psi(\xi,\mu)}{\partial\xi}\right] \\
&+\left[\frac{(\mu^2-1)(\xi-1)}{(\log(1-\xi)-1)^4}\frac{\partial^3\Psi(\xi,\mu)}{\partial\mu^3}\frac{\partial\Psi(\xi,\mu)}{\partial\xi}\right] \\
&+\left[\frac{2\ \ \mu(\xi-1)^2}{(\mu^2-1)(\log(1-\xi)-1)^2}(\frac{\partial\Psi(\xi,\mu)}{\partial\xi})^2\right] \\
&+\left[\frac{(2\xi-\xi^2-1)}{(\log(1-\xi)-1)^2}\frac{\partial\Psi(\xi,\mu)}{\partial\xi}\frac{\partial^2\Psi(\xi,\mu)}{\partial\xi\partial\mu}\right] \\
&+\left[\frac{(1-\mu^2)(\xi-1)}{(\log(1-\xi)-1)^4}\frac{\partial\Psi(\xi,\mu)}{\partial\mu}\frac{\partial^3\Psi(\xi,\mu)}{\partial\xi\partial\mu^2}\right] \\
&+\left[\frac{(\xi-1)^2(3\log(1-\xi)-5)}{(\log(1-\xi)-1)^3}\frac{\partial\Psi(\xi,\mu)}{\partial\mu}\frac{\partial^2\Psi(\xi,\mu)}{\partial\xi^2}\right] \\
&+\left[\frac{2\ \ \mu\ (\xi-1)^3}{(\mu^2-1)(\log(1-\xi)-1)^2}\frac{\partial\Psi(\xi,\mu)}{\partial\xi}\frac{\partial^2\Psi(\xi,\mu)}{\partial\xi^2}\right] \\
&+\left[\frac{(\xi-1)^3}{(1-\mu^2)(\log(1-\xi)-1)^2}\frac{\partial\Psi(\xi,\mu)}{\partial\xi}\frac{\partial^3\Psi(\xi,\mu)}{\partial\xi^2\partial\mu}\right] \\
&+\left[\frac{(\xi-1)^3}{(\log(1-\xi)-1)^2}\frac{\partial\Psi(\xi,\mu)}{\partial\mu}\frac{\partial^3\Psi(\xi,\mu)}{\partial\xi^3\partial\xi}\right].
\end{aligned}
\tag{6.1.3}
$$

We define:

$$\Psi(\xi,\mu) = \Psi(n,\xi,\mu). \tag{6.1.4}$$

We then expand Ψ as

$$\Psi(n,\xi,\mu) = \Psi_0(\xi,\mu) + \epsilon\Psi_t(n,\xi,\mu), \tag{6.1.5}$$

where

$$\Psi_0(\xi,\mu) = = \frac{(1-\mu^2)(\log(1-\xi))^2(-3+2\log(1-\xi))}{4(-1+\log(1-\xi))}. \tag{6.1.6}$$

Ψ_0 is the Stokes expansion in terms of ξ and μ.

By substituting equations (6.1.2), (6.1.3), (6.1.4), (6.1.5) and (6.1.6) into (6.1.1), we get an equation of the form

$$A_1\Psi_t(n+1,\xi,\mu) = B_1\Psi_t(n,\xi,\mu) + C_1, \tag{6.1.7}$$

where A_1 contains (ξ, μ, and ϵ), B_1 contains (ξ, μ, Re and ϵ) and C_1 contains (ξ, μ and Re).

We write the first derivative of $\Psi_t(n+1,\xi,\mu)$ as

$$\begin{aligned}\frac{\partial\Psi_t(n+1,\xi,\mu)}{\partial\xi} &= \frac{\Psi_t(n+1,k+1,j) - \Psi_t(n+1,k-1,j)}{2\delta\xi},\\ \frac{\partial\Psi_t(n+1,\xi,\mu)}{\partial\mu} &= \frac{\Psi_t(n+1,k,j+1) - \Psi_t(n+1,k,j-1)}{2\delta\mu}\end{aligned} \tag{6.1.8}$$

and the first derivative of $\Psi_t(n,\xi,\mu)$ as

$$\begin{aligned}\frac{\partial\Psi_t(n,\xi,\mu)}{\partial\xi} &= \frac{\Psi_t(n,k+1,j) - \Psi_t(n,k-1,j)}{2\delta\xi},\\ \frac{\partial\Psi_t(n,\xi,\mu)}{\partial\mu} &= \frac{\Psi_t(n,k,j+1) - \Psi_t(n,k,j-1)}{2\delta\mu}.\end{aligned} \tag{6.1.9}$$

After replacing the derivatives of $\Psi_t(n+1,\xi,\mu)$ and $\Psi_t(n,\xi,\mu)$ in equation (6.1.7) with the finite difference schemes, the form of equation (6.1.7) becomes

$$\vec{A_2}\vec{\Psi_t^{n+1}} = \vec{B_2}\vec{\Psi_t^n}. \tag{6.1.10}$$

We define

$$\Psi_t(n,k,j) = \Phi(n,k,j), \tag{6.1.11}$$

where

$$\Phi(n,k+x,j+y) = e^{(x\ ik_\xi\delta\xi + y\ k_\mu\delta\mu)}\Phi(n,k,j). \tag{6.1.12}$$

After substituting equations (6.1.11) and (6.1.12) into equation (6.1.10) we get an equation of the form

$$A_3\Phi(n+1,k,j) = B_3\Phi(n,k,j) + C_3, \tag{6.1.13}$$

where A_3 and B_3 are coefficient matrices of $\Phi(n+1,k,j)$ and $\Phi(n,k,j)$ respectively. The entries of matrices A_3 and B_3 contains (Re, $\delta\xi$ and $\delta\mu$). C_3 is a matrix which only contains values of ξ and μ.

For stability

$$|\ \frac{B_3}{A_3}\ | \leq 1. \tag{6.1.14}$$

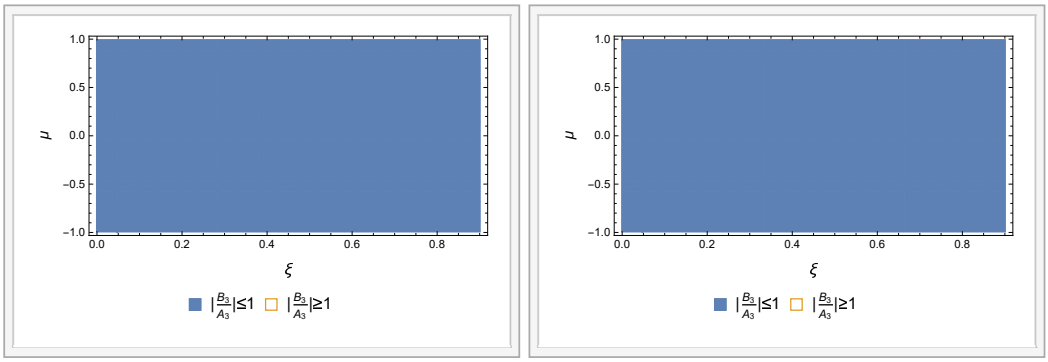
If B_3 grows faster than A_3 then the numerical solution to the PDE will become unstable.

6.2 Results

We require $B_3/A_3 \leq 1$ for the FDM to be stable. The stability of the FDM is depended on the values of Re, $\delta\xi$ and $\delta\mu$. We need $\delta\xi$ and $\delta\mu$ to be small enough for the numerical code to work as Re increases. The numerical results showed that the vortices formed at $Re = 50.00$.

Figure 18 shows the region plot for the stability of the FDM using 10×10 grid points. The FDM is stable at $Re = 0.01$, 1.00 and 10.00. The FDM is conditionally stable because the region of stability shrinks at $Re = 50.00$.

(a) Re = 0.01 (b) Re = 1.00



(c) Re = 10.00 (d) Re = 50.00

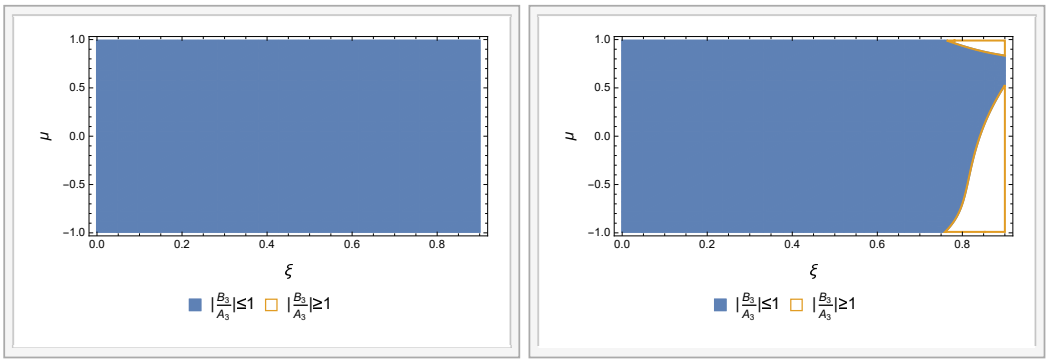
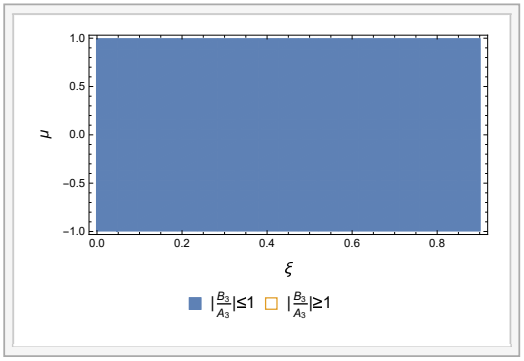


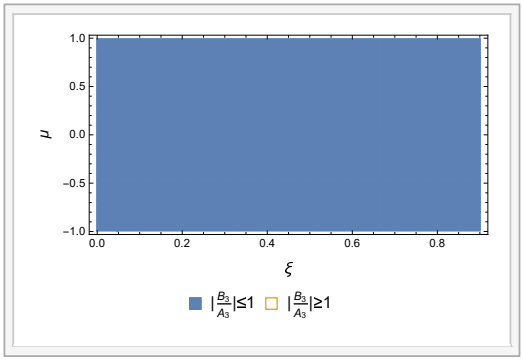
Figure 18: Region plot for $\delta\xi = 0.1$ and $\delta\mu = 0.22$ at various Reynolds numbers. The stable region is blue and unstable is white.

Figure 19 illustrates the stability conditions of the FDM using 40×40 grid points. The results are in agreement with the numerical results from figure 9. The FDM is stable at $Re = 0.01$, 1.00 and 10.00. The FDM becomes unstable at $Re = 50.00$.

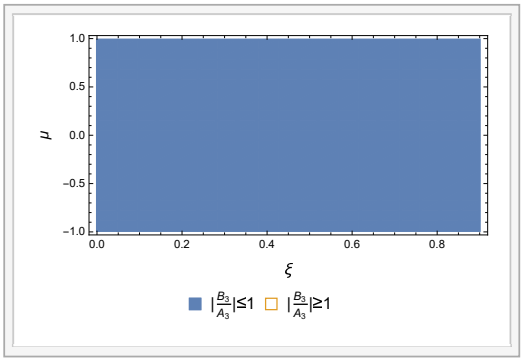
(a) Re = 0.01



(b) Re = 1.00



(c) Re = 10.00



(d) Re = 50.00

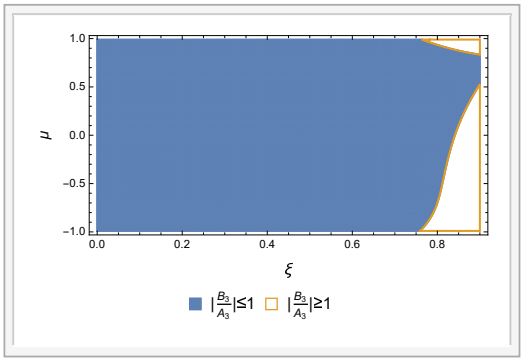
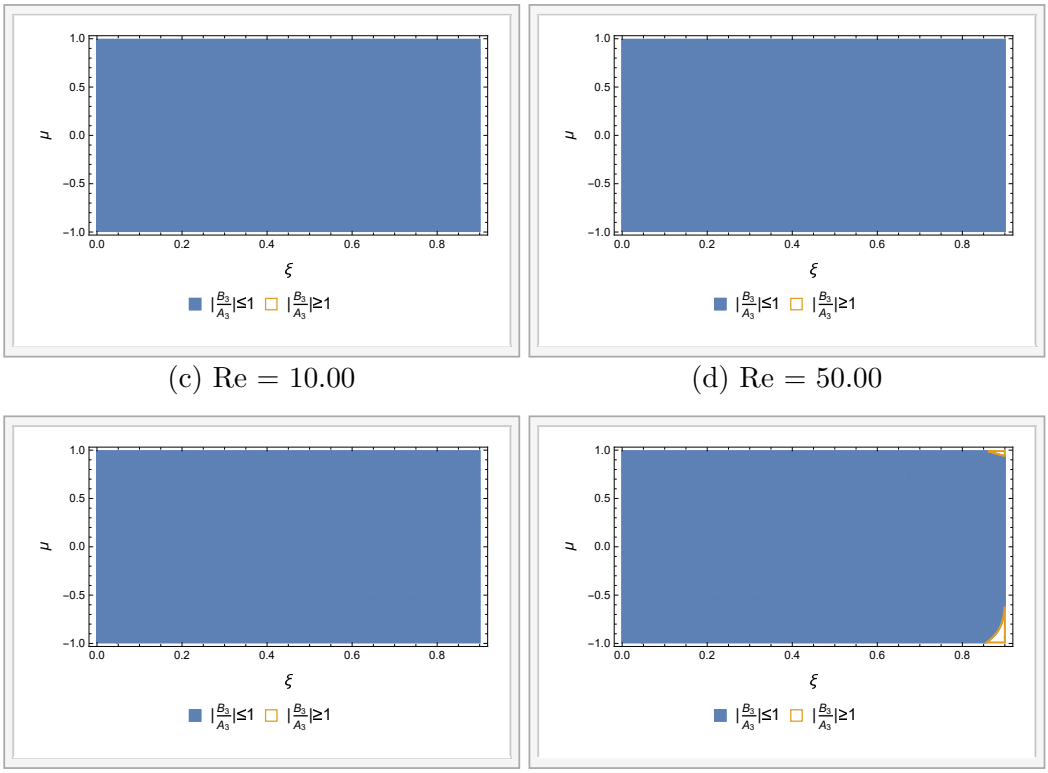


Figure 19: Region plots for $\delta\xi = 0.0230769$ and $\delta\mu = 0.0507692$ at various Reynolds numbers. The stable region is blue and unstable is white.

In figure 20, we have evaluated the stability of the FDM for 80×80 grid points. We picked $\delta\xi = 0.0113924$ and $\delta\mu = 0.0250633$ in order to be able to compare the stability results with the numerical results from figure 10. We find that the FDM is also stable at $Re = 0.01$, 1.00 and 10.00. The FDM becomes unstable at $Re = 50.00$.

(a) Re = 0.01 (b) Re = 1.00



(c) Re = 10.00 (d) Re = 50.00

Figure 20: Region plot for $\delta\xi = 0.0113924$ and $\delta\mu = 0.0250633$ at various Reynolds numbers. The stable region is blue and unstable is white.

6.3 Conclusion

We used the Von Neumann stability analysis to check the stability of the FDM for $Re = 0.01$, 1.00, 10.00 and 50.00 at various values of step sizes ($\delta\xi$ and $\delta\mu$). The stability results show that the FDM is conditionally stable. Figure 18 demonstrated that the FDM is stable at $Re = 0.01$, 1.00 and 10.00 for $\delta\xi = 0.1$ and $\delta\mu = 0.22$. The region of stability shrinks at $Re = 50.00$. We decreased the step sizes values to $\delta\xi = 0.0230769$ and $\delta\mu = 0.0507692$ and the region plot indicated that the FDM is still stable at $Re = 0.01$, 1.00 and 10.00. At $Re = 50.00$, the FDM becomes unstable and it is the same value at which the vortex forms as illustrated by the streamlines in figure 9. We can see that the stability analysis results are in agreement with the FDM numerical results. We decreased the step sizes values again to $\delta\xi = 0.0113924$ and $\delta\mu = 0.0250633$ and the FDM is still stable at $Re = 0.01$, 1.00 and 10.00. Now the region where the FDM becomes unstable becomes smaller at $Re = 50.00$.

From the stability analysis results for $Re = 0.01$, 1.00, 10.00 and 50.00 at various values of step sizes ($\delta\xi$ and $\delta\mu$), we note that the FDM is stable for small Reynolds numbers and the FDM becomes unstable at high Reynolds numbers. We can achieve stable if we keep the step sizes small. The stability is also dependent on the value of ξ because the region plots indicated that the FDM becomes unstable at ξ closer to 1.

7 Conclusion

In this dissertation we have studied the slow viscous incompressible flow past a stationary sphere. We have reproduced the solution of zero order problem that was obtained by Stokes [3] for slow viscous incompressible flow past a sphere. We also derived the solution of the first order problem and attempted to find the solution of the second order problem. We then reproduced the second term of Oseen expansion. We improved the solution of the first order problem by matching the Stokes and Oseen expansions to determine the constants of integration. We also tried to write an algorithm to obtain higher approximations of the flow using Mathematica. We used the second-order finite difference method (FDM) to solve the Navier-Stokes equations via the stream function approach (SFA). We compared the analytical and numerical (FDM) solution of the stream function. We also compared the solution of the FDM with the direct numerical simulation (DNS). Then we checked the stability of the FDM using the Von Neumann stability analysis.

The analytical solutions indicated that the zero order problem satisfies the boundary conditions at the surface of the sphere and far from the sphere. The solution of the first order problem does not satisfy the boundary conditions at infinity because the expansion breaks down for large r and the breakdown of the expansion is called the Whitehead paradox. Ossen resolved the Whitehead paradox by linearizing the inertia terms. The first order solution was improved by matching the Stokes expansion to the Oseen expansion. We could not find the solution of the second order problem using the Stokes expansion because we could not determine the constants that will satisfy the boundary conditions. The log r terms makes the equations to result in complex expressions. Proudman and Pearson [5] were able to determine the constants by matching the Stokes expansion to the Oseen expansion. We could not write an algorithm to obtain higher approximations of the flow using Mathematica because the trigonometric powers resulted in complex expressions that could not be reproduced algorithmically. We were able to find the zero and first order solutions using Mathematica.

We found the numerical solution of the stream function using the second-order FDM for various Reynolds numbers. The transformation of r and θ to ξ and μ allowed the computational domain to get arbitrarily closer to infinity. The transformation has an effect in the visualisation of the flow because it reduces the domain. The graph of ξ and r in figure 8 illustrated that ξ gets closer to 1 very quickly at about $r = 5$. The solution for the first two terms of the stream function was obtained using 40×40 and 80×80 data points for r interval [1, 3.30259] (ξ interval [0, 0.9]) at $Re = 0.01$, 1.00, 10.00, 50.00. The solution behaves the same for the 40×40 and 80×80 data points. The streamlines indicates that the solution is in agreement with previous authors results. The vortex did not form at $Re \leq 1$ which agrees with the Stokes expansion. Also the vortex did not form at $Re = 10.00$ but it formed at $Re = 50.00$ which is also in good agreement with previous studies results. We also found the solution of the first six terms of the stream function using 80×80 data points. The results are also in agreement with previous authors results. The solution of the first eleven terms of the stream function is also in agreement with previous results the were obtained by many authors.

The solution of the first two terms of the stream function breaks for large r when we use the r interval [1, 10.2103] (ξ interval [0, 0.9999]). The streamlines showed that the vortex forms at $Re = 0.5$ which is not in agreement with results for r interval [1, 3.30259] (ξ interval [0, 0.9]). We note that the solution breaks as r increases. It is important to note that the analytical solution of ψ_1 does not satisfy the boundary condition at infinity and it is not valid for large r. The FDM solution of the stream function is also not valid for large r as illustrated by the streamlines in figure 13. It looks like it is related to the Whitehead paradox. We note the that the Whitehead paradox is strong in the Stokes expansion because it is not only affecting the analytical solution but it is also present in the numerical solution. However we are able to bypass the Whitehead paradox using the FDM to approximate the solution of the stream function only for r closer to the sphere.

Analytical and numerical solutions were generated using 40×40 data points for r interval [1, 3.30259] (ξ interval [0, 0.9]) at $Re = 0.01$, 1.00, 10.00, 50.00. The comparison of the analytical solution with the numerical solution for the first two terms of ψ and Ψ indicated that the two solutions are in agreement for $Re \leq 1$. This is because the analytical solutions are valid for Reynolds numbers less or equal to 1. The numerical solution is also valid for $Re \leq 1$ because the solution of the zero order problem was used as an initial condition for the first order problem. The analytical and numerical solutions are not in agreement for Reynolds numbers greater than 1, this is because the analytical solution breaks for $Re > 1$. The analytical solution breaks for $Re > 1$ because the solution satisfies the boundary condition at the surface of the sphere and it does not satisfy the boundary condition at infinity. There is no choice of the constants of integration to correct it. The numerical solution does not break for r interval [1, 3.30259] (ξ interval [0, 0.9]) closer to the sphere. We observed that a vortex forms at $Re = 50.00$.

The DNS and FDM solutions were generated using 40×40 data points for r interval [1, 3.30259] (ξ interval [0, 0.9]). The streamlines of the DNS solution indicated that the vortex does not form at $Re = 0.01$, 1.00, 10.00 and it is in agreement with the streamlines of the FDM solution. The vortex forms at $Re = 50.00$ in both solutions. The numerical values of both solutions are in good agreement because the order of magnitude in both solutions is almost the same. The Mathematica code of the FDM approximates the solution of the stream function equation for any number of terms of Ψ and it runs faster than the DNS Mathematica code for solving the full Navier-Stokes equations directly. We can pick any Ψ solutions from the stream function numerical results and plot the solutions.

The Von Neumann stability analysis showed the FDM is conditionally stable because it is stable at $Re = 0.01$, 1.00, 10.00 and for small values of $\delta\xi$ and $\delta\mu$. The region plot of the stability results show that the scheme becomes unstable at $Re = 50.00$ which is in good agreement with the numerical results from figure 9. The stability results indicates that we can increase Re and achieve stability as long as we keep the values of $\delta\xi$ and $\delta\mu$ small compared to Re.

In future work we will explore the development of a numerical algorithm for the Oseen approximation as well as extending the code to include more general coordinates to allow for the investigation of Stokes flow passed an object of arbitrary shape.

A Algorithms

A.1 Analytical Code for ψ_0

$u = \frac{1}{r^2 \mathrm{Sin}[\theta]} D[\psi[r,\theta],\theta];$

$v = -\frac{1}{r \mathrm{Sin}[\theta]} D[\psi[r,\theta],r];$

$U = \{u, v, 0\};$

$W = \mathrm{Curl}[U, \{r,\theta,\phi\}, \text{“Spherical”}]//\mathrm{Expand}//\mathrm{FullSimplify};$

$\mathrm{LHS} = \mathrm{Curl}[\mathrm{Curl}[W, \{r,\theta,\phi\}, \text{“Spherical”}], \{r,\theta,\phi\},$

“Spherical”][[3]]//Expand//FullSimplify;

$\psi[\mathrm{r_}, \theta_]{:=}f[r]\mathrm{Sin}[\theta]^2$

$\mathrm{Equation} = \mathrm{LHS} == 0//\mathrm{FullSimplify};$

$f[r] = \mathrm{Limit}\left[\mathrm{DSolveValue}\left[\left\{\mathrm{Equation}, f[1] == 0, f'[1] == 0, f[R] == \frac{R^2}{2}, f'[R] == R\right\}, f[r], r\right], R \to \infty\right];$

$\psi[r,\theta] = f[r]\mathrm{Sin}[\theta]^2;$

A.2 Analytical Code for ψ_1

$u = \frac{1}{r^2 \text{Sin}[\theta]} D[\psi[r,\theta],\theta];$

$v = -\frac{1}{r \text{Sin}[\theta]} D[\psi[r,\theta],r];$

$U = \{u, v, 0\};$

$W = \text{Curl}[U, \{r,\theta,\phi\}, \text{“Spherical”}]//\text{Expand}//\text{FullSimplify};$

LHS = Curl[Curl[$W, \{r,\theta,\phi\}$, “Spherical”], $\{r,\theta,\phi\}$,

“Spherical”][[3]]//Expand//FullSimplify;

$\psi[\text{r_}, \theta_]:= \left(\frac{(-1+r)^2(1+2r)}{4r}\right) \text{Sin}[\theta]^2 + \text{re}\ \psi 1[r,\theta]$

RHS = reCurl[Cross[U, W], $\{r,\theta,\phi\}$, “Spherical”][[3]];

$\psi 1[\text{r_}, \theta_]:= f[r]\text{Cos}[\theta]\text{Sin}[\theta]^2$

Equation = LHS==Series[RHS, $\{\text{re}, 0, 1\}$]//Normal//FullSimplify;

$f[r] = \text{Limit}[\text{DSolveValue}[\{\text{Equation}, f[1] == 0, f'[1] == 0, f[R] == 0,$

$f'[R] == 0\}, f[r], r], R \to \infty];$

$\psi 1[r,\theta] = f[r]\text{Cos}[\theta]\text{Sin}[\theta]^2$

A.3 Numerical Code for Ψ

$$
\begin{aligned}
&\text{LHS[i_, j_]:=}\\
&(\mu(-\psi[i,-1+j]+\psi[i,1+j]))/(2g(1-\text{Log}[1-\xi])^4)-\\
&(\mu^3(-\psi[i,-1+j]+\psi[i,1+j]))/(2g(1-\text{Log}[1-\xi])^4)-\\
&(\mu(1-\mu^2)(-\psi[i,-1+j]+\psi[i,1+j]))/(2g(1-\text{Log}[1-\xi])^4)+\\
&(4(1-\mu^2)(\psi[i,-1+j]-2\psi[i,j]+\psi[i,1+j]))/(g^2(1-\text{Log}[1-\xi])^4)-\\
&(4\mu^2(1-\mu^2)(\psi[i,-1+j]-2\psi[i,j]+\psi[i,1+j]))/(g^2(1-\text{Log}[1-\xi])^4)+\\
&((1-\mu^2)(\psi[i,-2+j]-4\psi[i,-1+j]+6\psi[i,j]-4\psi[i,1+j]+\psi[i,2+j]))/\\
&(g^4(1-\text{Log}[1-\xi])^4)-\\
&(2\mu^2(1-\mu^2)(\psi[i,-2+j]-4\psi[i,-1+j]+6\psi[i,j]-4\psi[i,1+j]+\\
&\psi[i,2+j]))/(g^4(1-\text{Log}[1-\xi])^4)+\\
&(\mu^4(1-\mu^2)(\psi[i,-2+j]-4\psi[i,-1+j]+6\psi[i,j]-4\psi[i,1+j]+\\
&\psi[i,2+j]))/(g^4(1-\text{Log}[1-\xi])^4)-\\
&(2\mu(1-\mu^2)(-\psi[i,-2+j]+2\psi[i,-1+j]-2\psi[i,1+j]+\psi[i,2+j]))/\\
&(g^3(1-\text{Log}[1-\xi])^4)+\\
&(2\mu^3(1-\mu^2)(-\psi[i,-2+j]+2\psi[i,-1+j]-2\psi[i,1+j]+\psi[i,2+j]))/\\
&(g^3(1-\text{Log}[1-\xi])^4)-\tfrac{1}{2h}(1-\mu^2)(-\psi[-1+i,j]+\psi[1+i,j])+\\
&\tfrac{1}{2h}(1-\mu^2)\xi(-\psi[-1+i,j]+\psi[1+i,j])+\\
&\tfrac{1}{h^2}7(1-\mu^2)(\psi[-1+i,j]-2\psi[i,j]+\psi[1+i,j])-\\
&\tfrac{1}{h^2}14(1-\mu^2)\xi(\psi[-1+i,j]-2\psi[i,j]+\psi[1+i,j])+\\
&\tfrac{1}{h^2}7(1-\mu^2)\xi^2(\psi[-1+i,j]-2\psi[i,j]+\psi[1+i,j])+\\
&(2(1-\mu^2)((\psi[-1+i,-1+j]-2\psi[-1+i,j]+\psi[-1+i,1+j])/(g^2h^2)-\\
&(2(\psi[i,-1+j]-2\psi[i,j]+\psi[i,1+j]))/(g^2h^2)+\\
&(\psi[1+i,-1+j]-2\psi[1+i,j]+\psi[1+i,1+j])/(g^2h^2)))/
\end{aligned}
$$

$$
\begin{aligned}
&(1-\mathrm{Log}[1-\xi])^2- \\
&(2\mu^2\,(1-\mu^2)\,((\psi[-1+i,-1+j]-2\psi[-1+i,j]+\psi[-1+i,1+j])\,/(g^2h^2)- \\
&(2(\psi[i,-1+j]-2\psi[i,j]+\psi[i,1+j]))\,/(g^2h^2)+ \\
&\left(\psi[1+i,-1+j]-2\psi[1+i,j]+\psi[1+i,1+j]\right)/(g^2h^2)))/ \\
&(1-\mathrm{Log}[1-\xi])^2- \\
&(4\,(1-\mu^2)\,\xi\,((\psi[-1+i,-1+j]-2\psi[-1+i,j]+\psi[-1+i,1+j])\,/(g^2h^2)- \\
&(2(\psi[i,-1+j]-2\psi[i,j]+\psi[i,1+j]))\,/(g^2h^2)+ \\
&\left(\psi[1+i,-1+j]-2\psi[1+i,j]+\psi[1+i,1+j]\right)/(g^2h^2)))/ \\
&(1-\mathrm{Log}[1-\xi])^2+ \\
&(4\mu^2\,(1-\mu^2)\,\xi\,((\psi[-1+i,-1+j]-2\psi[-1+i,j]+\psi[-1+i,1+j])\,/(g^2h^2)- \\
&(2(\psi[i,-1+j]-2\psi[i,j]+\psi[i,1+j]))\,/(g^2h^2)+ \\
&\left(\psi[1+i,-1+j]-2\psi[1+i,j]+\psi[1+i,1+j]\right)/(g^2h^2)))/ \\
&(1-\mathrm{Log}[1-\xi])^2+ \\
&(2\,(1-\mu^2)\,\xi^2\,((\psi[-1+i,-1+j]-2\psi[-1+i,j]+\psi[-1+i,1+j])\,/(g^2h^2)- \\
&(2(\psi[i,-1+j]-2\psi[i,j]+\psi[i,1+j]))\,/(g^2h^2)+ \\
&\left(\psi[1+i,-1+j]-2\psi[1+i,j]+\psi[1+i,1+j]\right)/(g^2h^2)))/ \\
&(1-\mathrm{Log}[1-\xi])^2- \\
&(2\mu^2\,(1-\mu^2)\,\xi^2\,((\psi[-1+i,-1+j]-2\psi[-1+i,j]+\psi[-1+i,1+j])\,/(g^2h^2)- \\
&(2(\psi[i,-1+j]-2\psi[i,j]+\psi[i,1+j]))\,/(g^2h^2)+ \\
&\left(\psi[1+i,-1+j]-2\psi[1+i,j]+\psi[1+i,1+j]\right)/(g^2h^2)))/ \\
&(1-\mathrm{Log}[1-\xi])^2- \\
&(4\,(1-\mu^2)\,((-\psi[-1+i,-2+j]+\psi[1+i,-2+j])\,/(8g^2h)- \\
&(-\psi[-1+i,j]+\psi[1+i,j])\,/(4g^2h)+ \\
&\left(-\psi[-1+i,2+j]+\psi[1+i,2+j]\right)/(8g^2h)))\,/(1-\mathrm{Log}[1-\xi])^3+ \\
&(4\mu^2\,(1-\mu^2)\,((-\psi[-1+i,-2+j]+\psi[1+i,-2+j])\,/(8g^2h)-
\end{aligned}
$$

$$
\begin{aligned}
&(-\psi[-1+i,j]+\psi[1+i,j])/(4g^2h)+\\
&(-\psi[-1+i,2+j]+\psi[1+i,2+j])/(8g^2h)))/(1-\mathrm{Log}[1-\xi])^3+\\
&(4(1-\mu^2)\xi((-\psi[-1+i,-2+j]+\psi[1+i,-2+j])/(8g^2h)-\\
&(-\psi[-1+i,j]+\psi[1+i,j])/(4g^2h)+\\
&(-\psi[-1+i,2+j]+\psi[1+i,2+j])/(8g^2h)))/(1-\mathrm{Log}[1-\xi])^3-\\
&(4\mu^2(1-\mu^2)\xi((-\psi[-1+i,-2+j]+\psi[1+i,-2+j])/(8g^2h)-\\
&(-\psi[-1+i,j]+\psi[1+i,j])/(4g^2h)+\\
&(-\psi[-1+i,2+j]+\psi[1+i,2+j])/(8g^2h)))/(1-\mathrm{Log}[1-\xi])^3-\\
&(2(1-\mu^2)((-\psi[-1+i,-2+j]+\psi[1+i,-2+j])/(8g^2h)-\\
&(-\psi[-1+i,j]+\psi[1+i,j])/(4g^2h)+\\
&(-\psi[-1+i,2+j]+\psi[1+i,2+j])/(8g^2h)))/(1-\mathrm{Log}[1-\xi])^2+\\
&(2\mu^2(1-\mu^2)((-\psi[-1+i,-2+j]+\psi[1+i,-2+j])/(8g^2h)-\\
&(-\psi[-1+i,j]+\psi[1+i,j])/(4g^2h)+\\
&(-\psi[-1+i,2+j]+\psi[1+i,2+j])/(8g^2h)))/(1-\mathrm{Log}[1-\xi])^2+\\
&(2(1-\mu^2)\xi((-\psi[-1+i,-2+j]+\psi[1+i,-2+j])/(8g^2h)-\\
&(-\psi[-1+i,j]+\psi[1+i,j])/(4g^2h)+\\
&(-\psi[-1+i,2+j]+\psi[1+i,2+j])/(8g^2h)))/(1-\mathrm{Log}[1-\xi])^2-\\
&(2\mu^2(1-\mu^2)\xi((-\psi[-1+i,-2+j]+\psi[1+i,-2+j])/(8g^2h)-\\
&(-\psi[-1+i,j]+\psi[1+i,j])/(4g^2h)+\\
&(-\psi[-1+i,2+j]+\psi[1+i,2+j])/(8g^2h)))/(1-\mathrm{Log}[1-\xi])^2+\\
&\tfrac{1}{h^4}(1-\mu^2)(\psi[-2+i,j]-4\psi[-1+i,j]+6\psi[i,j]-4\psi[1+i,j]+\psi[2+i,j])-\\
&\tfrac{1}{h^4}4(1-\mu^2)\xi(\psi[-2+i,j]-4\psi[-1+i,j]+6\psi[i,j]-4\psi[1+i,j]+\\
&\psi[2+i,j])+\\
&\tfrac{1}{h^4}6(1-\mu^2)\xi^2(\psi[-2+i,j]-4\psi[-1+i,j]+6\psi[i,j]-4\psi[1+i,j]+\\
&\psi[2+i,j])-
\end{aligned}
$$

$\frac{1}{h^4}4\,(1-\mu^2)\,\xi^3(\psi[-2+i,j]-4\psi[-1+i,j]+6\psi[i,j]-4\psi[1+i,j]+$

$\psi[2+i,j])+$

$\frac{1}{h^4}\,(1-\mu^2)\,\xi^4(\psi[-2+i,j]-4\psi[-1+i,j]+6\psi[i,j]-4\psi[1+i,j]+$

$\psi[2+i,j])-$

$\frac{1}{h^3}3\,(1-\mu^2)\,(-\psi[-2+i,j]+2\psi[-1+i,j]-2\psi[1+i,j]+\psi[2+i,j])+$

$\frac{1}{h^3}9\,(1-\mu^2)\,\xi(-\psi[-2+i,j]+2\psi[-1+i,j]-2\psi[1+i,j]+\psi[2+i,j])-$

$\frac{1}{h^3}9\,(1-\mu^2)\,\xi^2(-\psi[-2+i,j]+2\psi[-1+i,j]-2\psi[1+i,j]+\psi[2+i,j])+$

$\frac{1}{h^3}3\,(1-\mu^2)\,\xi^3(-\psi[-2+i,j]+2\psi[-1+i,j]-2\psi[1+i,j]+\psi[2+i,j])/.$

$\xi\to\xi_i/.\mu\to\mu_j;$

RHS[i_, j_]:=

$(2\,(1-\mu^2)\,(-\psi[i,-1+j]+\psi[i,1+j])(\psi[i,-1+j]-2\psi[i,j]+\psi[i,1+j]))/$

$(g^3(1-\mathrm{Log}[1-\xi])^5)-$

$(2\mu^2\,(1-\mu^2)\,(-\psi[i,-1+j]+\psi[i,1+j])$

$(\psi[i,-1+j]-2\psi[i,j]+\psi[i,1+j]))\,/(g^3(1-\mathrm{Log}[1-\xi])^5)+$

$((-\psi[i,-1+j]+\psi[i,1+j])(-\psi[-1+i,j]+\psi[1+i,j]))/$

$(4gh(1-\mathrm{Log}[1-\xi])^4)-$

$(\mu^2(-\psi[i,-1+j]+\psi[i,1+j])(-\psi[-1+i,j]+\psi[1+i,j]))/$

$(4gh(1-\mathrm{Log}[1-\xi])^4)-$

$((1-\mu^2)\,(-\psi[i,-1+j]+\psi[i,1+j])(-\psi[-1+i,j]+\psi[1+i,j]))/$

$(4gh(1-\mathrm{Log}[1-\xi])^4)-$

$(\xi(-\psi[i,-1+j]+\psi[i,1+j])(-\psi[-1+i,j]+\psi[1+i,j]))/$

$(4gh(1-\mathrm{Log}[1-\xi])^4)+$

$(\mu^2\xi(-\psi[i,-1+j]+\psi[i,1+j])(-\psi[-1+i,j]+\psi[1+i,j]))/$

$(4gh(1-\mathrm{Log}[1-\xi])^4)+$

$((1-\mu^2)\,\xi(-\psi[i,-1+j]+\psi[i,1+j])(-\psi[-1+i,j]+\psi[1+i,j]))/$

$$
\begin{aligned}
&(4gh(1-\text{Log}[1-\xi])^4)- \\
&((1-\mu^2)\,(-\psi[i,-1+j]+\psi[i,1+j])(-\psi[-1+i,j]+\psi[1+i,j]))/ \\
&(2gh(1-\text{Log}[1-\xi])^3)+ \\
&((1-\mu^2)\,\xi(-\psi[i,-1+j]+\psi[i,1+j])(-\psi[-1+i,j]+\psi[1+i,j]))/ \\
&(2gh(1-\text{Log}[1-\xi])^3)- \\
&((1-\mu^2)\,(-\psi[i,-1+j]+\psi[i,1+j])(-\psi[-1+i,j]+\psi[1+i,j]))/ \\
&(4gh(1-\text{Log}[1-\xi])^2)+ \\
&((1-\mu^2)\,\xi(-\psi[i,-1+j]+\psi[i,1+j])(-\psi[-1+i,j]+\psi[1+i,j]))/ \\
&(4gh(1-\text{Log}[1-\xi])^2)+ \\
&((1-\mu^2)\,(-\psi[i,-2+j]+2\psi[i,-1+j]-2\psi[i,1+j]+\psi[i,2+j]) \\
&(-\psi[-1+i,j]+\psi[1+i,j]))\,/(4g^3h(1-\text{Log}[1-\xi])^4)- \\
&(\mu^2\,(1-\mu^2)\,(-\psi[i,-2+j]+2\psi[i,-1+j]-2\psi[i,1+j]+\psi[i,2+j]) \\
&(-\psi[-1+i,j]+\psi[1+i,j]))\,/(4g^3h(1-\text{Log}[1-\xi])^4)- \\
&((1-\mu^2)\,\xi(-\psi[i,-2+j]+2\psi[i,-1+j]-2\psi[i,1+j]+\psi[i,2+j]) \\
&(-\psi[-1+i,j]+\psi[1+i,j]))\,/(4g^3h(1-\text{Log}[1-\xi])^4)+ \\
&(\mu^2\,(1-\mu^2)\,\xi(-\psi[i,-2+j]+2\psi[i,-1+j]-2\psi[i,1+j]+\psi[i,2+j]) \\
&(-\psi[-1+i,j]+\psi[1+i,j]))\,/(4g^3h(1-\text{Log}[1-\xi])^4)- \\
&(\mu(-\psi[-1+i,j]+\psi[1+i,j])^2)\,/\,(2h^2(1-\text{Log}[1-\xi])^2)+ \\
&(\mu\xi(-\psi[-1+i,j]+\psi[1+i,j])^2)\,/\,(h^2(1-\text{Log}[1-\xi])^2)- \\
&(\mu\xi^2(-\psi[-1+i,j]+\psi[1+i,j])^2)\,/\,(2h^2(1-\text{Log}[1-\xi])^2)+ \\
&((1-\mu^2)\,(-\psi[i,-1+j]+\psi[i,1+j])(\psi[-1+i,j]-2\psi[i,j]+\psi[1+i,j]))/ \\
&(gh^2(1-\text{Log}[1-\xi])^3)- \\
&(2\,(1-\mu^2)\,\xi(-\psi[i,-1+j]+\psi[i,1+j]) \\
&(\psi[-1+i,j]-2\psi[i,j]+\psi[1+i,j]))\,/(gh^2(1-\text{Log}[1-\xi])^3)+ \\
&((1-\mu^2)\,\xi^2(-\psi[i,-1+j]+\psi[i,1+j])
\end{aligned}
$$

$$(\psi[-1+i,j]-2\psi[i,j]+\psi[1+i,j]))/(gh^2(1-\text{Log}[1-\xi])^3)+$$
$$(3(1-\mu^2)(-\psi[i,-1+j]+\psi[i,1+j])$$
$$(\psi[-1+i,j]-2\psi[i,j]+\psi[1+i,j]))/(2gh^2(1-\text{Log}[1-\xi])^2)-$$
$$(3(1-\mu^2)\xi(-\psi[i,-1+j]+\psi[i,1+j])$$
$$(\psi[-1+i,j]-2\psi[i,j]+\psi[1+i,j]))/(gh^2(1-\text{Log}[1-\xi])^2)+$$
$$(3(1-\mu^2)\xi^2(-\psi[i,-1+j]+\psi[i,1+j])$$
$$(\psi[-1+i,j]-2\psi[i,j]+\psi[1+i,j]))/(2gh^2(1-\text{Log}[1-\xi])^2)+$$
$$(\mu(-\psi[-1+i,j]+\psi[1+i,j])(\psi[-1+i,j]-2\psi[i,j]+\psi[1+i,j]))/$$
$$(h^3(1-\text{Log}[1-\xi])^2)-$$
$$(3\mu\xi(-\psi[-1+i,j]+\psi[1+i,j])(\psi[-1+i,j]-2\psi[i,j]+\psi[1+i,j]))/$$
$$(h^3(1-\text{Log}[1-\xi])^2)+$$
$$(3\mu\xi^2(-\psi[-1+i,j]+\psi[1+i,j])(\psi[-1+i,j]-2\psi[i,j]+\psi[1+i,j]))/$$
$$(h^3(1-\text{Log}[1-\xi])^2)-$$
$$(\mu\xi^3(-\psi[-1+i,j]+\psi[1+i,j])(\psi[-1+i,j]-2\psi[i,j]+\psi[1+i,j]))/$$
$$(h^3(1-\text{Log}[1-\xi])^2)-$$
$$((1-\mu^2)(-\psi[-1+i,j]+\psi[1+i,j])$$
$$(-((-\psi[-1+i,-1+j]+\psi[1+i,-1+j])/(4gh))+$$
$$(-\psi[-1+i,1+j]+\psi[1+i,1+j])/(4gh)))/(2h(1-\text{Log}[1-\xi])^2)+$$
$$((1-\mu^2)\xi(-\psi[-1+i,j]+\psi[1+i,j])$$
$$(-((-\psi[-1+i,-1+j]+\psi[1+i,-1+j])/(4gh))+$$
$$(-\psi[-1+i,1+j]+\psi[1+i,1+j])/(4gh)))/(h(1-\text{Log}[1-\xi])^2)-$$
$$((1-\mu^2)\xi^2(-\psi[-1+i,j]+\psi[1+i,j])$$
$$(-((-\psi[-1+i,-1+j]+\psi[1+i,-1+j])/(4gh))+$$
$$(-\psi[-1+i,1+j]+\psi[1+i,1+j])/(4gh)))/(2h(1-\text{Log}[1-\xi])^2)-$$
$$((1-\mu^2)(-\psi[i,-1+j]+\psi[i,1+j])$$

$$
\begin{aligned}
&((-\psi[-1+i,-2+j]+\psi[1+i,-2+j])/(8g^2h)-\\
&(-\psi[-1+i,j]+\psi[1+i,j])/(4g^2h)+\\
&(-\psi[-1+i,2+j]+\psi[1+i,2+j])/(8g^2h)))/(2g(1-\mathrm{Log}[1-\xi])^4)+\\
&(\mu^2(1-\mu^2)(-\psi[i,-1+j]+\psi[i,1+j])\\
&((-\psi[-1+i,-2+j]+\psi[1+i,-2+j])/(8g^2h)-\\
&(-\psi[-1+i,j]+\psi[1+i,j])/(4g^2h)+\\
&(-\psi[-1+i,2+j]+\psi[1+i,2+j])/(8g^2h)))/(2g(1-\mathrm{Log}[1-\xi])^4)+\\
&((1-\mu^2)\xi(-\psi[i,-1+j]+\psi[i,1+j])\\
&((-\psi[-1+i,-2+j]+\psi[1+i,-2+j])/(8g^2h)-\\
&(-\psi[-1+i,j]+\psi[1+i,j])/(4g^2h)+\\
&(-\psi[-1+i,2+j]+\psi[1+i,2+j])/(8g^2h)))/(2g(1-\mathrm{Log}[1-\xi])^4)-\\
&(\mu^2(1-\mu^2)\xi(-\psi[i,-1+j]+\psi[i,1+j])\\
&((-\psi[-1+i,-2+j]+\psi[1+i,-2+j])/(8g^2h)-\\
&(-\psi[-1+i,j]+\psi[1+i,j])/(4g^2h)+\\
&(-\psi[-1+i,2+j]+\psi[1+i,2+j])/(8g^2h)))/(2g(1-\mathrm{Log}[1-\xi])^4)-\\
&((1-\mu^2)(-\psi[i,-1+j]+\psi[i,1+j])\\
&(-\psi[-2+i,j]+2\psi[-1+i,j]-2\psi[1+i,j]+\psi[2+i,j]))/\\
&(4gh^3(1-\mathrm{Log}[1-\xi])^2)+\\
&(3(1-\mu^2)\xi(-\psi[i,-1+j]+\psi[i,1+j])\\
&(-\psi[-2+i,j]+2\psi[-1+i,j]-2\psi[1+i,j]+\psi[2+i,j]))/\\
&(4gh^3(1-\mathrm{Log}[1-\xi])^2)-\\
&(3(1-\mu^2)\xi^2(-\psi[i,-1+j]+\psi[i,1+j])\\
&(-\psi[-2+i,j]+2\psi[-1+i,j]-2\psi[1+i,j]+\psi[2+i,j]))/\\
&(4gh^3(1-\mathrm{Log}[1-\xi])^2)+\\
&((1-\mu^2)\xi^3(-\psi[i,-1+j]+\psi[i,1+j])
\end{aligned}
$$

$$(-\psi[-2+i,j]+2\psi[-1+i,j]-2\psi[1+i,j]+\psi[2+i,j]))/$$
$$(4gh^3(1-\text{Log}[1-\xi])^2)+(1/(2h(1-\text{Log}[1-\xi])^2))\,(1-\mu^2)$$
$$(-\psi[-1+i,j]+\psi[1+i,j])$$
$$((-\psi[-2+i,-1+j]+\psi[i,-1+j])/(8gh^2)-$$
$$(-\psi[-2+i,1+j]+\psi[i,1+j])/(8gh^2)-$$
$$(-\psi[i,-1+j]+\psi[2+i,-1+j])/(8gh^2)+$$
$$(-\psi[i,1+j]+\psi[2+i,1+j])/(8gh^2))-$$
$$(1/(2h(1-\text{Log}[1-\xi])^2))\,3\,(1-\mu^2)\,\xi(-\psi[-1+i,j]+\psi[1+i,j])$$
$$((-\psi[-2+i,-1+j]+\psi[i,-1+j])/(8gh^2)-$$
$$(-\psi[-2+i,1+j]+\psi[i,1+j])/(8gh^2)-$$
$$(-\psi[i,-1+j]+\psi[2+i,-1+j])/(8gh^2)+$$
$$(-\psi[i,1+j]+\psi[2+i,1+j])/(8gh^2))+$$
$$(1/(2h(1-\text{Log}[1-\xi])^2))\,3\,(1-\mu^2)\,\xi^2(-\psi[-1+i,j]+\psi[1+i,j])$$
$$((-\psi[-2+i,-1+j]+\psi[i,-1+j])/(8gh^2)-$$
$$(-\psi[-2+i,1+j]+\psi[i,1+j])/(8gh^2)-$$
$$(-\psi[i,-1+j]+\psi[2+i,-1+j])/(8gh^2)+$$
$$(-\psi[i,1+j]+\psi[2+i,1+j])/(8gh^2))-$$
$$(1/(2h(1-\text{Log}[1-\xi])^2))\,(1-\mu^2)\,\xi^3(-\psi[-1+i,j]+\psi[1+i,j])$$
$$((-\psi[-2+i,-1+j]+\psi[i,-1+j])/(8gh^2)-$$
$$(-\psi[-2+i,1+j]+\psi[i,1+j])/(8gh^2)-$$
$$(-\psi[i,-1+j]+\psi[2+i,-1+j])/(8gh^2)+$$
$$(-\psi[i,1+j]+\psi[2+i,1+j])/(8gh^2))/.\xi\to\xi_i/.\mu\to\mu_j/.\psi\to\psi 0/.$$
$$\text{re}\to 1;$$

$\mathrm{Ns} = 2;$

$\mathrm{N}\xi = 80;$

$\mathrm{N}\mu = 80;$

$a = 0;$

$b = 0.9;$

$c = 0.99;$

$d = -0.99;$

$h = \frac{b-a}{(\mathrm{N}\xi-1)};$

$g = \frac{d-c}{(\mathrm{N}\mu-1)};$

$\xi\mathrm{grid} = \mathrm{Range}[a, b, h];$

$\mu\mathrm{grid} = \mathrm{Range}[c, d, g];$

$\xi\mathrm{values} = \mathrm{NSolve}\left[\mathrm{Table}\left[\xi_i, \{i, 2, \mathrm{N}\xi + 1\}\right] == \xi\mathrm{grid}, \mathrm{Table}\left[\xi_i, \{i, 2, \mathrm{N}\xi + 1\}\right]\right] //$

Flatten;

$\mu\mathrm{values} = \mathrm{NSolve}\left[\mathrm{Table}\left[\mu_j, \{j, 2, \mathrm{N}\mu + 1\}\right] == \mu\mathrm{grid}, \mathrm{Table}\left[\mu_j, \{j, 2, \mathrm{N}\mu + 1\}\right]\right] //$

Flatten;

$\mathrm{Solution}[0] =$

$\mathrm{Table}\left[\frac{1}{4}\left(1 - {\mu_j}^2\right)\left(\frac{1}{1-\mathrm{Log}[1-\xi_i]} - 3\left(1 - \mathrm{Log}\left[1 - \xi_i\right]\right) + 2\left(1 - \mathrm{Log}\left[1 - \xi_i\right]\right)^2\right),\right.$

$\{i, 2, \mathrm{N}\xi + 1\}, \{j, 2, \mathrm{N}\mu + 1\}]/.\xi\mathrm{values}/.\mu\mathrm{values}//\mathrm{Flatten};$

$\psi 00\mathrm{Grid} = \mathrm{Table}[\psi 0[i, j], \{i, 2, \mathrm{N}\xi + 1\}, \{j, 2, \mathrm{N}\mu + 1\}]//\mathrm{Flatten};$

$\mathrm{sol}[0] = \ \mathrm{NSolve}[\psi 00\mathrm{Grid} == \mathrm{Solution}[0], \psi 00\mathrm{Grid}]//\mathrm{Flatten};$

$\mathrm{BC1} = \mathrm{Table}[\psi[2, j] == 0, \{j, 3, \mathrm{N}\mu\}]//\mathrm{Flatten};$

$\mathrm{BC2} = \mathrm{Table}[\psi[\mathrm{N}\xi + 1, j] == 0, \{j, 3, \mathrm{N}\mu\}, \{i, \mathrm{N}\xi + 1, \mathrm{N}\xi + 1\}]/.\xi\mathrm{values}/.\mu\mathrm{values}//$

Flatten;

$\mathrm{BC3} = \mathrm{Table}[\psi[i, 2] == 0, \{i, 2, \mathrm{N}\mu + 1\}]//\mathrm{Flatten};$

BC4 = Table[$\psi[i, \mathrm{N}\mu + 1] == 0, \{i, 2, \mathrm{N}\mu + 1\}$]//Flatten;

BC5 = NSolve[Table[$\psi[1, j] == \psi[3, j], \{j, 3, \mathrm{N}\mu\}$], Table[$\psi[1, j], \{j, 3, \mathrm{N}\mu\}$]]//

Flatten;

BC6 = NSolve[Table[$\psi 0[1, j] == \psi 0[3, j], \{j, 2, \mathrm{N}\mu + 1\}$],

Table[$\psi 0[1, j], \{j, 2, \mathrm{N}\mu + 1\}$]]//Flatten;

BC7 =

NSolve[Table[$\psi[\mathrm{N}\xi + 2, j] == \psi[\mathrm{N}\xi, j], \{j, 2, \mathrm{N}\mu + 1\}$],

Table[$\psi[\mathrm{N}\xi + 2, j], \{j, 2, \mathrm{N}\mu + 1\}$]]/.$\xi$values/.$\mu$values//Flatten;

BC8 =

NSolve $\left[\text{Table}\left[\psi 0[\mathrm{N}\xi + 2, j] == \psi 0[\mathrm{N}\xi, j] + 2 * h\left(\frac{\left(1-\text{Log}\left[1-\xi_{\mathrm{N}\xi+1}\right]\right)}{\left(1-\xi_{\mathrm{N}\xi+1}\right)}\left(1-{\mu_j}^2\right)\right),\right.\right.$
$\{j, 2, \mathrm{N}\mu + 1\}]$, Table[$\psi 0[\mathrm{N}\xi + 2, j], \{j, 2, \mathrm{N}\mu + 1\}$]]/.$\xi$values/.$\mu$values//

Flatten;

BC9 = NSolve[Table[$\psi[i, 1] == -\psi[i, \mathrm{N}\mu], \{i, 2, \mathrm{N}\xi + 1\}$],

Table[$\psi[i, 1], \{i, 2, \mathrm{N}\xi + 1\}$]]//Flatten;

BC10 = NSolve[Table[$\psi 0[i, 1] == -\psi 0[i, \mathrm{N}\mu], \{i, 2, \mathrm{N}\xi + 1\}$],

Table[$\psi 0[i, 1], \{i, 2, \mathrm{N}\xi + 1\}$]]//Flatten;

BC11 = NSolve[Table[$\psi[i, \mathrm{N}\mu + 2] == -\psi[i, 3], \{i, 2, \mathrm{N}\xi + 1\}$],

Table[$\psi[i, \mathrm{N}\mu + 2], \{i, 2, \mathrm{N}\xi + 1\}$]]//Flatten;

BC12 = NSolve[Table[$\psi 0[i, \mathrm{N}\mu + 2] == -\psi 0[i, 3], \{i, 2, \mathrm{N}\xi + 1\}$],

Table[$\psi 0[i, \mathrm{N}\mu + 2], \{i, 2, \mathrm{N}\xi + 1\}$]]//Flatten;

BOC = Join[BC5, BC6, BC7, BC8, BC9, BC10, BC11, BC12];

Equation1 =

Table[{LHS$[i, j]$ == RHS$[i, j]$}, $\{i, 3, \mathrm{N}\xi\}, \{j, 3, \mathrm{N}\mu\}$]/.BOC/.$\xi$values/.

μvalues//Flatten;

$$\text{Equation2} = \text{Join}[\text{Equation1}, \text{BC1}, \text{BC2}, \text{BC3}, \text{BC4}];$$

$$\text{For}[n = 1, n < \text{Ns}, n{+}{+},$$
$$\text{Equation}[n] = \text{Equation2}/.\text{sol}[n-1];$$
$$\text{variables}[n] = \text{Union}[\text{Cases}[\text{Equation}[n], \psi[_, _], \infty]];$$
$$\{B, A\} = \text{CoefficientArrays}[\text{Equation}[n], \text{variables}[n]];$$
$$\text{Solution}[n] = \text{LinearSolve}[A, -B];$$
$$\text{sol}[n] = \text{NSolve}[\psi 00\text{Grid} == \text{Solution}[n], \psi 00\text{Grid}]//\text{Flatten};$$
$$]$$

$$\psi\text{grid} = \text{Table}[\psi[i, j], \{i, 2, \text{N}\xi + 1\}, \{j, 2, \text{N}\mu + 1\}]//\text{Flatten};$$
$$\text{Data1} = \text{Solution}[0] + \text{Sum}\left[\text{re}^{n}\text{Solution}[n], \{n, 1, \text{Ns} - 1\}\right];$$
$$\text{Data2} = \text{NSolve}[\psi\text{grid} == \text{Data1}, \psi\text{grid}]//\text{Flatten};$$

$$\text{BC13} = \text{NSolve}[\text{Table}[\psi[1, j] == \psi[3, j], \{j, 2, \text{N}\mu + 1\}],$$
$$\text{Table}[\psi[1, j], \{j, 2, \text{N}\mu + 1\}]]//\text{Flatten};$$
$$\text{BC14} = \text{NSolve}[\text{Table}[\psi[i, 1] == -\psi[i, \text{N}\mu], \{i, 2, \text{N}\xi + 1\}],$$
$$\text{Table}[\psi[i, 1], \{i, 2, \text{N}\xi + 1\}]]//\text{Flatten};$$
$$\text{BC15} = \text{NSolve}[\text{Table}[\psi[i, \text{N}\mu + 2] == -\psi[i, 3], \{i, 2, \text{N}\xi + 1\}],$$
$$\text{Table}[\psi[i, \text{N}\mu + 2], \{i, 2, \text{N}\xi + 1\}]]//\text{Flatten};$$
$$\text{BC16} =$$
$$\text{NSolve}\left[\text{Table}\left[\psi[\text{N}\xi + 2, j] == \psi[\text{N}\xi, j] + 2 * h\left(\frac{\left(1-\text{Log}\left[1-\xi_{\text{N}\xi+1}\right]\right)}{\left(1-\xi_{\text{N}\xi+1}\right)}\left(1-{\mu_j}^2\right)\right),\right.\right.$$
$$\left.\left.\{j, 1, \text{N}\mu + 1\}\right], \text{Table}[\psi[\text{N}\xi + 2, j], \{j, 1, \text{N}\mu + 1\}]]/.\xi\text{values}/.\mu\text{values}//$$
$$\text{Flatten};$$

$$\text{D1} =$$
$$\text{Table}\left[\{\{(1 - \text{Log}\left[1 - \xi_i\right])\,\mu_j, (1 - \text{Log}\left[1 - \xi_i\right])\,\text{Sqrt}\left[1 - {\mu_j}^2\right]\}\right.,$$

$\{u[i,j]\mu_j - v[i,j]\text{Sqrt}\left[1-{\mu_j}^2\right], u[i,j]\text{Sqrt}\left[1-{\mu_j}^2\right] + v[i,j]\mu_j\}\},$

$\{i, 2, \text{N}\xi + 1\}, \{j, 2, \text{N}\mu + 1\}]/.\xi\text{values}/.\mu\text{values};$

$u[\text{i_}, \text{j_}]:= -\frac{1}{r^2}\left(\frac{(\psi[i,j+1]-\psi[i,j-1])}{2*g}\right)/.r \to (1 - \text{Log}\left[1-\xi_i\right])$

$v[\text{i_}, \text{j_}]:=$

$-\frac{1}{r\text{Sin}[\theta]}\left(e^{1-r}\right)\left(\frac{(\psi[i+1,j]-\psi[i-1,j])}{2*h}\right)/.r \to (1 - \text{Log}\left[1-\xi_i\right])/.$

$\frac{1}{\text{Sin}[\theta]} \to \frac{1}{\text{Sqrt}[1-{\mu_j}^2]}$

$\text{D2} = \text{Flatten}[\text{D1}, 1]/.\text{BC13}/.\text{BC14}/.\text{BC15}/.\text{BC16}/.\text{Data2}/.\xi\text{values}/.\mu\text{values};$

$\text{Manipulate}[\text{ListStreamDensityPlot}[\text{Out}[46], \text{AspectRatio} \to 1/2,$

$\text{ImageSize} \to \text{Large}, \text{PlotRange} \to \text{All}, \text{ColorFunction} \to \text{“SunsetColors”},$

$\text{RegionFunction} \to \text{Function}\left[\{x, y\}, x^2 + y^2 > 1\right], \text{FrameStyle} \to \text{Directive}[\text{Bold}, 15],$

$\text{FrameLabel} \to \{\text{x}, \text{y}\}], \{\text{re}, 0, 1000, 10\}]$

References

[1] D. Abrecht, An analytical solution method for the unsteady, unbounded, incompressible three-dimensional Navier-Stokes equations in cartesian coordinates using coordinate axis symmetry degeneracy. http://authors.library.caltech.edu/28596/1/Abrecht_20111225_NS.pdf , 1-2, 2011.

[2] Suprijadi, M. R. A. Sentosa, P. Subekti, and S. Virid, Application of computational physics: Blood vessel constrictions and medical infuses. AIP Conference Proceedings, 1587.1, 1, 2014.

[3] G. G. Stokes, On the effect of the internal friction of fluids on the motion of pendulums. Cambridge: Pitt Press, 9, 8, 1851.

[4] A. N. Whitehead, Second approximations to viscous fluid motion. Quart. J. Math, 23, 143-152, 1889.

[5] L. Proudman and J. R. A. Pearson, Expansions at small Reynolds numbers for the flow past a sphere and a circular cylinder. Journal of Fluid Mechanics, 2.3, 237-262, 1957.

[6] C. W. Oseen, Stokes' formula and a related theorem in hydrodynamics, Arkiv. Mat. Astron. Fysik, 6, 20, 1910.

[7] S. Kaplun and P. A. Lagerstrom, Asymptotic expansions of Navier-Stokes solutions for small Reynolds numbers. Journal of Mathematics and Mechanics, 6, 585-593, 1957.

[8] M. D. Van Dyke, Perturbation Methods in Fluid Mechanics. New York: Academic Press, 136, 1964.

[9] J. S. B. Gajjar, Asymptotic expansions and perturbation methods math44011/64011. http://www.maths.manchester.ac.uk/∼gajjar, 7-15, 2010.

[10] M. Kohr, An application of the method of matched asymptotic expansions for low Reynolds number flow past a cylinder of arbitrary cross section. International Journal of Mathematics and Mathematical Sciences, 47, 2525-2535, 2004.

[11] S. Datta and S. Singhal, Small Reynolds Number Steady Flow Past a Sphere with a Source at its Centre. Applications and Applied Mathematics: An International Journal (AAM), 6.1, 201-210, 2011.

[12] A. Umemura, Matched-asymptotic analysis of low-Reynolds-number flow past two equal circular cylinders. Journal of Fluid Mechanics, 121, 345-363, 1982.

[13] D. K. Srivastava, R. R. Yadav, and S. Yadav, Steady Oseen's flow past a deformed sphere: an analytical approach. Journal of Theoretical and Applied Mechanics, 51.3, 661-673, 2013.

[14] C. Thieulot, Analytical solution for viscous incompressible Stokes flow in a spherical shell. Solid Earth, 8.6, 1181, 2017.

[15] J. J. L. Higdon and M. Kojima, On the calculation of Stokes flow past porous particles. Int. J. Multiphase Flow, 7.6, 719-727, 1981.

[16] H. C. Brinkman, A calculation of the viscous force exerted by a flowing fluid in dense swarm of particles. Appl. Sci. Res, A1, 27-34, 1947.

[17] B. S. Padmavathi, T. Amaranath, and S. D. Nigam, Stokes flow past a porous sphere using Brinkman's model. Zeitschrift für angewandte Mathematik und Physik ZAMP, 44.5, 929-939, 1993.

[18] K. D. Housiadas, G. C. Georgiou, and R. I. Tanner, A note on the unbounded creeping flow past a sphere for Newtonian fluids with pressure-dependent viscosity. International Journal of Engineering Science, 86, 1-9, 2015.

[19] L. Zhao, Hydrodynamics of Highly Viscous Flow past a Compound Particle: Analytical Solution. Fluids, 1.4, 36, 2016.

[20] A. A. Ragab, K. M. Hemida, M. S. Mohamed, M. A. El Salam, and N. City, Solution of time-fractional Navier–Stokes equation by using homotopy analysis method. Gen Math Notes, 13.2, 13-21, 2012.

[21] J. V. R. Murthy and M. P. Kumar, Effect of slip parameter on the flow of viscous fluid past an impervious sphere. International Journal of Applied Science and Engineering, 12.3, 203-223, 2014.

[22] M. O. Bristeau, G. Roland, and J. Periaux, Numerical methods for the Navier-Stokes equations. Applications to the simulation of compressible and incompressible viscous flows. Computer Physics Reports, 6.1-6, 73-187, 1987.

[23] Y. Li and K. Li, Operator splitting methods for the Navier-Stokes equations with nonlinear slip boundary conditions. International Journal of Numerical Analysis and Modeling, 7, 785-805, 2010.

[24] J. Djoko and J. Koko, Numerical methods for the Stokes and Navier–Stokes equations driven by threshold slip boundary conditions. Computer Methods in Applied Mechanics and Engineering, 305, 936-958, 2016.

[25] A. J. Chorin, The numerical solution of the Navier-Stokes equations for an incompressible fluid. Bulletin of the American Mathematical Society, 73.6, 928-931, 1967.

[26] C. I. Christov and P. K. Volkov, Numerical investigation of the steady viscous flow past a stationary deformable bubble. Journal of Fluid Mechanics, 158, 341-364, 1985.

[27] B. Fornberg, Steady viscous flow past a sphere at high Reynolds numbers. Journal of Fluid Mechanics, 190, 471-489, 1988.

[28] L. B. Zhang, A second-order upwinding finite difference scheme for the steady Navier-Stokes equations in primitive variables in a driven cavity with a multigrid solver. ESAIM: Mathematical Modelling and Numerical Analysis, 24.1, 133-150, 1990.

[29] G. H. Juncu, A numerical study of steady viscous flow past a fluid sphere. International journal of heat and fluid flow, 20.4, 414-421, 1999.

[30] H. Johnston and J.G Liu, Finite difference schemes for incompressible flow based on local pressure boundary conditions. Journal of Computational Physics, 180.1, 120-154, 2002.

[31] M. C. Lai, Fourth-order finite difference scheme for the incompressible Navier–Stokes equations in a disk. International journal for numerical methods in fluids, 42.8, 909-922, 2003.

[32] Z. Li and C. Wang, A fast finite difference method for solving navier-stokes equations on irregular domains. Communications in Mathematical Sciences, 1.1, 180-196, 2003.

[33] J. P. De Angeli, A. M. Valli, N. C. Reis, and A. F. De Souza, Finite difference simulations of the Navier-Stokes equations using parallel distributed computing. In Computer Architecture and High Performance Computing, 15, 149-156, 2003.

[34] M. Quadrio and P. Luchini, The numerical solution of the incompressible Navier–Stokes equations on a low-cost, dedicated parallel computer. Preprint, 2004.

[35] M. Svärd, M. H. Carpenter, and J. Nordström, A stable high-order finite difference scheme for the compressible Navier–Stokes equations, far-field boundary conditions. Journal of Computational Physics, 225.1, 1020-1038, 2007.

[36] A. B. Usov, Finite-difference method for the Navier-Stokes equations in a variable domain with curved boundaries. Computational Mathematics and Mathematical Physics, 48.3, 464-476, 2008.

[37] S. Mcgee and P. Seshaiyer, Finite difference methods for coupled flow interaction transport models. In Electron. J. Differ. Equ. Conf, 17, 171-184, 2009.

[38] H. Kumar and R. Rajathy, Steady flow past a sphere in an aligned magnetic field at high Reynolds numbers. International Journal of Engineering, Science and Technology, 6.1, 1-19, 2014.

[39] G. A. D. Reis, I. V. M. Tasso, L. F. D. Souza, and J. A. Cuminato, A compact finite differences exact projection method for the Navier–Stokes equations on a staggered grid with fourth-order spatial precision. Computers and Fluids, 118, 19-31, 2015.

[40] E. Sterner, Semi-implicit Runge-Kutta schemes for the Navier-Stokes equations. BIT Numerical Mathematics, 37.1, 164-178, 1997.

[41] T. A. Johnson and V. C. Patel, Flow past a sphere up to a Reynolds number of 300. J. Fluid Mech, 378, 19-70, 1999.

[42] C. S. Peskin, Flow patterns around heart valves: a digital computer method for solving the equations of motion. IEEE Transactions on Biomedical Engineering, 4, 316-317, 1973.

[43] R. Campregher, J. Militzer, and A. D. S. Neto, Computations of the flow past a still sphere at moderate Reynolds numbers using an immersed boundary method. Journal of the Brazilian Society of Mechanical Sciences and Engineering, 31.4, 344-352, 2009.

[44] A. L. E. Silva, A. Silveira-Neto, and J. J. R. Damasceno, Numerical simulation of two dimensional flows over a circular cylinder using the immersed boundary method. J. Comp. Phys, 189, 351-370, 2003.

[45] G. Muhammad and N. A. Shah, Calculation of creeping flow past a sphere using direct boundary element method. Journal of American Science, 6.6, 162-165, 2010.

[46] E. Poon, G. Iaccarino, A. S. Ooi, and M. Giacobello, Numerical studies of high Reynolds number flow past a stationary and rotating sphere. In Proceedings of the 7th International Conference on CFD in the Minerals and Process Industries, 2009.

[47] J. Smagorinsky, General circulation experiments with the primitive equations. Monthly weather review, 91, 99-164, 1963.

[48] D. R. Mikulencak and J. F. Morris, Stationary shear flow around fixed and free bodies at finite Reynolds number. Journal of Fluid Mechanics, 520, 215-242, 2004.

[49] A. Masud and R. A. Khurram, A multiscale finite element method for the incompressible Navier–Stokes equations. Computer Methods in Applied Mechanics and Engineering, 195.13-16, 1750-1777, 2006.

[50] J. Li, Y. He, and Z. Chen, A new stabilized finite element method for the transient Navier–Stokes equations. Computer Methods in Applied Mechanics and Engineering, 197.1-4, 22-35, 2007.

[51] M. A. Aigo, Numerical solution of Navier stokes equation using control volume and finite element method. International Journal of Applied Mathematical Research, 5.1, 63-68, 2016.

[52] J. Camano, G. N. Gatica, R. Oyarzúa, and G. Tierra, An Augmented Mixed Finite Element Method for the Navier-Stokes Equations with Variable Viscosity. SIAM Journal on Numerical Analysis, 54.2, 1069-1092, 2016.

[53] A. Danilov, A. Lozovskiy, M. Olshanskii, and Y. Vassilevski, A finite element method for the Navier-Stokes equations in moving domain with application to hemodynamics of the left ventricle. Russian Journal of Numerical Analysis and Mathematical Modelling, 32.4, 225-236, 2017.

[54] M. Abdelwahed, N. Chorfi, and M. Hassine, A stabilized finite element method for Stream function vorticity formulation of Navier-Stokes equations. Electronic Journal of Differential Equations, 2017.24, 1-10, 2017.

[55] S. Boivin, F. Cayré, and J. M. Herard, A finite volume method to solve the Navier–Stokes equations for incompressible flows on unstructured meshes. International journal of thermal sciences, 39.8, 806-825, 2000.

[56] P. Chandrashekar, Finite volume discretization of heat equation and compressible Navier–Stokes equations with weak Dirichlet boundary

condition on triangular grids. International Journal of Advances in Engineering Sciences and Applied Mathematics, 8.3, 174-193, 2016.

[57] A. Sadikin, N. A. M. Yunus, K. Abdullah, and A. N. Mahommed, Numerical Study of Flow Past a Solid Sphere at Moderate Reynolds Number. Applied Mechanics and Materials, 660, 674-678, 2014.

[58] A. W. Vreman, The projection method for the incompressible Navier–Stokes equations: the pressure near a no-slip wall. Journal of Computational Physics, 263, 353-374, 2014.

[59] M. M. Krasnov, P. A. Kuchugov, M. E. Ladonkina, A. E. Lutsky, and V. F. Tishkin, Numerical solution of the Navier-Stokes equations by discontinuous Galerkin method. Journal of Physics: Conference Series, 815.1, 2017.

[60] H. P. Langtangen, K. Mardal, and R. Winther, Numerical methods for incompressible viscous flow. Advances in Water Resources, 25.8-12, 1125-1146, 2002.

[61] R. M. Valladares, P. Goldstein, C. Stein, and A. Calles, Simulation of the motion of a sphere through a viscous fluid. Revista mexicana de física, 49.2, 166-174, 2003.

[62] H. J. Wilson, Stokes flow past three spheres. Journal of Computational Physics, 245, 302-316, 2013.

[63] J. R. Grace and M. E. Weber, Bubbles, drops, and particles. Academic Press Inc, 3-9, 1978.

[64] S. Goldstein, The steady flow of viscous fluid past a fixed spherical obstacle at small Reynolds numbers. Proc. R. Soc. Lond. A 123.791, 225-235, 1929.

[65] B. Seibold, A compact and fast Matlab code solving the incompressible Navier-Stokes equations on rectangular domains mit18086 navierstokes. m. Massachusetts Institute of Technology, 2008.